

**GROUNDWATER POTENTIAL IN TERTIARY
AND
TRIASSIC SEDIMENTS IN KIDIANI
AREA, KWALE DISTRICT, KENYA**

THIS THESIS HAS BEEN ACCEPTED FOR
THE DEGREE OF MSc 1991.....
AND A COPY MAY BE PLACED IN THE
UNIVERSITY LIBRARY.

CHARLES M. GICHABA

A thesis submitted in accordance with the requirements for
partial fulfilment of the Degree of Master of Science of
the University of Nairobi.

DEPARTMENT OF GEOLOGY

UNIVERSITY OF NAIROBI

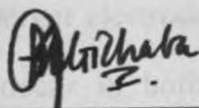
Nairobi, 1991.

ABSTRACT

DECLARATION

This is my original work and has not been submitted for a degree in any other University.

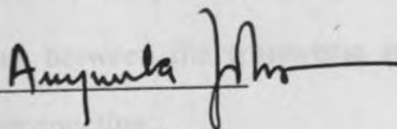
Signed: _____



Charles M. Gichaba.

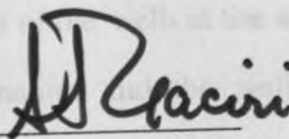
This thesis has been submitted for examination with our knowledge as University Supervisors:

Signed: _____



Dr. J. Anyumba.

Signed: _____



Dr. S.J. Gaciri.

ABSTRACT

This thesis describes the results of a hydrogeological project carried out in Kidiani Area of Kwale District, about 60 kilometres south-west of Mombasa.

With a view to evaluate the groundwater potential in Kidiani Area, Kwale District, geophysical resistivity method was applied. Here, the vertical electrical sounding (VES) was done using the Schlumberger electrode configuration. The VES results show that potable water zones occur in both Magarini sands and Mazeras sandstones. Iterative, non-automatic inversion of VES data, coupled with borehole information, resolved with some confidence the conductive / non-conductive water interfaces and revealed some correspondence between the lithostratigraphic units and resistivity values.

Maps of resistivity and transverse resistance values agree reasonably with the general hydrogeological conditions in the area. Within the Mazeras sandstones the results suggest that groundwater is strongly associated with the presence of structural features in the subsurface where seasonal recharge is likely. Correlations have been established between the conductive zone resistivity and the water salinity and to a lesser extent between the transverse resistance and the potential area(s) for groundwater prospecting.

From the available Recovery test data of the wells in the area, Jacob's straight line method of analysis depicted the nature and the well characteristics mainly transmissivity, (T) and specific capacity,(Q/S) with sufficient confidence. Determination of some aquifer limitations and to a lesser extent, relative well

efficiency were also made.

ACKNOWLEDGEMENTS

Further, groundwater analysis was carried out to determine its quality and possible uses. Generally, it is observed that groundwater in the Tertiary Magarini and Kilindini sands has lower salinity than the water in the Triassic Mazaras sandstones.

From the observations made in this study, it can be concluded that the Cenozoic Magarini and Kilindini sands have a higher groundwater potential than the Tertiary Mazaras sandstones. Moreover, these observations could be used to assist in the exploration and evaluation of groundwater resources in new target areas in the Coast Province where lithostratigraphical and hydrogeological information is very limited.

My sincere thanks also go to the Project Manager, Mr. J.K. Mwangi, Mears S.C. Mwalongo, M.M. Lichaba and the rest of the staff of Fresh Water and Sanitation Project for providing invaluable assistance and backing during the execution of the fieldwork. The chemical analysis of the water samples was made possible by the kind assistance of Mears P.K. Bor and J.O. Mwangi of the Ministry of Environment and Natural Resources, Nairobi, and the Kenya Bureau of Standards, Nairobi, respectively. Many thanks are also due to the entire staff of the Department of Geology, University of Nairobi, who in a way contributed immensely to the completion of this work.

Last but not least, I would like to heartily thank my parents for their continuous, unwavering support and unparalleled patience during the entire duration of the project. My wife, Mrs. Mary Wanjau, is warmly acknowledged for her faithfulness, understanding and display of strong courage during those difficult periods that I went through on this project.

ACKNOWLEDGEMENTS

I wish to express my sincere gratitude to the University of Nairobi for awarding me a scholarship which enabled me to successfully carry out this project. My special thanks are due to my supervisors, Dr. S.J. Gaciri and Dr. J. Anyumba, for their intellectual stimulation, guidance and encouragements during the course of this work. They painstakingly read through the manuscript and made very useful suggestions for improvement.

I also wish to register my deepest appreciations to the Ministry of Water Development for all the facilities that were put at my disposal during the entire period of this project. My sincere thanks also go to the Project Manager, Mr. L.K. Biwott, Messrs S.G. Mathenge, M.M. Lidonde and the rest of the staff of Kwale Water and Sanitation Project for providing invaluable assistance and backup during the execution of the fieldwork. The chemical analysis of the water samples was made possible by the kind assistance of Messrs P.K. Bor and J.G. Mwangi of the Ministry of Environment and Natural Resources, Nairobi, and the Kenya Bureau of Standards, Nairobi, respectively. Many thanks are also due to the entire staff of the Department of Geology, University of Nairobi, who in a way contributed immensely to the completion of this work.

Last but not least, I would like to heartily thank my parents for their continuous, unwavering support and unparalleled patience during the entire duration of the project. My wife, Mrs Mary Wanjiru, is warmly acknowledged for her fathomless understanding and display of strong courage during those difficult periods that I was away on this project.

CONTENTS

	Page
Abstract	iii
Acknowledgement	v
Table of Contents	vi
List of Figures	xi
List of Plates	xiii
List of Tables	xiv
 CHAPTER 1 INTRODUCTION	
1.1 General Information	1
1.2 Location	2
1.3 Physiography	
1.3.1 Topography	2
1.3.2 Drainage	2
1.4 Climate	4
1.5 Population	5
1.6 Soils and Land Use	
1.6.1 Soils	5
1.6.2 Land Use	5
1.7 Communication	6
1.8 Justification	6
1.9 Aims and Scope	7
1.10 Previous Related Work	8

CHAPTER 2 GEOLOGY AND HYDROGEOLOGY

2.1	General Introduction	13
2.1.1	Duruma Sandstones	13
2.1.2	Magarini Sands	16
2.1.3	Kilindini sands	17
2.2	Geologic History and Tectonism	18
2.3	Hydrogeology	
2.3.1	Mazeras Sandstones	20
2.3.2	Magarini Sands	21
2.3.3	Kilindini Sands	21

CHAPTER 3 METHODOLOGY OF WORK

3.1	Fieldwork	23
3.1.1	Resistivity Survey	23
3.1.1.1	Field Equipment	23
3.1.1.2	Field Measurement Procedure	28
3.1.1.2.1	Calculation of Apparent Resistivity	29
3.1.1.3	Choice of the Method	33
3.1.1.4	Field Limitations and data Quality	34
3.1.2	Well Tests	36
3.1.2.1	Measurements	36
3.1.2.1.1	Water Level Measurements	37
3.1.2.1.2	Discharge Rate Measurements	38
3.1.2.2	Duration of the Test	38
3.1.2.3	Field Limitations of the Test and Data Quality	40

3.1.3	Water Sampling Operations	41
-------	---------------------------------	----

CHAPTER 4 DATA ANALYSIS

4.1	Resistivity Data Analysis	43
4.1.1	Qualitative Analysis	43
4.1.2	Quantitative Analysis	50
4.1.2.1	Curve Matching and Auxiliary Point Method	51
4.1.2.1.1	Disadvantage of this Analytical Method	51
4.1.2.2	Computer Model Curve Generating Method	52
4.1.2.2.1	Advantages of this Method	53
4.1.2.2.2	Limitations of Computer Modelling Method	54
4.1.2.3	Limitations of the Two Applied Analytical Method	54
4.2	Well Tests	
4.2.1	General Principles	59
4.2.2	Recovery Test	62
4.2.2.1	Advantages of using Recovery Test Data	63
4.3	Water Quality	65

CHAPTER 5 INTERPRETATION OF THE RESULTS AND DISCUSSIONS

5.1	General Introduction	69
5.1.1	Description and Interpretation of Apparent Resistivity Maps	69
5.2	Interpreted Geo-electric cross-sections and stratigraphic correlation	74

5.2.1	Profile B-B'	74
5.2.2	Profile T-T'	79
5.2.3	Profile X-X'	82
5.2.4	Discussions on the VES Data Results	85
5.3	Interpretation of the Well Tests Data: Results and Discussions	
5.3.1	Introduction	90
5.3.2	Effects of some Hydrogeologic Factors on the interpreted Results	91
5.3.3	Discussions on the Recovery Test Results	100
5.3.4	Comparison between Interpreted VES and Well Test Analyses Results	107
5.4	Interpretation of Water Quality Analysis: Results and Discussion	
5.4.1	Dominant Ions	109
5.4.2	Minor Ions	111
5.4.2.1	Iron	111
5.4.2.2	Fluoride	111
5.4.2.3	Silica	112
5.4.2.4	PH	112
5.4.2.5	Specific Conductance and Total Dissolved Solids	113
5.4.3	Discussions on the Water Quality Analysis	114
5.4.3.1	Water Quality and Use	114
5.4.3.1.1	Domestic Use	114
5.4.3.1.2	Industrial Use	115
5.4.3.1.3	Irrigation Use	116
5.4.3.2	Relation to Geology	119

5.4.4	Correlation between Aquifer Resistivity and Salinity	123
5.4.5	Groundwater Potential Distribution in Kidiani Area	127
5.4.5.1	Rainfall/Recharge	128
5.4.5.2	Well Characteristics	130
5.4.5.3	Borehole Distribution	130

CHAPTER 6 CONCLUSIONS AND RECOMMENDATIONS

6.1	Vertical Electrical Soundings (VES)	
6.1.1	Conclusions	133
6.1.2	Recommendations	134
6.2	Well Tests	
6.2.1	Conclusions	136
6.2.2	Recommendations	137
6.3	Water Quality	
6.3.1	Conclusions	138
6.3.2	Recommendations	138

REFERENCES	141
------------------	-----

Figure 5.3 (a) Interpreted geo-electric cross-section along profile
line B-B' in Kidiani Area, Kwale upto a depth of 100m75

List of Figures

Figure 1 Location of the project area3

Figure 2 (a) Geological map of Kidiani Area14

Figure 2 (b) Geological cross-section along line A-A'14

Figure 3.1 Controls and Terminals of SAS 300B Terrameter25

Figure 3.2 Vertical Electrical Sounding sites, Boreholes
and Sampling sites in Kidiani Area, Kwale27

Figure 3.3 Schlumberger Electrode Configuration28

Figure 4.1 (a) Examples of the four Types of three-layer
Schlumberger curves for three-layer Earth models44

Figure 4.1 (b) Examples of three of the eight possible Types of
Schumberger curves for four-layer Earth models44

Figure 4.1 (c) Dominant Types of resistivity curves in Kidiani Area46

Figure 4.2 Sounding curves of 'Traverse B-B' drawn on same X-axis48

Figure 4.3 Sounding curves of traverse B-B' drawn on the same axes ..49

Figure 4.4 Modelled curves showing Equivalence by Longitudinal
Conductance (S) for F35 57

Figure 4.5 Modelled curves showing Equivalence by Transverse
Resistance (T_r) for F3558

Figure 4.6 Single Borehole Recovery Test63

Figure 5.1 Apparent resistivity map at AB/2 spacing = 13m71

Figure 5.2 Apparent resistivity map at AB/2 spacing = 50m72

Figure 5.3 Apparent resistivity map at AB/2 spacing = 100m73

Figure 5.4 Interpreted geo-electric cross-section along profile
line B-B' in Kidiani Area, Kwale75

Figure 5.5 (a)	Interpreted geo-electric cross-section along profile	99
Figure 5.10	line B-B' in Kidiani Area, Kwale upto a depth of 100m	75
Figure 5.5 (b)	Borehole logs stratigraphic correlation along profile	102
Figure 5.20	B-B' in Kidiani Area, Kwale	75
Figure 5.6	Interpreted geo-electric cross-section along profile	104
Figure 5.22	line T-T' in Kidiani Area, Kwale	80
Figure 5.7 (a)	Interpreted geo-electric cross-section along profile	
	line T-T' in Kidiani Area, Kwale upto a depth of 100m	80
Figure 5.7 (b)	Borehole logs stratigraphic correlation along profile	
	T-T' in Kidiani Area, Kwale	80
Figure 5.8	Interpreted geo-electric cross-section along profile	
	line X-X' in Kidiani Area, Kwale	84
Figure 5.9 (a)	Interpreted geo-electric cross-section along profile	129
Figure 5.27	line X-X' in Kidiani Area, Kwale upto a depth of 100m	84
Figure 5.9 (b)	Borehole logs stratigraphic correlation along profile	
	X-X' in Kidiani Area, Kwale	84
Figure 5.10	Map showing Recharge and discharge areas in	
Plan 1	Kidiani Area, Kwale	88
Figure 5.11	Transverse Resistance map of the Aquifer zone	
	in Kidiani Area, Kwale	89
Figure 5.12	Residual drawdown curve against ratio t/t' for C7087	92
Figure 5.13	Time drawdown curve for pumping phase for C7087	93
Figure 5.14	Residual drawdown curve against ratio t/t' for C7934	95
Figure 5.15	Time drawdown curve for pumping phase for C7934	96
Figure 5.16	Residual drawdown curve against ratio t/t' for C8221	98

Figure 5.17	Time drawdown curve for pumping phase for C822199
Figure 5.18	Residual drawdown curve against ratio t/t' for C7090101
Figure 5.19	Residual drawdown curve against ratio t/t' for C6673102
Figure 5.20	Residual drawdown curve against ratio t/t' for C6721103
Figure 5.21	Residual drawdown curve against ratio t/t' for C7097104
Figure 5.22	Trilinear Diagrams110
Figure 5.23	Classification of irrigation water based on SAR and Conductivity118
Figure 5.24	Comparison between Aquifer Resistivity and groundwater salinity in Mazeras sandstones in Kidiani area, Kwale124
Figure 5.25	Comparison between Aquifer Resistivity and groundwater salinity in Magarini sands in Kidiani area, Kwale126
Figure 5.26	Mean monthly rainfall distribution patterns129
Figure 5.27	Groundwater potential distribution map132
Table 4.3	Aquifer(s) characteristics in Magarini sands and Mazeras sandstones in Kidiani Area, Kwale66
List of Plates		
Plate I	SAS 300B Terrameter and its Accessories25
Plate II	Electric Dipper used for depth measurements during Well Test39
Table 5.1	Correlation between Resistivity and Formation characteristics of Mazeras sandstones in Kidiani Area, Kwale78
Table 5.2	Well log for borehole no CS76782

List of Tables

Table 1	Mean monthly rainfall data of some stations in Kidiani Area	4
Table 2	Stratigraphical succession of the Mombasa-Kwale Area	15
Table 3.1	Range of time intervals between water level measurements in the pumped borehole during the pumping phase	37
Table 3.2	Range of time intervals between water level measurements in the pumped borehole during the recovery phase	38
Table 3.3	Desired type and duration of pumping test program on various types of boreholes	40
Table 4.1	Layer parameters of three Equivalent model curves by Longitudinal Conductance (S) for F35	56
Table 4.2	Layer parameters of three Equivalent model curves by Transverse Resistance (T_r) for F40	59
Table 4.3	Aquifer(s) characteristics in Magarini sands and Mazeras sandstones in Kidiani Area, Kwale	66
Table 4.4	Detection limits of AA6 Tectron AAS machine	67
Table 4.5	Chemical characteristics of groundwater in Magarini sands and Mazeras sandstones in Kidiani Area, Kwale between 1987-1988	68
Table 5.1	Correlation between Resistivity and Formation characteristics of Mazeras sandstones in Kidiani Area, Kwale	78
Table 5.2	Well log for borehole no C5767	82

INTRODUCTION

Table 5.3 Correlation between Resistivity and Formation characteristics of Magarini sands in Kidiani Area, Kwale83

Table 5.4 Categorization of groundwater based on TDS114

Table 5.5 Drinking water standards; KBS (1985)115

Table 5.6 SAR values for borehole water samples in Magarini sands and Mazeras sandstones in Kidiani Area, Kwale117

Table 5.7 Salinity and Aquifer resistivity values of some boreholes in Mazeras sandstones in Kidiani Area, Kwale123

Table 5.8 Salinity and Aquifer resistivity values of some boreholes in Magarini sands in Kidiani Area, Kwale125

APPENDICES

Appendix A Field sheet of Resistivity Data (showing AB/2, MN/2 and geometric factor, K)A1-A2

Appendix B Computer generated model curves and Field DataB1-B26

Appendix C Well Test data: Recovery phaseC1-C8

Appendix D Well logs dataD1-D4

CHAPTER 1

INTRODUCTION

1.1 General Information

Much of Kenyan land is arid and semi-arid. Like other developing countries, Kenya faces immense difficulties in trying to meet the water requirements for her rapidly growing population that are both sufficient and safe.

The present project area falls within a marginal zone. The cultivated land is generally below 10% (Survey of Kenya, 1970) since there is not sufficient water for irrigation purposes. Currently the population density is low, 19-39 people per square kilometre. However, with the present national population incremental rate of about 3.6% p.a. (Ojany and Ogendo, 1973), it is expected that the water needs will rise even higher.

Currently, the main sources of water are the "traditional" shallow village wells usually dug in dry stream beds. These wells often provide foul water which leads to occasional outbreaks of water related diseases. However, in the recent past, several boreholes have been drilled. Some existing springs have also been rehabilitated in an effort to provide clean, potable water to the local population.

It is, therefore, the intended purpose of this project not only to collect and correlate geophysical and well log data but also to analyse the well test data and determine the quality of the water in order to adequately evaluate the groundwater potential in the project area. This will augment the present water supplies thereby enabling the local people to set up better health facilities, improve livestock rearing

and, more importantly, carry out some horticultural cultivation projects whose market would be the vast tourist hotel industry in the coast.

1.2 Location

The project area is situated in Kwale District of the Coast Province of Kenya. It comprises part of the land extent of the lower central region of Msambweni, top-sheet 200/4 of the Survey of Kenya. It is about 60 kilometres to the south-west of Mombasa and bounded by latitudes $4^{\circ} 23' 12''$ S and $4^{\circ} 28' 12''$ S and longitudes $39^{\circ} 21' 05''$ E and $39^{\circ} 26' 05''$ E (Fig 1). It covers an area of approximately 100 square kilometres.

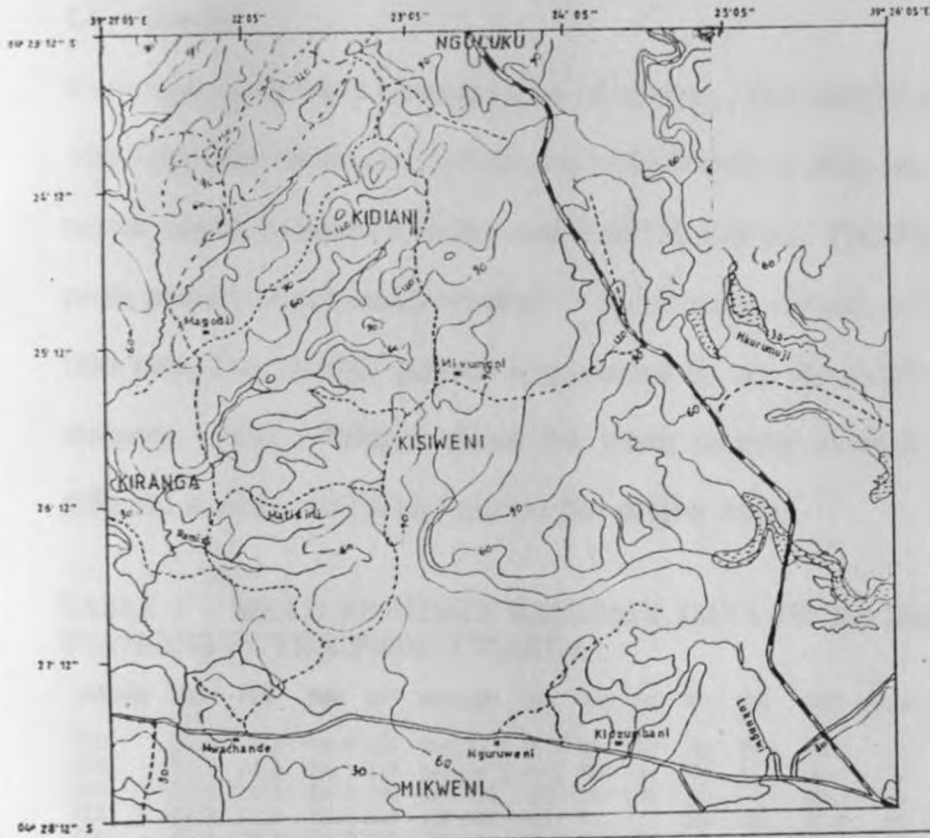
1.3 Physiography

1.3.1 Topography

Kidiani area falls under the physiographic unit referred to as the Foot Plateau by Gregory (1921), Caswell (1953, 1956) and Miller (1952). This forms part of the land between the low lying Coastal Plains and the eminent Shimba Hills which comprise the Coastal Ranges (Caswell, 1953; Dindi, 1983). The Foot Plateau lies between 60 and 135 m above sea level and is generally a flat plain.

1.3.2 Drainage

There are two major rivers that traverse the project area. These are River Ramisi to the west and south-west and River Mkurumuji to the eastern part. River Ramisi has developed drainage channels through the sandstones along some easily weathered geological zones. These channels were observed as fractures and/or miniature faults which are recognisable on aerial photographs as photo lineaments.



- LEGEND**
- All weather road
 - Loose surface
 - Dry weather road
 - Main motorable tracks and other footpaths
 - River
 - Area of seasonal flooding
 - 90 Contours
 - KIDIANI Area name
 - Hwachande Shopping centre



Fig 1 LOCATION OF THE PROJECT AREA.

River Mkurumuji drains the sandy, flat area to the east of the project area. Often it flows into swamps and shows signs of reaching maturity by meandering in several parts. The Shimba Hills situated on the northern side of the project area form the major catchment and serve as the source of numerous streams and rivers which are seasonal and drain the area.

1.4 Climate

The project area has a monsoon type of climate. The rainfall pattern is bi-modal with long rainy season occurring from mid-March to May while the short rainy season comes between October and mid-December. The highest precipitation peaks occur in April and November. The average annual precipitation is about 1250 mm. The rainfall pattern is governed by the direction of the prevailing monsoon winds. Table 1 shows the mean monthly rainfall data recorded at different stations within and around the project area.

1.4.1 Soils and Land Use

TABLE 1 MEAN MONTHLY RAINFALL DATA UP TO 1988 OF THE STATIONS IN THE PROJECT AREA

STATION	JAN	FEB	MAR	APR	MAY	JUN	JUL	AUG	SEP	OCT	NOV	DEC	NO.OF YRS
KAS	33.0	17.5	59.4	154	231	99.1	79.7	64	67	105	99.1	79.5	75
NCO	34.9	24.8	54	115	165	54.3	64.7	59	44	79	83.8	68	37
SHS	37.8	14.5	69.1	209	293	118	103	78	69	130	118	72.1	34
KKS	33.8	17.9	74.5	210	267	118	111	82	77	104	122	87.4	30
KFS	45.2	34.5	64.9	116	257	122	94.6	64	78	121	123	95.5	11
TCC	23.6	13.1	50.1	226	308	98.3	86.3	76	80	83	82.9	64.2	35
MDO	18.2	13.2	62.4	258	371	143	103	79	69	90	94.6	47.3	50

(Source : Meteorological Department)

- KEY**
- KAS - KWALE AGRIC. STATION
 - NCO - NDAVAYA CHIEF'S CAMP
 - SHS - SHIMBA HILLS SETTLEMENT
 - KKS - KIKONENI AGRIC. STATION
 - KFS - KWALE FOREST STATION
 - TCC - TIWI CHIEF'S CAMP
 - MDO - MSAMBWENI DISTRICT OFFICE

Temperatures are generally high with averages ranging from 20° C during the months of July and August to 35° C in February and March. According to

Meteorological Department (1988), the mean annual minimum temperature is 22° C.

Humidity varies between 60-95% depending on the locality of the area relative to the coastal zone (Met. Dept., 1988).

1.5 Population

The Kidiani area with over 205,000 people (Ojany and Ogendo, 1973) is predominantly inhabited by the Digo. However, Kambas form a major proportion of the population especially in the hilly areas towards the Shimba Hills. A few Makonde and Luo people are found in the labour camp of the Ramisi sugar farms. The source of income and employment for this population is limited. However, majority of the people are employed by the tourist industry at the coast.

1.6 Soils and Land Use

1.6.1 Soils

The type of soil in the project area depend very much on the parent rock. Except perhaps in the flood plains, the soils in the area derived from the sandstones are usually red sandy and silty ones. Magarini sands provide soils ranging from whitish-grey to dark-brownish nearly red sandy soils. Soils from the Kilindini sands are generally dark coloured and also finer than those of Magarini sands.

1.6.2 Land Use

The inhabitants of this area are hard working subsistence farmers. However, they face the hardships of low rainfall while the soils are likely to be unproductive due

to high soil salinities. People have developed some land on which they grow some food crops such as cassava, groundnuts, guavas, bananas and maize. Others have grown cash crops mainly cashewnuts, coconuts, mangoes, oranges and, to a lesser extent bixa. In addition, they also keep livestock such as the indigenous cattle, sheep and goats.

1.7 Communication

Characteristically, the infrastructure as in most other parts of the district, is poor. The nearest tarmac road is the Mombasa-LungaLunga road which passes about five kilometres to the east of the project area. Other motorable tracks (murrum roads) which traverse through the area are the Msambweni-Kikoneni and Msambweni-Nguluku roads (Fig 1). A number of other smaller dusty roads also exists. However, most of these roads are rendered immotorable during the rainy seasons.

(v) To evaluate the groundwater potential distribution in the area.

1.8 Justification

None of the earlier research works has adequately covered the project area though a general over-view of the groundwater assessment has been provided. The major problem facing either small scale or large scale developments in the area is lack of adequate natural water resources necessary for its general development.

These conditions were also generally noted.

Presently, water is obtained from rivers, earth dams or ponds and some springs. Such water is, however, not safe for consumption. To cater for the increased population, irrigation of new farming lands and initiation of small-scale industrial projects, potable water resources are an obvious requirement.

1.9 Aims and Scope

To evaluate the groundwater potential in this area, the project was carried out with the following objectives:-

- (i) Examine the extent to which vertical electrical sounding (VES) can provide reliable results in relation to the quality of the groundwater.
- (ii) Establish some hydrogeophysical correlations which would be used in other areas of similar geological and hydrogeological conditions at the coast.
- (iii) Estimate the well hydraulic parameters, i.e., yields (Q), drawdowns (s), specific capacity, (Q/S) and transmissivity, (T) of the various boreholes within the different formations in the project area.
- (iv) To determine the general quality and use of the groundwater in the project area.
- (v) To evaluate the groundwater potential distribution in the area.

To achieve these objectives, all the already existing resistivity, borehole logs and well test data were collected and analyzed. These were, however, very little and generally inadequate. Fresh resistivity data was acquired. Single borehole pumping tests were performed and recorded for the newly drilled boreholes. These boreholes were also geologically logged.

Hydrologic and climatic data were also incorporated. Water quality analysis was done on some randomly selected boreholes spread throughout the project area.

It is, therefore, anticipated that it will be possible to get a clearer "regional" picture of the groundwater potential in this area. This will go a long way in augmenting the current inadequate water supplies in the area.

1.10 Previous Related Work

A number of surveys have been conducted in the south coastal regions of Kenya in connection with mineral and water explorations. However, none of these investigations has embraced the present project area. The following review, therefore, looks at all the work that has been undertaken in the south coast. Since some of these works are of a regional nature, they, no doubt, have some bearing on the present area of interest.

Caswell (1953 and 1956) investigated the general geology of Mombasa-Kwale and Kilifi areas, respectively. His conclusions on groundwater resources agree with those drawn by Miller (1952). He went further and strongly recommended the pre-Cenozoic valleys as the best targets for groundwater development as they had higher yields and better quality water.

Sanders (1959 and 1963), while studying the mid-Galana and Voi-South Yatta areas, commented on the water supply of the area. He observed that the Lower Duruma sandstone were deposited in a semi-arid environment and evaporites associated with such environmental conditions have contributed to the salinity of groundwater in the area.

Sanders (1959) further observed that Upper Duruma sandstones deposited in sub-aerial environments have low permeability. The quality of water from boreholes drilled in this formation is better than that obtained from the lower members of the same formation. He also observed that the Magarini sands are unconsolidated and a very permeable formation. Springs are a common feature at their contact with the underlying Jurassic formations.

Gentle (1968) attempted a systematic resistivity geophysical work in the area around Tiwi and Ukunda and the area to the north in corals, beaches and lagoonal deposits. Existing boreholes and wells within this area provided the controls. He noted from the resistivity data that the top layer in the corals have generally high resistivities which rapidly decrease with depth perhaps due to groundwater salinity. However, the middle coral layers form the main fresh water aquifer of considerable thickness.

Terra Surveys Ltd. of Canada (1978) carried out a combined towed-bird time-domain "INPUT" airborne electromagnetic and magnetic survey in the area between Malindi to the north and Shimoni to the south. From the "INPUT" data, anomalous areas of low conductivity (high resistivity) were delineated. Some of these anomalous areas were interpreted to be due to fresh groundwater.

Austromineral of Austria (1980) conducted a large scale systematic geophysical survey for groundwater in the area extending from Likoni near Mombasa to Muhaka near Msambweni. This area is covered by lagoonal Kilindini sands. During the survey, numerous resistivity measurements were carried out both in the

corals and the lagoonal sands. In addition, two seismic reflection lines were made: one in the strike direction of the corals and the other one perpendicular to it into the lagoonal deposits.

From the resistivity investigation, relationships that govern resistivity of sands and coral limestones were distinguished, but rather tentatively. It was established that in the sands, high/low resistivity values depend on the presence or absence of clay horizons, respectively. Problems arise in distinguishing the clay layers from sands filled with brackish water or shales from saline water saturated sands. This is because the resistivity values in both cases are about the same. The uncertainty further increases when sequences of sands, saline water and shales or clay layers, sands and sand with brackish water are to be determined from the resistivity data.

Austromineral (1980) like Caswell (1953) and Gentle (1968) agreed that the lagoonal sands are indeed favourable aquifers. The sandy aquifer varies in thickness from 30-100 m at Tiwi (Austromineral, 1980). The resistivity of the aquifer saturated with fresh water seems to be over 50 ohm-m. The presence of clay layers prevents the saline water from reaching the top layers of the aquifer. The saline water in the lower horizons is probably responsible for the lowering of the resistivities in Gentle's observations.

Mwangi (1981) carried out a detailed resistivity survey of Msambweni area east of the present study area. This was a ground follow-up of the "INPUT" anomaly A6-2. He reported that the fresh / saline water interface is marked by the interpreted 6 ohm-m true resistivity along the shoreline. He concluded that the

thickness of the saline/brackish water zone is from a few metres to just over 100m. Its corresponding depth is from 10 to 40 m. This brackish water layer is thicker in the NE and SW areas of Msambweni.

He further reported that the thickness of the coral limestone seems to be approximately 310-400 m and there is a possibility of its interfingering with Kilindini sands at various places. The boundary, however, between the sands and the coral may be difficult to detect by resistivity contrast. The low resistivity values in the western side of the Msambweni area (bordering the present area of study) are probably due to clays.

Further, he estimated the depth to the Jurassic shales to be about 310-400 m. The shales have low resistivity although this would be due to saturation with saline/brackish water. The shales outcrop around the area north of the project area. There is a greater possibility that they are buried deeper in the southern part than in the north as suggested by Caswell (1953).

Dindi (1983) carried out a gravity survey of the Jombo Hill area situated in the south-western part of the project area. Though his survey covered the area of interest, its spacing was, however, very large (1-2 km). Two deep faults trending in NE-SW direction and passing under the project area were mapped.

Mailu (1983), while studying the Athi Basin, covered some formations that are also prevalent in the project area. He observed that two types of aquifers can be distinguished, namely the weathered and fault zone aquifers mainly found within

the Mazeras sandstone and the unconsolidated sediment aquifer on the Cainozoic Magarini sands. Accordingly, groundwater recharge is more significant along fault zones and within areas covered by loose sediments.

2.1 General Introduction

Other reports which have a bearing on the present investigation are by Sheikh and Biwott (1985) and Norconsult (1986). It should, however, be noted that these reports have little or no detailed geophysical investigation that cover the sedimentary formations found in this area. In these reports, the authors recommended further and detailed resistivity investigation.

According to all these reports, the oldest rocks are the Basement rocks of the Precambrian found in the south-west of the study area. Other rocks are the Tertiary rocks found in the south-east of the study area. Using this model, he delineated the fresh-sea water interface more accurately than was previously the case.

Thambu (1987) describes the hydrogeology, quantity and quality of the groundwater in the south-coast area of Kenya. He makes no attempt to carry out any geophysical investigation. He, however, suggests that the real extent and thickness of the Msambweni-Gazi aquifer can only be determined by electrical profiling and sounding, respectively.

2.1.1 Tertiary Sediments

The tertiary rocks consist of the Upper Tertiary formations of the Kenya System (Wood, 1933; Gregory, 1933). They consist of Mazeras sandstones and the Magarini sands. These rocks were deposited in a shallow sea. Thus, they form the Tertiary Coastal

CHAPTER 2

GEOLOGY AND HYDROGEOLOGY

2.1 General Introduction

The earliest description of the sedimentary rock sequence of the Coastal Kenya was provided by Gregory (1921). However, the general geology of Kwale District has been described by Caswell (1953) and Miller (1952). More work involving the re-mapping of the area was done in 1978 by the staff of Mines and Geology Department, Ministry of Environment and Natural Resources (Winani, 1977). According to all these reports, the oldest rocks are the Basement rocks of the Precambrian age found to the north-west of the project area. Other rocks are the younger sedimentary rocks found towards the Shimba hills and the Indian Ocean to the east. The general stratigraphical succession of the south coast and the tectonism of the area is shown in Table 2.

The project area is covered by sedimentary rocks. The three outcropping geological formations (Fig 2) include:

- (i) The Duruma sandstones, mainly comprising Mazeras sandstone formation,
- (ii) The Magarini sands and
- (iii) The Kilindini sands.

2.1.1 Duruma Sandstones

These sandstones form the Upper Triassic formation of the Karroo System (Wood, 1930; Gregory, 1921). They consist of Mazeras sandstones and the Shimba grits; the latter being more resistant to weathering. Thus, they form the hilly Coastal

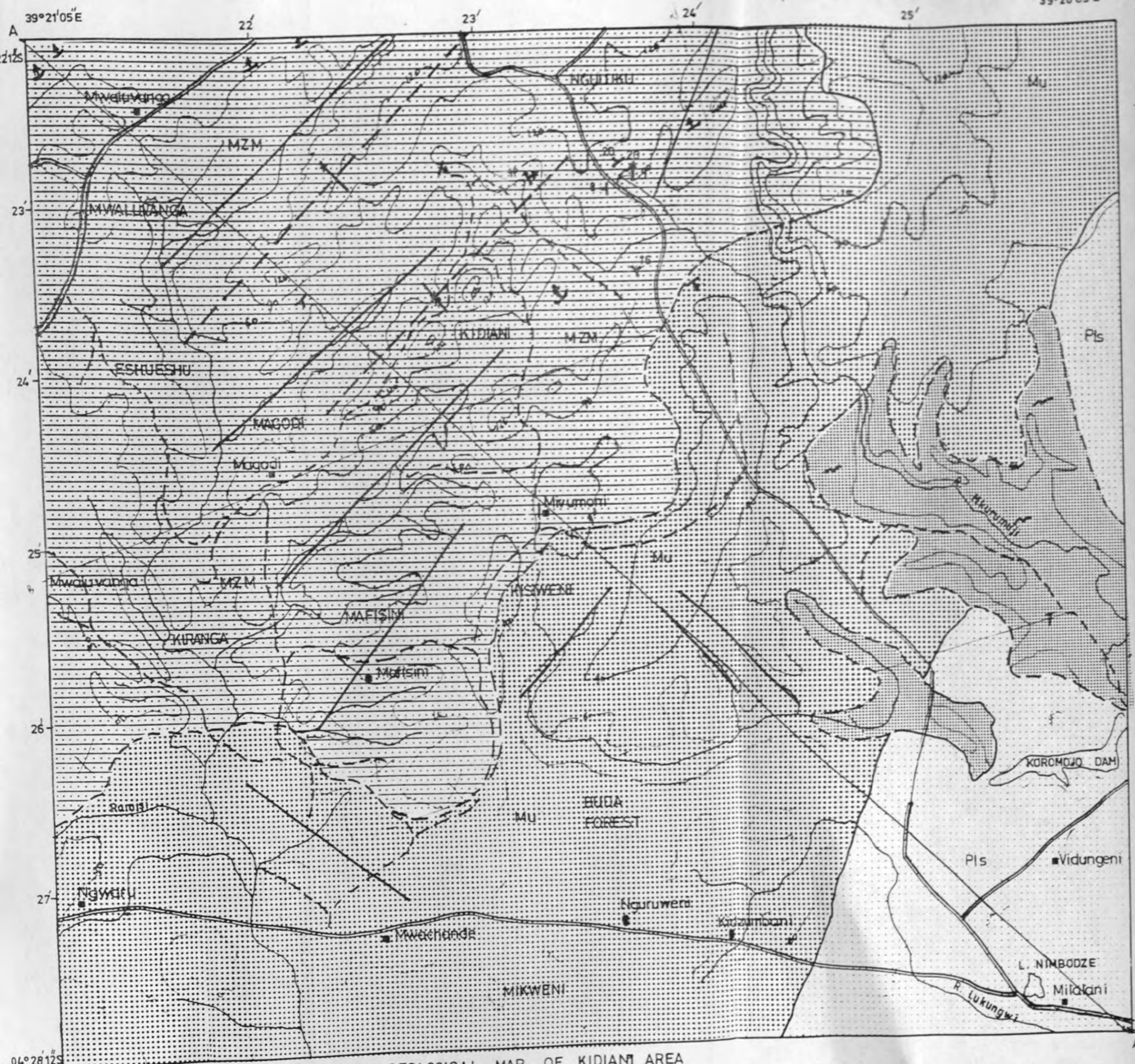
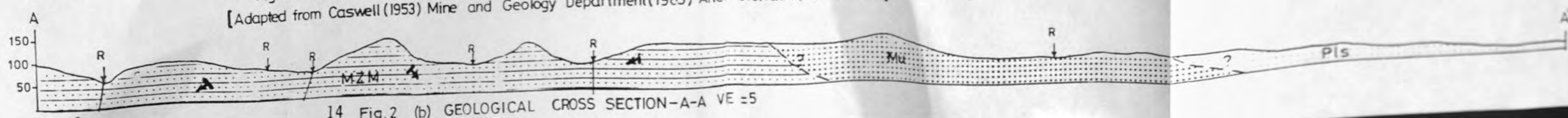
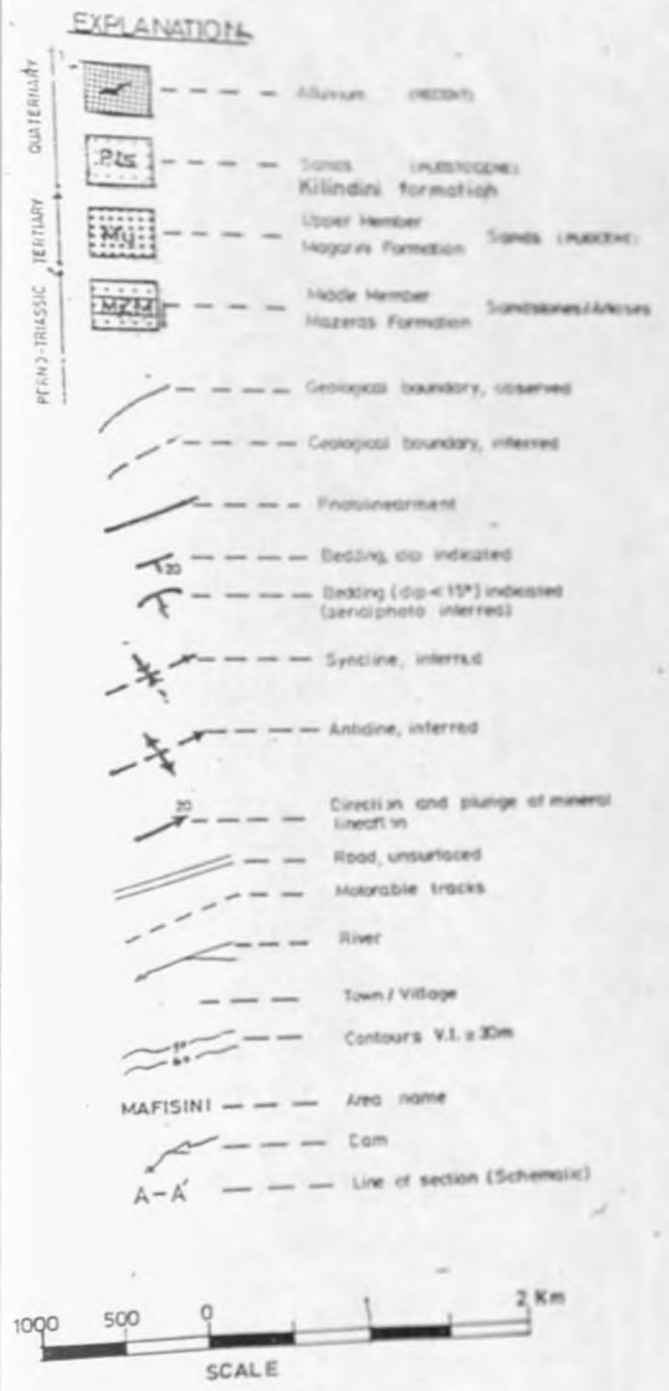


Fig. 2 (a) GEOLOGICAL MAP OF KIDIAMA AREA
 [Adapted from Caswell (1953) Mine and Geology Department (1985) After Gichaba (1989) Mod.]



14 Fig. 2 (b) GEOLOGICAL CROSS SECTION-A-A VE =5

Ranges physiographic unit represented by the hills around Kidiani in the north-western part of the project area.

The Upper Proterozoic Magarini sands were derived from the Mazeras sandstones. The Mazeras sandstones series is composed of grits, sandstones and shales. According to Caswell (1953), this series seems to have been deposited under lacustrine, deltaic and possibly neritic conditions. The sandstones and grits are massive, cross-bedded and quartzo-feldspathic with interbedded shales in the lower horizons. The feldspars are generally weathered and often kaolinised, cemented together by mica, feldspar, silica or calcite. The former two are most common. As they form the cementing material, the rocks readily disintegrate to sand.

Caswell (1956) observed that the Upper Duruma Mazeras sandstones rest unconformably on the underlying Mariakani sandstones. During their deposition, denudation of the Mozambiquian prevailed; continental deposits accumulated under lacustrine or sub-aerial conditions with one or more marine intercalations.

Mathu, et. al., (1989) have observed that this formation, arkosic in nature with poorly rounded grains, has silicified fossil wood in certain horizons. Further, the sediments were most probably deposited under shallow water conditions with the more massive members having most likely been formed in an aeolian environment.

2.1.2 Magarini Sands.

According to Caswell (1953), Magarini sands comprise some of the Tertiary sediments in this area. They form the Foot Plateau physiographic unit overlying unconformably the down-faulted Jurassic and Cretaceous shales. They form a belt

of low lying hills running parallel to the coast. The base of the Kilindini sands is probably over 200 m deep (Cawson, 1961). The thickness of the Magarini sands. The Upper Pliocene Magarini sands were derived from the Mazeras sandstones. They abut against the Duruma Series in the project area. It is extremely difficult to delimit their outcrops as both the weathered Duruma sandstones and the Magarini sands, which are also weathered products of the Duruma series, bear very close resemblance.

The Magarini sands are predominantly quartzose. According to Caswell (1953), these sands contain fragments of Jurassic shales, rounded fragments of silicified fossil wood and well rounded pebbles of gneiss from the Mozambiquian Belt System. The outcrop is usually poorly stratified, ill-sorted and unconsolidated. It varies from silty clay to coarse boulder gravel.

The nature and the constitution of the Magarini sands indicate that they were most probably deposited as river gravels and coastal dunes under conditions of intense erosion by streams rushing seawards from the Shimba Hills. These brought with them vast quantities of debris that were scattered all over the Coastal Plains.

2.1.3 Kilindini Sands.

These sands cover the Coastal Plains physiographic unit. In the present project area, Kilindini sands are only found in the south-eastern part. They are unconsolidated and ill-sorted. These sands lie on a wave cut platform on the Jurassic shales. They are erosional products of Magarini sands that were deposited in a lagoon fringed by the coral limestones in the Pleistocene. These sands are

intercalated by clay layers in several places. The base of the Kilindini sands is probably over 200 m deep (Mwangi, 1981). The thickness of the Magarini sands ranges from 120 m (Caswell, 1956) to 150 m (Thomson, 1954) while Mazeras sandstones have a thickness ranging from less than 200 m to about 300 m (Caswell, 1953 ; Thomson, 1954 ; K.A.M.E., 1977).

2.2 Geologic History and Tectonism.

In groundwater investigations, the geologic history and tectonic structures are vital aspects which should be considered. The two aspects not only have a direct impact on the water quality by the "order of encounter" (Freeze and Cherry, 1979) but also on the occurrence and distribution of this natural resource.

Generally, the coastal belt of the sedimentary sequence is considered to have arisen due to deposition in a down-faulted NE-SW trending trough. According to Caswell (1953), this trough is envisaged to have been initiated towards the end of the Palaeozoic as a gentle downwarp possibly caused by the weight of the ice sheet. Deposition of the post-Basement complex rocks began with the Karroo. Observations from the geophysical surveys in the coastal Tanzania (Kent, et. al., 1971) indicate that the sedimentary sequence unconformably overlies the Basement.

According to Kent, et. al., (1971), deposition of the Karroo started off at a rapid rate becoming slower towards the top of the Karroo. Caswell (1953) suggested that structural weakness that led to faulting coupled with the great weight of their overlying sediments may have been the cause of the partial collapse of the initial

trough. This tends to explain the marine invasion that followed and which resulted in the deposition of Jurassic sediments consisting of limestones, shales and sandstones.

The history of the fault movements is parallel to that of the Gregory Rift further inland. Similarities occur in the stress conditions (Kent, et. al., 1971; Kaitera, 1967). Compressional structures are absent (Caswell, 1953; Kent, et. al., 1971; K.A.M.E. project, 1977) and fault patterns indicate predominantly vertical movements with complete absence of transcurrent displacement. Initial NNE-SSW trending faulting is considered to have occurred in early Palaeozoic with middle Jurassic faulting being the main tectonic episode in the area. In north-eastern Tanzania (south of the project area), faults of this age are characterised by displacements of the order of 3000-6000 metres.

Further faulting is reported to have occurred in the late Cretaceous prior to the igneous intrusion consisting of the Jombo complex. These faults have an ESE trend (K.A.M.E. project, 1977).

The third phase of faulting resulted in the activation of the old faults marking the contacts between the Jurassic and the Duruma sediments (Caswell, 1953; K.A.M.E. project, 1977). It was characterised by small displacements. Today, this phase is represented by fault scarps. These episodes preceded the deposition of the Plio-Pleistocene deposits so that the latter are generally unaffected by faulting. Such is the case for both Magarini and Kilindini sand in the project area.

In the Mazaras sandstone formation encountered in the project area, there is evidence of NE-SW trending vertical movements without any displacements. This confirms the observations by Caswell (1953) and K.A.M.E. project (1977). These fractures / minor faults form drainage channels [Fig 2 (b)]. During the execution of this project, very low formation dips (less than 15°) were measured. Compressional NE-SW trending structures of syncline and anticline were inferred from these dips [Fig 2 (a)]. It was, however, difficult to confirm the existence of these features due to limited rock exposures on which dips could be measured. If confirmed, these features would enhance the groundwater potential as the syncline would provide a reservoir for this resource. Some of the bedding dips were interpreted from the aerial photographs as done by Lissa, et. al., (1987) in the Nyanza Province.

2.3 Hydrogeology

In the project area, the hydrogeology may be studied in three zones, namely, the Mazaras sandstones, Magarini sands and Kilindini sands.

2.3.1 Mazaras Sandstones

Generally, the Mazaras sandstones comprise the hilly north-western parts of the project area. These rocks have been mildly folded and fractured (Figs 2 (a) and (b)). The Shimba Hills form an ideal recharge zone for aquifers within this formation. Seasonal springs are also frequently found. However, a few of them are perennial and drain the unconfined sandstone aquifers which appear to be structurally controlled. Other tectonic structures such as incongruent fold axes and the many small faults running in various directions induce localised sub-

surface flow directions. The water quality from these springs may be poor especially due to bacteriological contamination (Lidonde and Mathenge, 1989, personal communication).

Boreholes drilled in this formation are usually successful with sufficient water. However, some boreholes yield mineralized water of which a good example is the Fuombi borehole (No. 8221) with a chloride content of 1475 ppm and total dissolved solids amounting to 3434 ppm.

2.3.2 Magarini Sands

These sands constitute a highly pervious formation since they are unconsolidated. They rest upon a sea-ward sloping surface of impervious Jurassic rocks so that sub-surface flowage is directed toward the later Cainozoic deposits (Caswell,1953). The junction of the Magarini sands and the Jurassic rocks is frequently marked by springs, most of which are seasonal.

The highly pervious Magarini sands formation constitutes a "relatively richer" unconfined aquifer least affected by any tectonic structures. Boreholes drilled in the Magarini sands formation yield good quality and often reliable water quantities. On average, they have a yield of about 4 m³/hr which, when compared to other formations, is relatively high.

2.3.3 Kilindini Sands.

Kilindini sands form the most favoured unconfined aquifers along the south coast. The water yields are high an example of which is the Kombani borehole (no

6674) with a tested yield of 20 m³/hr. However, these sandy aquifers are intercalated by clay horizons. The quality of water from this aquifer is good and is thus more potable. However, Austromineral (1980) cautioned about the risk of seawater intrusion. This phenomenon was not observed by the author during the execution of this project.

Resistivity (Vertical Electrical Sounding) Survey

Well Tests

Water Supplying Operations

1. Resistivity Survey

1.1 Field Equipment

For the purposes of measuring the apparent resistivity of the subsurface, a transmitter SAS (Signal Averaging System) 300 B from AHEM, a Swedish company, was used. This instrument consists of three main units, all housed in a metal casing. These include the transmitter, the receiver and the microprocessor.

The electrically isolated transmitter sends out well-defined and regulated signal current. The receiver discriminates noise and measures voltages correlated with transmitted signal current (resistivity survey mode) and also measures uncorrelated direct current (DC) potentials with the same discrimination of noise rejection. The microprocessor monitors and controls operations and records results. The results are usually the ratio of the potential difference (V) to the current (I), V/I, i.e., resistance.

CHAPTER 3

METHODOLOGY OF WORK

3.1 Fieldwork

The fieldwork was carried out in three phases. These were:

- (i) Resistivity (Vertical Electrical Sounding) Survey
- (ii) Well Tests
- (iii) Water Sampling Operations.

3.1.1 Resistivity Survey

3.1.1.1 Field Equipment

For the purposes of measuring the apparent resistivity of the subsurface, a Terrameter SAS (Signal Averaging System) 300 B from ABEM, a Swedish company, was used. This instrument contains three main units, all housed in a single casing. These include the transmitter, the receiver and the microprocessor.

The electrically isolated transmitter sends out well defined and regulated signal current. The receiver discriminates noise and measures voltages correlated with the transmitted signal current (resistivity survey mode) and also measures spurious, uncorrelated direct current (DC) potentials with the same discrimination and noise rejection. The microprocessor monitors and controls operations and calculates results. The results are usually the ratio of the potential difference (**V**) to the current (**I**), V/I , i.e., resistance.

The instrument is made in such a way that consecutive readings are taken automatically and the results averaged continuously. The continuous updated average is displayed in digital form in kilo-ohms, ohms and milli-ohms. The advantage of using Terrameter SAS 300 B in resistivity surveys is that it permits natural or induced signals to be measured at extremely low levels, with excellent penetration and low power consumption. Moreover, it can be used in a wide variety of applications where effective signal/noise discrimination is needed.

The source of power for this instrument is a Ni-Cd battery pack. This pack is fitted conveniently onto the bottom of the instrument.

To facilitate vertical electrical sounding by this instrument, a sounding cable set has been provided. The cable incorporates heavier gauge conductors and much better insulation, both of which improve the electrical survey results. Moreover, there are convenient, short hook-up cables for easier expandability. The sounding cable set consists of:

- (i) Current cables wound on two separate plastic reels, each containing 750 m (length) of 0.75 mm^2 (cross-sectional area)
- (ii) Potential cables comprising two separate 50 m lengths of 1 mm^2 wire wound in parallel to a single reel that is provided with a short reel-to-instrument hook-up cable.

A set of the Terrameter SAS 300 B together with the accessories, i.e., sounding cable sets is shown on Plate 1.

The following are the controls and terminals of the Terrameter



Plate 1 SAS 300B TERRAMETER and its accessories

ON/OFF Switch.

Selection panel on and off range

CURRENT selector.

This diagrammatic sketch shows the controls and terminals



TERMINALS

The various electrical terminals are at right on the control panel.

Fig 3.1 SAS 300B controls and terminals

The following are the controls and terminals of the Terrameter SAS 300B (Fig 3.1).

CONTROLS

SAS selector (also called the **CYCLES selector**).

This 4-position selector is used to choose either the single reading mode of 1, 4, 16 or 64 automatically averaged readings. For this investigation mode 4 was chosen.

Function selector.

This selector selects either the resistivity range or the voltage range. When this selector is turned to the battery check position, the battery voltage is measured.

ON/OFF Switch.

Switches power on and off period

CURRENT Selector.

This 11-position selector selects the current for the built-in transmitter (0.2 mA to 20 mA, in seven steps)

MEASURE Push button.

When the button is pushed, the microprocessor runs through its automatic diagnostic program and if all is satisfactory, starts the Terrameter SAS 300 B measurement procedure automatically.

TERMINALS.

The current electrode terminal are at right on the control panel. The potential electrode ones are at left.

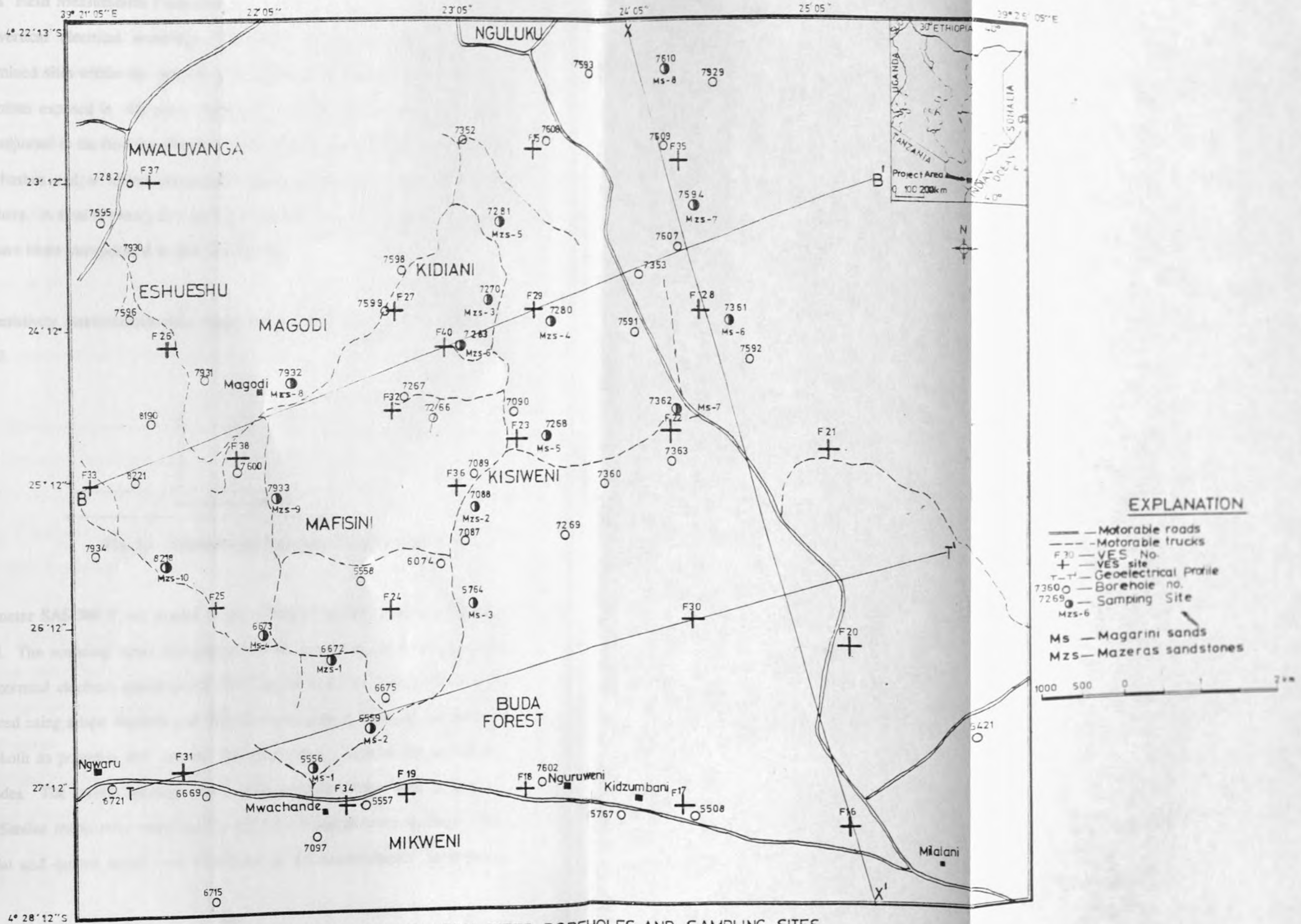


Fig.3.2 RESISTIVITY SOUNDING SITES, BOREHOLES AND SAMPLING SITES IN KIDIANI AREA, KWALE.

3.1.1.2 Field Measurement Procedure

The vertical electrical soundings (VES) were made on some already pre-determined sites within the project area. These sites cover all the geological formations exposed in this area. However, the locations of some of these sites were adjusted as the field conditions dictated. Often they were inaccessible or had thick bushes and/or forests overgrowing there. Consequently, they were shifted elsewhere. A total of twenty five vertical electrical soundings (Fig 3.2) were made and have been incorporated in this field survey.

The resistivity measurements were made using a Schlumberger array shown in Fig 3.3.

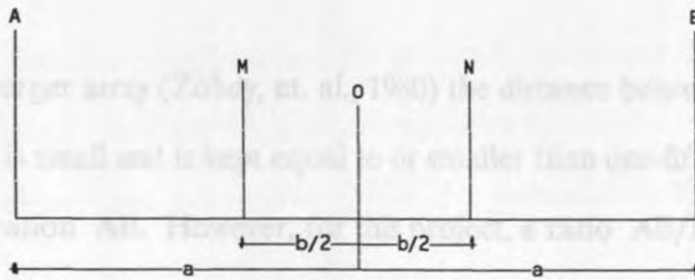


Fig. 3.3 Schlumberger Electrode Configuration

Terrameter SAS 300 B was placed at the centre, O in Fig 3.3, of the sounding spread. The sounding centre was marked on the ground by use of a metal rod. The potential electrode positions for $MN/2$ equal to 0.5 m, 5m and 10 m were measured using a tape measure and marked on the ground. Steel electrodes were used both as potential and current electrodes due to lack of the porous pot electrodes. The current spacings, $AB/2$, were carefully marked with a masking tape. Similar marks were made for the $MN/2$ of 5 and 10 metre spacings. The potential and current cables were reeled out as the measurements were being

taken. After acquiring the required data at a given site the cables were wound back. This not only minimised the cable breakage but also ensured that the insulation on these sounding cables did not come off quickly during the fieldwork.

The current electrode spacings, $AB/2$, were increased in the manner shown in Appendix A. It was envisaged that, with these separations, no information in between the spacings was missed out or repeated. As the current electrode spacing was increased, the potential difference (p.d.) decreased. Occasionally, this decrease in the p.d. was too great that the signal/noise ratio became rather too small for any accurate measurements. Such readings were repeated with different current input until more reasonable and consistent measurements were obtained.

In the Schlumberger array (Zohdy, et. al., 1980) the distance between the potential electrodes MN is small and is kept equal to or smaller than one-fifth of the current electrode separation AB. However, for this project, a ratio AB/MN of between 3 and 5 was acceptable provided reasonable and consistent apparent resistivity readings were obtained.

3.1.1.2.1 Calculation of Apparent Resistivity

Apparent resistivity is the most convenient quantity used to represent the distribution of true resistivity in the subsurface on the basis of surface measurements. It is a function of several variables: the electrode spacings AM, AN, BM and BN, the geometry of the electrode array (Fig 3.3), the true resistivity and other characteristics of the subsurface materials, such as layer thicknesses, angles of dip and anisotropic properties. Several authors have described the

calculation of apparent resistivity (Parasnis, 1979; Dobrin, 1976; Zohdy, et. al., 1980; Mwangi, 1981; Kunetz, 1966; Unz, 1953; Orellana and Mooney, 1966).

The basic equation for the potential V due to a point source of the current in a homogeneous half space of infinite extent is expressed as:

$$V = \frac{I\rho}{2\pi r} \quad \text{Eqn 3.1}$$

where I = current emanating from a source

ρ = resistivity of a medium and

r = distance from a point source

The net potential difference between the potential electrodes M and N (Fig 3.3) can be obtained for a homogeneous earth by considering the distribution of the potential at these electrodes. Thus, the potential at M due to positive electrode A is :

$$V_M^A = \frac{I\rho}{2\pi (AM)} \quad \text{Eqn 3.2}$$

while the potential at M due to the negative electrode B is :

$$V_M^B = \frac{I\rho}{2\pi (BM)} \quad \text{Eqn 3.3}$$

The total potential at M due to A and B is given by combining eqns 3.2 and 3.3 :

$$V_M^{AB} = \frac{I\rho}{2\pi} \left(\frac{1}{AM} - \frac{1}{BM} \right) \quad \text{Eqn 3.4}$$

Similarly, the total potential at N due to A and B is given by a combined equation of :

$$V_N^{AB} = \frac{I\rho}{2\pi} \left(\frac{1}{AN} - \frac{1}{BN} \right) \quad \text{Eqn 3.5}$$

The measurable net potential difference between M and N is given by subtracting eqn 3.5 from eqn 3.4 :

$$V = \frac{I\rho}{2\pi} \left(\frac{1}{AM} - \frac{1}{BM} - \frac{1}{AN} + \frac{1}{BN} \right) \quad \text{Eqn 3.6}$$

Re-arranging eqn 3.6, resistivity can be expressed by

$$\rho_a = \frac{V}{I} \left(\frac{2\pi}{\frac{1}{AM} - \frac{1}{BM} - \frac{1}{AN} + \frac{1}{BN}} \right) \quad \text{Eqn 3.7}$$

The factor

$$K = \frac{2\pi}{\left(\frac{1}{AM} - \frac{1}{BM} - \frac{1}{AN} + \frac{1}{BN} \right)}$$

is the geometrical factor, K, of the electrode configuration. Thus,

$$\rho_a = \frac{V}{I} K \quad \text{Eqn 3.8}$$

whereas

$$K = \frac{\left(\frac{AB}{2} \right)^2 - \left(\frac{MN}{2} \right)^2}{MN} \quad \text{Eqn 3.9}$$

for the symmetrical Schlumberger array used in this project (Fig 3.1)

and

$$\rho_a = \text{apparent resistivity.}$$

Hence, after recording the measured V/I (read off from the instrument) the corresponding apparent resistivity values were calculated by multiplying these measurements with the pre-calculated geometric factor K using eqn 3.9 above.

The apparent resistivity values were then plotted against $AB/2$ readings on a bi-logarithmic graph paper of the same modulus as the master curves (62.5 mm). The plotting was done before the current electrode operators moved to the next spacing. This served as a counter-checking method whenever the current electrodes were wrongly positioned giving spurious results.

The bi - log presentation of resistivity data ensured that a wide range of resistivity values were plotted in the field and enhanced both the variations in thickness and low resistivity values at shallow depths. Further, the use of these graph papers permitted the preservation of the shape of both the field curves and the theoretically computed curves. However, it proved difficult to distinguish between layers with low resistivity contrast at great depths.

All the soundings were done up to $AB/2$ spacing of 250 m. Sometimes obstructions such as houses, very thick bushes and cattle fences could not allow the soundings to be expanded to the required spread. However, this occurred at only a few sites.

A good number of the soundings were made at/near existing boreholes. This was intended to calibrate the boreholes by using resistivity sounding measurements obtained thus, rendering the survey more credible and reliable.

3.1.1.3 Choice of the Method

The Schlumberger array used in this investigation was chosen mainly due to its several advantages over the other commonly used arrays. Firstly, it must be emphasized that it was absolutely necessary that as much data be collected as quickly as possible due to the limited time and funds available for the project. Therefore, by using Schlumberger array, considerable time was saved since the potential electrodes M and N were moved only a few times in a single sounding. Besides, the manpower required was only minimal compared with the other commonly used Wenner array where all the four electrodes are moved between each movement.

The depth to which the probing was aimed at was only 250 m. This is what the author considered to be economical depth as far as drilling and extraction of groundwater for domestic purposes is concerned since drilling is generally an expensive exercise; more so if deep boreholes are considered. With Schlumberger array, even deeper soundings could have been possible since the two current electrodes could be expanded up to 750 m. In any case, Schlumberger array has greater probing depth and resolving power than the Wenner array for equal $AB/2$ electrode spacing.

The effects of near surface lateral inhomogeneities are less apt to affect Schlumberger measurements since these inhomogeneities are easily detected as "jumps". Thus, these "jumps" are easily corrected by only smoothing the curve.

Usually drifting or unstable potential difference is created upon driving two metal stakes/electrodes into the ground, a situation less encountered with Schlumberger array than with the Wenner array (Zohdy, et. al., 1980). Besides, Keller, et. al., (1966) add that any stray current in industrial areas and telluric current that are measured with long spreads affect measurements made with Wenner array more readily than those made with the Schlumberger array.

3.1.1.4 Field Limitations and Data Quality

During the course of this sounding survey, a few problems were encountered. These problems could therefore, affect the quality of the data. Initially, a major problem was with the personnel. They were not used to the procedure and a lot of time was therefore, spent on teaching them. This rendered the process of data collection rather slow and expensive.

A related and frequent problem was lack of walkie-talkie radios which resulted in poor voice communication between the current electrode crew and the recorder at the centre of the array. This generally resulted in wrong electrode measurement especially after $AB/2 = 130$ m, giving rise to "jumps" on the field curves.

Other "jumps" occurred as well due to lateral inhomogeneities in the surface layers. This phenomenon was quite prevalent in areas covered by the unconsolidated Magarini sands. This problem was corrected by shifting the current electrode to a more compact and seemingly homogeneous point/surface thereby improving the electrode/ground contact.

Bad connections at the current electrodes in the instrument were a frequent problem. However, this was easily detected by the instrument. Generally, when the soundings were done during the dry weather in February and March, this was a very persistent problem. It was caused by the ground surface having too high resistances for the selected current. When this happened, all the connections were checked. The current electrodes were hammered deeper into the ground. If the error persisted, then the current was reduced step by step until consistent readings were obtained.

Another problem detectable by the instrument was due to persistent overloading, i.e., signal plus excessive noise. Often this resulted in negative readings especially, when measurements were made on sands. This was corrected by reducing the transmitter current a step at a time till consistent resistivity measurements were obtained.

The high temperatures in this area especially, during February to March, might have affected the SAS 300 B Terrameter readings rendering it less sensitive. Thus, several soundings were so erratic that they could not be interpreted. Indeed, these soundings had to be repeated during the wet season, April to May, and sure enough, very good curves were obtained.

A persistent problem throughout the investigation was that of keeping the profile line straight. The tape measure used could only stretch to a maximum of 50 m. As such, any subsequent measurements were "falsely" centred. Thus, the profile was hardly ever straight, especially after AB/2 spacing of 150 m. A significant error

could, therefore, have occurred in determining the geometrical factor. However, a compass was used to keep the profile as straight as was possible thus reducing this error. This was quite successful despite thick bushes which often necessitated shortening the configurations. Test readings were taken at brief intervals. These (Table 3.1) were gradually increased as pumping continued. After the

Despite these limitations, the vertical electrical soundings (VES) data quality in this project is generally high and fairly reliable. on the rate of rise decreased. A

3.1.2 Well Tests

These well tests were performed in the absence of piezometers or observation wells where the discharge and the water level only in the pumped well were measured. The boreholes in the project area were drilled by using either Percussion Hydrometer or Percussion Rustom Bycyrus rigs. Once the recommended depth was reached, drilling was stopped and the aquifer allowed to attain equilibrium conditions whereby the water level rose until it reached a static level. Afterwards, a reciprocating piston pump was installed and pumping and subsequent development of the test started.

3.1.2.1. Measurements

The performance of the well test comprised regular measurements of depths to the water level and discharge rate of the pumped well. Water level measurements were taken during both the pumping phase and the recovery test.

Time	Water Level (m)
0-10	10.0
10-20	10.0
20-30	10.0
30-40	10.0
40-50	10.0
50-60	10.0
60-70	10.0
70-80	10.0
80-90	10.0
90-100	10.0

3.1.2.1.1. Water Level Measurements

Water level measurements were taken as many times during the course of the test with as much accuracy as possible. Since the water levels were dropping fast during the initial stage of the test, readings were taken at brief intervals. These intervals (Table 3.1) were gradually increased as pumping continued. After the pumping was stopped, the water level in the well started to rise, i.e., recovery test. Initially, the level rose rapidly, but as time went on, the rate of rise decreased. A typical schedule of time intervals for the recovery measurements as used in the test is shown in Table 3.2

Water level measurements were taken by use of an electric dipper (Plate II). This comprised a double electric wire with two electrodes at the lower end attached to a calibrated steel tape. The upper ends of the wire were connected to a battery and an indicator. When the tape was lowered into the well and the electrodes touched the water, an electric circuit closed. This was shown by the indicator. The depth to the water level was then read off directly from the tape.

A normal chronometer was used to record each instant the water level was taken.

Table 3.1 Range of time Intervals between water level measurements in the pumped well during the pumping phase

Time since pumping started (minutes)	Time Intervals (minutes)
0-10	1
10-20	2
20-40	5
40-90	10
90-180	15
180-pump shutdown	30

Table 3.2 Range of Time Intervals between water level measurements in the pumped well during the Recovery Test

Time since pumping started (minutes)	Time Intervals (minutes)
0-5	1
5-10	2
10-60	5
60-120	15
120-180	30
180-720	60
720-end of test	120

3.1.2.1.2 Discharge Rate Measurements

As much as possible, the discharge rate was kept constant during the test. It was measured frequently with any variations being recorded and any necessary adjustments made in order to keep it constant. At the end of the test, an average discharge rate was calculated.

Several methods of measuring the discharge rate for a pumping well exist (Driscoll, 1986; Groundwater Manual, 1981; Hazel, 1975). For the purposes of this study and owing to the unavailability of the other methods, a 220-litre drum was used. Often a 110 litre drum was also used. This was considered a simple and fairly accurate method. All that was done was to measure the time taken to fill the container.

3.1.2.2. Duration of the Test

The question of how long a pumping test should last is difficult to answer because the period of pumping essentially depends on the type of aquifer and the degree of accuracy desired in establishing its hydraulic characteristics. Better and more

reliable data are obtained if pumping continues until the cone of depression



Plate II Electric Dipper used for Water Level Measurements

stabilizes and does not seem to be expanding further as pumping continues. It is for this reason that the pumping was done until there was hardly any significant change in the water levels for the last three hours. This was exemplified by the drawdown remaining constant for that duration.

Hazel (1975), in Table 3.3, gives the duration for which various tests should be done. This, however, depends on the purposes for which the water is required. Generally, for livestock and domestic purposes, pumping tests should be done for between four to six hours. For this study, a pumping period of between six to eight hours was considered appropriate and adequate. In some instances, pumping

was done up to fourteen hours. Rarely was it done for twenty four hours.

Table 3.3 Desired type and duration of pumping test programme on various types of Boreholes. (After Hazel,1975)

Type of Borehole	Type and Duration of Test
Livestock and Domestic	Constant Discharge or Constant Drawdown (4-6 hrs)
Irrigation	Constant Discharge (24 hrs) with optional steps in closing stages
Town water supply and Industrial	As for irrigation boreholes but duration for a 100 hrs duration

3.1.2.3 Field Limitations of the Test and Data Quality

The hydraulic data collected during the well pumping test was possibly affected by any one of the following :-

- (i) During the pumping test, the vibrations caused by the pump affected the tape. Consequently the accuracy of the water level measurements was not as high as desired.
- (ii) The initial drawdown was influenced by an additional loss in the hydraulic head due to turbulent flow conditions in or immediately around the well; this means that the discharge, Q , was from the water stored in the borehole (before pumping) and not from the aquifer itself.
- (iii) The clearance between the draw pipe and the outside casing was not large enough to let through the electric dipper. This resulted in abandoning measuring the water level in boreholes where this problem persisted.

(iv) Occasionally a pump operator would increase its speed during the test. This affected the discharge rate thereby violating the principle upon which this method is based-the constancy of the discharge rate throughout the test.

However, since the recovery data was collected after pumping was stopped, the above limitations were eliminated to a great extent. This rendered these data more reliable and of relatively good quality.

3.1.3 Water Sampling Operations

In order to determine the quality of the water in the project area, it was necessary to collect some samples from the boreholes for chemical analysis. Eighteen boreholes were randomly selected from the project area. It was anticipated that these boreholes provided representative samples for analysis.

The water samples were collected from the selected boreholes in clean half litre plastic bottles. These bottles had screw cap stoppers to prevent leakage during transportation were initially cleaned with metal free nitric acid and then rinsed several times with distilled water. Each bottle was again rinsed thoroughly with the water about to be sampled from the borehole. These samples were taken after the water was allowed to flow after pumping for some time. This was to ensure that the sample collected was as representative as possible of the borehole source.

The parameters which required immediate determination such as specific conductivity and pH were determined in the field. Specific conductivity was measured by using an Electrolytic Conductivity, Measuring set, Model MC-1, Mark V. It was recorded in microsiemen/cm. The pH was measured by using a pH meter. To preserve the samples for later analysis of other parameters, about 5 millilitres of nitric acid was added to the sample bottles. This ensured that the samples could be analyzed much later without necessarily showing any significant changes in the concentration of the parameters to be determined.

Qualitative Analysis

The samples were analyzed for the presence of various ions in the field. The classification of the samples was on the basis of the results of the field analysis. A classification of the results was also done in the laboratory.

The four possible types of sections which are referred to as H, K, N, and Q are used to describe the relative positions of the various elements $P_1, P_2,$ and P_3 and their linear geometric relations with the elements $S_1, S_2,$ and S_3 .

The four possible type types resulting from the explanations of the values of $P_1, P_2,$ and P_3 are:

- 1. H-Type where $P_1 > P_2 > P_3$ referred to as H-Type section,
- 2. K-Type where $P_1 < P_2 > P_3$ referred to as K-Type section,
- 3. N-Type where $P_2 < P_1 < P_3$ referred to as N-Type section,
- 4. Q-Type where $P_1 > P_3 > P_2$ referred to as Q-Type section,

(as in Fig. 4.1.18).

CHAPTER 4

DATA ANALYSIS

4.1 Resistivity Data Analysis

In order to acquire as much information as possible about the nature of the subsurface in the project area, resistivity data were analyzed both qualitatively as well as quantitatively. According to Zohdy, et. al., (1980), qualitative analysis should always precede the quantitative one for electrical sounding.

4.1.1 Qualitative Analysis

The first step in this analysis was to classify the observed apparent resistivity curves into types. This classification was primarily made on the basis of the shapes of the electrical sounding curves. A correlation of this classification with the area's geology was attempted.

Zohdy, et. al., (1980) have given a method in which letters H, A, K, and Q are generally used to describe the relation between the various resistivities ρ_1 , ρ_2 , and ρ_3 in a three-layer geoelectric section which has thicknesses h_1 , h_2 , and h_3 respectively. The four possible type curves resulting from the combinations between the values of ρ_1 , ρ_2 and ρ_3 are:-

- (i) Minimum Type where $\rho_1 > \rho_2 < \rho_3$ referred to as H-Type section,
 - (ii) Maximum Type where $\rho_1 < \rho_2 > \rho_3$ referred to as K-Type section,
 - (iii) Ascending Type where $\rho_1 < \rho_2 < \rho_3$ referred to as A-Type section,
 - (iv) Descending Type where $\rho_1 > \rho_2 > \rho_3$ referred to as Q-Type section,
- as illustrated in Fig 4.1 (a).

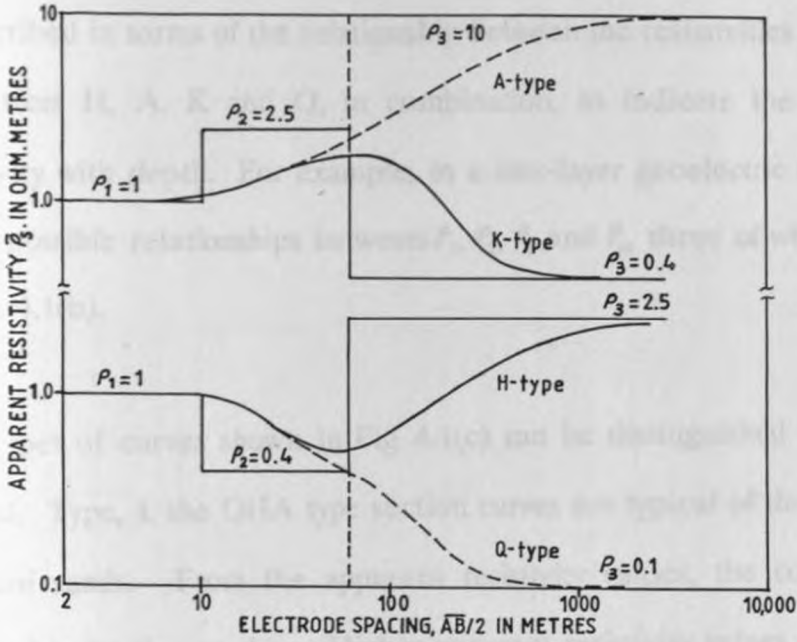


Fig 4.1(a) Examples of the four types of three-layer Schlumberger curves for three-layer Earth models

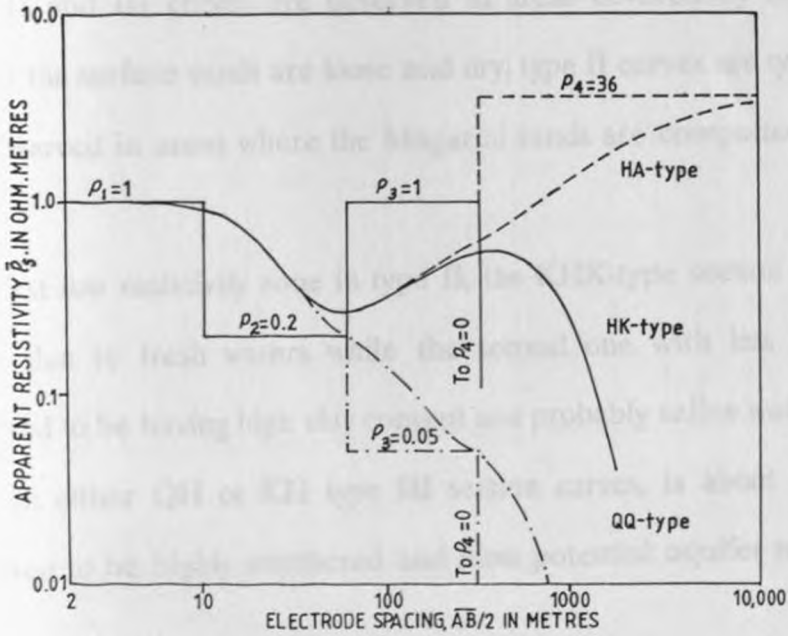


Fig 4.1(b) Examples of three of the eight possible types of Schlumberger curves for four-layer Earth models

If the subsurface is composed of more than three horizontal layers of resistivities $\rho_1, \rho_2, \rho_3, \dots, \rho_n$ and thicknesses $h_1, h_2, h_3, \dots, h_n = \infty$ respectively, the geoelectric section is described in terms of the relationship between the resistivities of the layers, and the letters H, A, K and Q, in combination, to indicate the variation of the resistivity with depth. For example, in a four-layer geoelectric section, there are eight possible relationships between ρ_1, ρ_2, ρ_3 and ρ_4 , three of which are shown in Figure 4.1(b).

Four types of curves shown in Fig 4.1(c) can be distinguished by this analytical method. Type I, the QHA type section curves are typical of the area covered by Kilindini sands. From the apparent resistivity values, the conductive zone is expected to be due to clays. Higher apparent resistivity values of the lower non-conductive layer may be due to coral Limestone. Mwangi (1981) observed that the Kilindini sands inter-finger with the coral limestones.

Type II and III curves are observed in areas covered by the Magarini sands. Where the surface sands are loose and dry, type II curves are typical while type III are observed in areas where the Magarini sands are compacted.

The first low resistivity zone in type II, the KHK-type section curves, is expected to be due to fresh waters while the second one with less than 10 ohm-m is expected to be having high clay content and probably saline water. The conductive zone in either QH or KH type III section curves, is about 100 m deep. It is expected to be highly weathered and most potential aquifer zone.

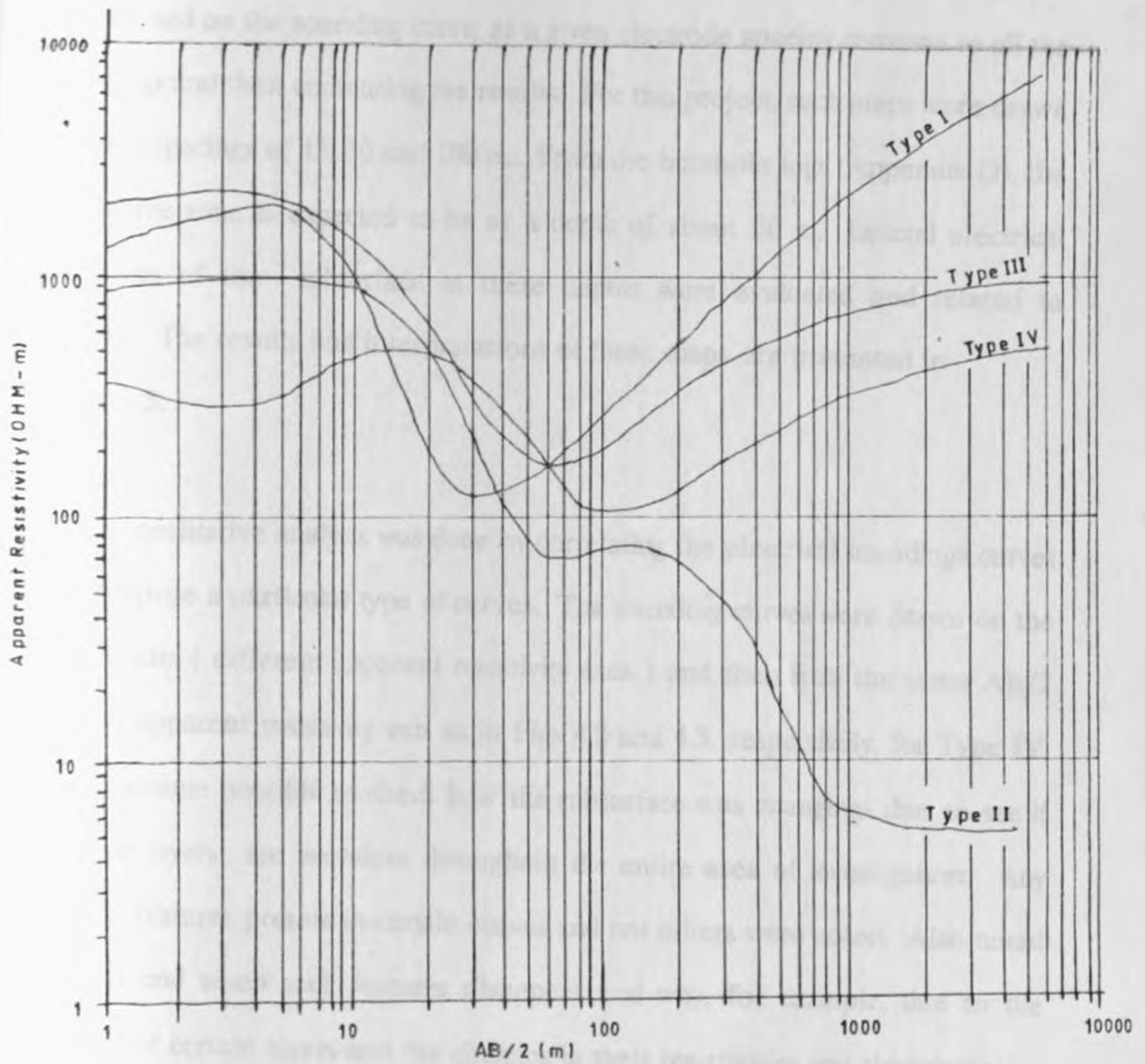


Fig 4.1(c) DOMINANT TYPE OF RESISTIVITY CURVES IN KIDIYANI AREA, KWALE

Type IV, section curves, are observed in areas covered by Mazeras sandstone. Two conductive zones can be discerned. The first shallow one is suspected to be a moist/damp layer just below the surface while the second one is suspected to be a highly weathered aquifer zone. More qualitative analysis involved the preparation of apparent resistivity maps. Zohdy, et. al., (1980) emphasize that each map is prepared by plotting the apparent resistivity values, as registered and smoothed on the sounding curve, at a given electrode spacing common to all the soundings and then contouring the results. For this project, such maps were drawn at AB/2 spacings of 13, 50 and 100 m. From the borehole logs (Appendix D), the conductive zone is expected to be at a depth of about 50 m. Lateral electrical properties of the subsurface at these depths were evaluated and related to geology. The results and interpretations of these maps are presented in Chapter 5.

Further qualitative analysis was done by correlating the electrical soundings curves that comprise a particular type of curves. The sounding curves were drawn on the same X-axis (different apparent resistivity axes) and then with the same AB/2 axis and apparent resistivity axis as in Figs 4.2 and 4.3, respectively, for Type IV. It thus became possible to check how the subsurface was changing- thus to see if the same layers are prevalent throughout the entire area of investigation. Any common features present in certain curves and not others were noted. Also noted is where and when such features disappear and why, for example, due to the presence of certain layers and the changes in their resistivities and thicknesses.

Fig. 4.2: SOUNDING CURVES OF TRAVEL B-E DRAWN ON THE SAME X-AXIS.

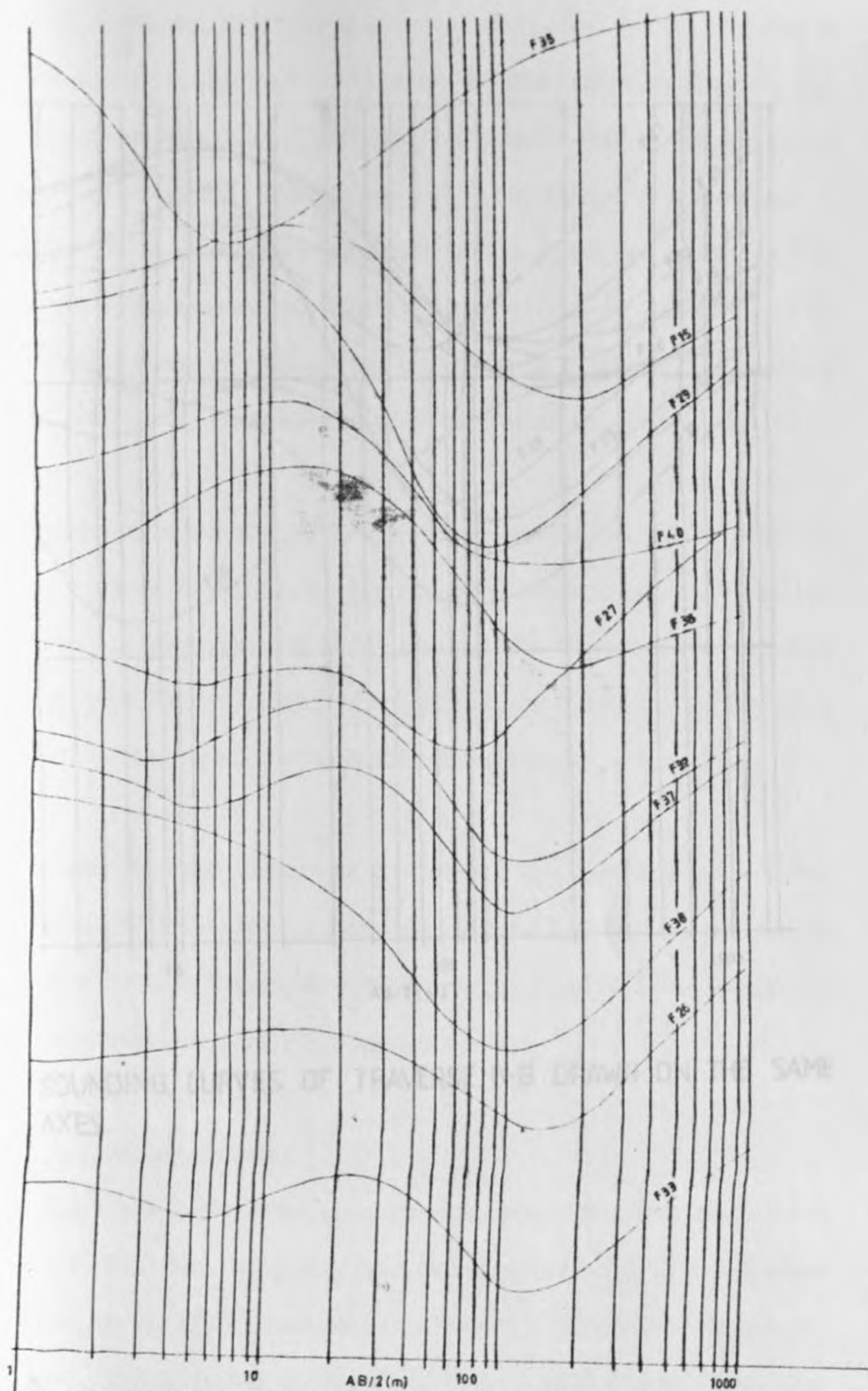


Fig. 4.2: SOUNDING CURVES OF TRAVERSE B-B' DRAWN ON THE SAME X-AXIS.

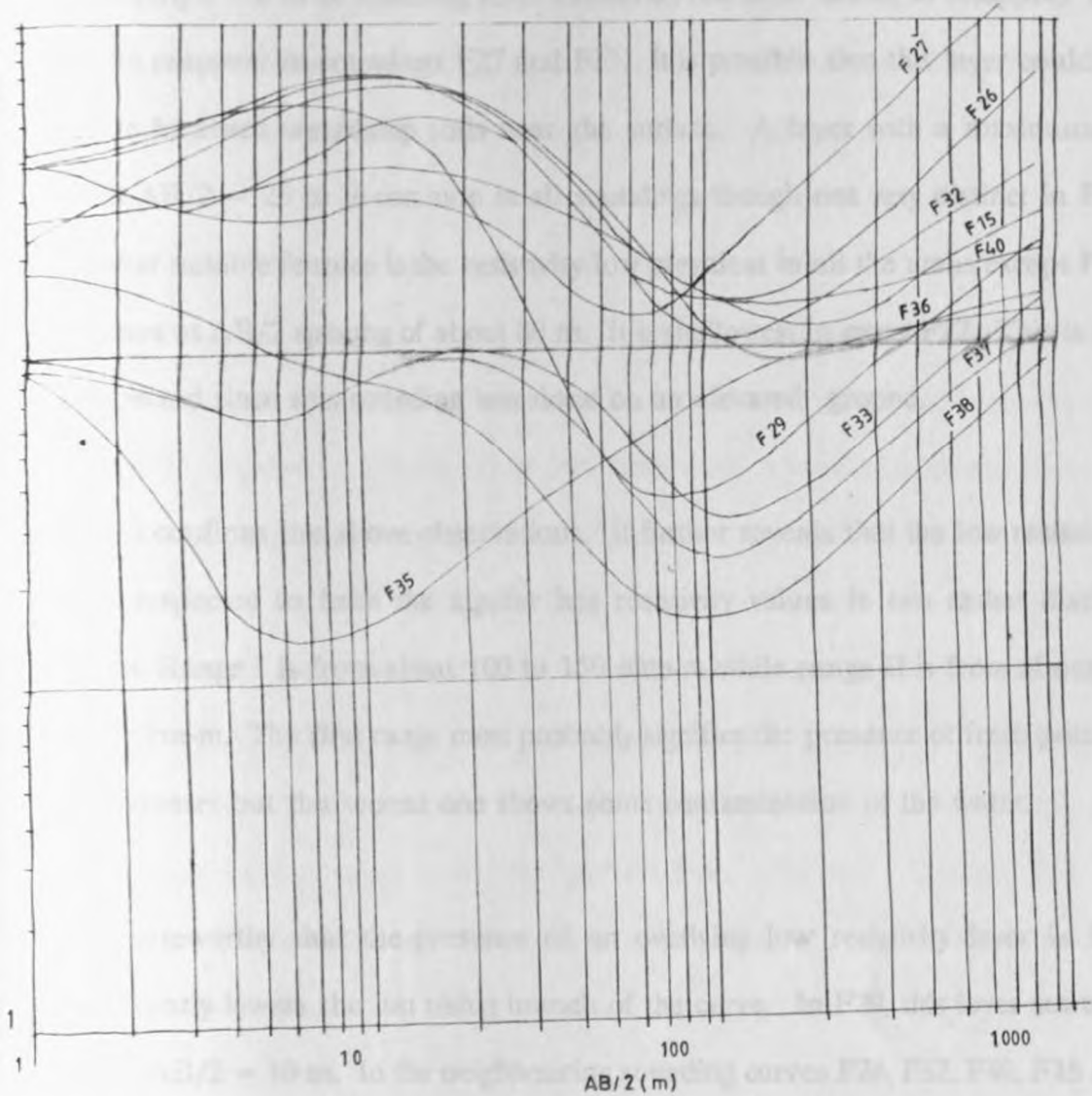


Fig. 4.3 SOUNDING CURVES OF TRAVERSE B-B' DRAWN ON THE SAME AXES.

Quantitative Analysis

which was applied for quantitative analysis of the electrical sounding curves. The methods have extensively been discussed by Mariani (1951), Kozford (1952), et al. (1955), Keller and Frischmeyer (1966, 1971), Mathews and (1965), Dobry (1970), Kaufman and Keller (1983), Morris (1984), and

From Fig 4.2, it appears that there is a low resistivity layer with a minimum at about $AB/2 = 6$ m in sounding F35. However, this layer seems to disappear and only to reappear in soundings F27 and F33. It is possible that this layer could be due to localised wet/damp soils near the surface. A layer with a maximum at about $AB/2 = 25$ m is common in all soundings though not very distinct in F38. Another notable feature is the resistivity low prevalent in all the areas except F35. It occurs at $AB/2$ spacing of about 80 m. It is shallowest in curve F27. This is not unexpected since this sounding was done on an elevated ground.

Fig 4.3 confirms the above observations. It further reveals that the low resistivity layer suspected to form the aquifer has resistivity values in two rather distinct ranges. Range I is from about 100 to 150 ohm-m while range II is from about 20 to 35 ohm-m. The first range most probably signifies the presence of fresh potable groundwater but the second one shows some contamination of the water.

It is noteworthy that the presence of an overlying low resistivity layer in F29 significantly lowers the last rising branch of the curve. In F29, this layer starts at about $AB/2 = 10$ m. In the neighbouring sounding curves F26, F32, F40, F15 and F36, this layer begins at about $AB/2$ spacing of 30 m.

4.1.2 Quantitative Analysis

Several methods are employed for quantitative analysis of the electrical sounding data. These methods have adequately been discussed by Mwangi (1981), Koefoed (1979), Zohdy, et. al.,(1980), Keller and Frischknecht (1966, 1970), Mathies and Huyot (1966), Dobrin (1976), Kaufman and Keller (1983), Morris (1964), Van

Dam and Menlenkamp (1968) and many others. In this project, electrical sounding data were quantitatively analyzed by using the methods of curve matching and computer model curve generating. Quantitative analysis involved the determination of the layer parameters namely, thickness and resistivity values.

4.1.2.1 Curve Matching and Auxiliary Point Method

The field curves exhibited the presence of at least four layers. For the initial approximation of these layer parameters, theoretical curves for a single overburden and auxiliary graphs (Bhattacharya and Patra, 1968) were employed. This was supplemented by three-layer Rijkswaterstaat's (1980) standard graphs.

A detailed description of the auxiliary method is not necessary as several authors (Cagniard, 1952; Koefoed, 1960; Homilius and Mundry, 1979; Orellana and Mooney, 1966) have presented the basic principles of this method. It is worth noting that, by this method, the determined layer thickness (Zohdy, 1965) is usually greater than the true thickness by a factor of ρ_v / ρ_h , where ρ_v is the vertical resistivity and ρ_h the horizontal resistivity of the layer.

4.1.2.1.1 Disadvantages of this Analytical Method

The application of a combination of curve matching and auxiliary point as an analytical technique has the following disadvantages :-

- (i) the method only yields approximate and often wild layer parameters which may be geologically ambiguous,
- (ii) usually most of the available standard curves are only up to three layers. This, therefore, inhibits their application in interpretation especially if the

curve has more layers. Besides one may lack a suitably matching master curve from the available catalogues,

- (iii) for the application of this method, it must be ascertained that each layer has a considerable effect on the field curve, otherwise a layer without such an effect may not be noticed in the subsurface,
- (iv) the method is tedious and time consuming.

Despite the above limitations, curve matching and auxiliary point method still remains a valuable tool of interpretation, especially in and during the field work. When used correctly, it can provide reliable results. However, the availability of computer programs is rendering this method almost obsolete.

4.1.2.2 Computer Model Curve Generating Method

Generally the interpretations by the curve matching method were useful as they provided the initial model parameters for the computer program. These parameters were, however, changed until a suitable best fit was obtained. The changing of the layer parameters was done by non-automatic iterative method. This method involved changing the parameters by personal judgement based mainly on the operator's experience. More often than not, some guess work was involved. The choice of the changes that had to be applied in the value of a layer parameter involves two steps. The first of these determined which layer was to be changed in order to eliminate error in a given section of the curve; the second concerned the amount by which the value of the layer parameter had to be changed. This, however, was not an easy process especially because several permutations of resistivity and thickness parameters were involved for each layer.

For this project, computer model curve generation of the electrical soundings was quantitatively analyzed by using a Vertical Electrical Sounding (VES) program. This program was coded on the basis of Ghosh's convolution method using inverse O'Neill filters (O'Neill, 1975). An IBM compatible Olivetti M24 micro-computer was used. Generally this program provided the data-base for the geo-electrical sounding data calculated the apparent resistivity curve with O'Neill filter coefficients and plotted these curves. This filter is for a sampling distance of a sixth of a decade. It generally took 16-20 seconds to plot one such a curve. The computer model curves generated are presented in Appendix B.

4.1.2.2.1 Advantages of this Method

Computer curve generating method provided several advantages over that of curve matching; the most obvious one being that the interpretation was faster and more reliable. From literature, field observations and experience, it may be highly acceptable that the computer interpretation method gives higher accuracy than the traditional methods.

The other advantage of the computer model curve generating method was that the layer parameters, particularly resistivity, could be specified more clearly while the other parameters were adjusted such that reasonable and desirable fits to the field curves were produced. For example, if the resistivity of a layer could be determined more reliably in one field curve, the same value could be used in other field curves in the same profile provided there was evidence that the same layer existed. This, however, could only be true if the assumption that the resistivity of a layer does not change so abruptly along a given profile held. Gradual variations

might have been detected only where the layer was thick enough. The sensitivity of this method of analysis seemed to diminish with depth.

4.1.2.2.2 Limitation(s) of Computer Modelling Method

Even though the interpretation of resistivity data by use of a computer modelling was considered to be more accurate and faster than the traditional curve matching method, it nonetheless, had some limitations.

The most serious limitation, especially to the particular VES program applied in this project, is its inability to give the percentage error on the final computed curves. This means that a "good fit" to the field data does not necessarily indicate an accurate determination of the layer parameters. It was, therefore, necessary to check the interpreted results against the drilling results obtained from nearby boreholes.

The other minor limitation was the declining of the resolution especially at greater depths. This could be associated with the decrease in the current penetration to the deeper layers such that the apparent resistivity measured at large current electrode spacings are only representative of resistivity structures at shallower depths.

4.1.2.3 Limitations of the Two Applied Analytical Methods

During the analysis by both curve matching and auxiliary point and computer model curve generating methods, two limitations which often reduced the reliability of the interpretations were experienced. One was the principle of suppression

while the other was the principle of equivalence.

Electrical potential at the ground surface does not depend on the absolute values of resistivity (ρ) and thickness (h) of the layer, but by the ratio of its thickness to resistivity when the thickness and resistivity of the intermediate layer are considerably smaller than those of the layers above and below it, and the product of the thickness and resistivity if the thickness of the intermediate layer is small and the resistivity large compared with the values of the layers above and below it (Njau, 1981; Brown, et. al., 1972). These are the principles of equivalence by longitudinal conductance (S) and transverse resistance (T_r), respectively, (Zohdy, et. al., 1980; Koefoed, 1979).

Computer model curve generating method provided yet another advantage over curve-matching while investigating the principle of suppression. If there was evidence of the existence of a layer whose effects have been suppressed in the field curve, its layer parameters could be extrapolated from the interpretations of the neighbouring curves and a satisfactorily fitting curve generated. For example, F20 had initially been interpreted as a four-layer KH-type curve. However, from F16 nearby within the same geological formation, it became apparent that another intermediate layer exists. Its layer parameters were deduced to be 65 m and 350 ohm-m. When these parameters were fixed in the F20 curve, no significant shift was observed. Upon little adjustment by non-automatic iterative method, the layer parameters were changed to 55 m and 500 ohm-m. This, therefore, proved the existence of such a layer.

Field curve F35 has been used to illustrate the principle of equivalence by longitudinal conductance (S). The low resistivity layer had its parameters changed such that the ratio $h/\rho = 0.6$ remained constant. Three acceptable curves are shown in Fig 4.4 while Table 4.1 summarises the layer parameters for three curves. From the well logs correlation analysis, curve "c" was the most acceptable one.

Equivalence by transverse resistance (T.) was illustrated by using the field curve F40. Initial curve "a" had its parameters altered in such a manner that the product $h \times \rho = 8976$ for the high resistivity layer remained constant. This resulted in two other equivalent and acceptable curves "b" and "c" shown in Fig 4.5. The summary of the layer parameters is tabulated in Table 4.2

Table 4.1 Layer parameters of three Equivalent model curves by Longitudinal Conductance (S) for F35

LAYER	1	2	3	4
MODEL				
a	$h = 1$ $\rho = 100$	$h = 8$ $\rho = 13.8$	$h = 11$ $\rho = 40$	$\rho = 110$
b	$h = 1$ $\rho = 100$	$h = 7.5$ $\rho = 12.5$	$h = 11.5$ $\rho = 40$	$\rho = 110$
c	$h = 1$ $\rho = 100$	$h = 6$ $\rho = 10$	$h = 13$ $\rho = 40$	$\rho = 110$

h = thickness (m)
 ρ = resistivity (ohm-m)

Due to these two principle limitations, different layer resistivity structures could be produced by the same sounding graph as illustrated above. Therefore, to obtain true resistivities and thicknesses in terms of the subsurface hydrogeological

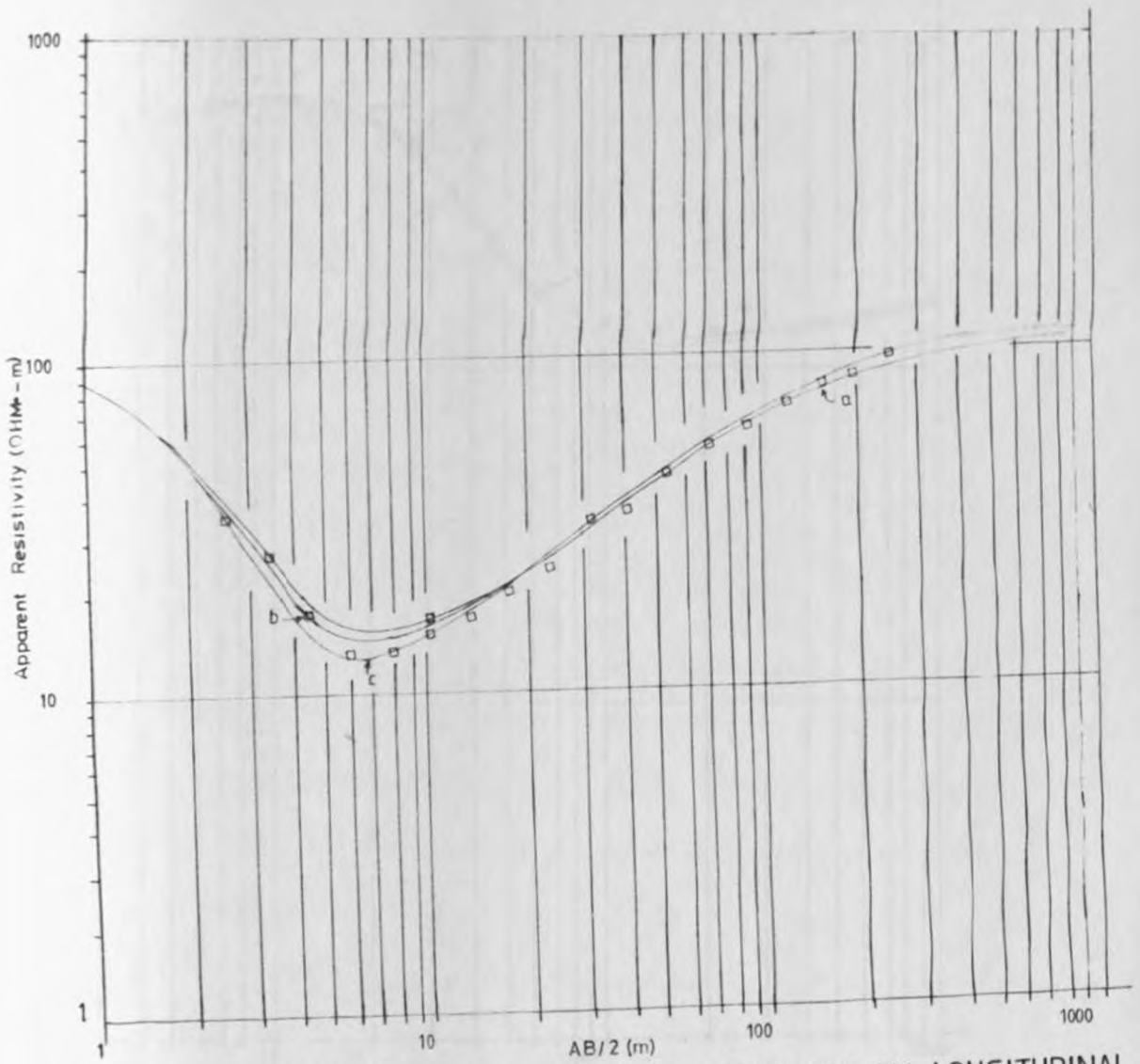


Fig. 4.4 MODELLED CURVES SHOWING EQUIVALENCE BY LONGITUDINAL CONDUCTANCE (S) OF F35.

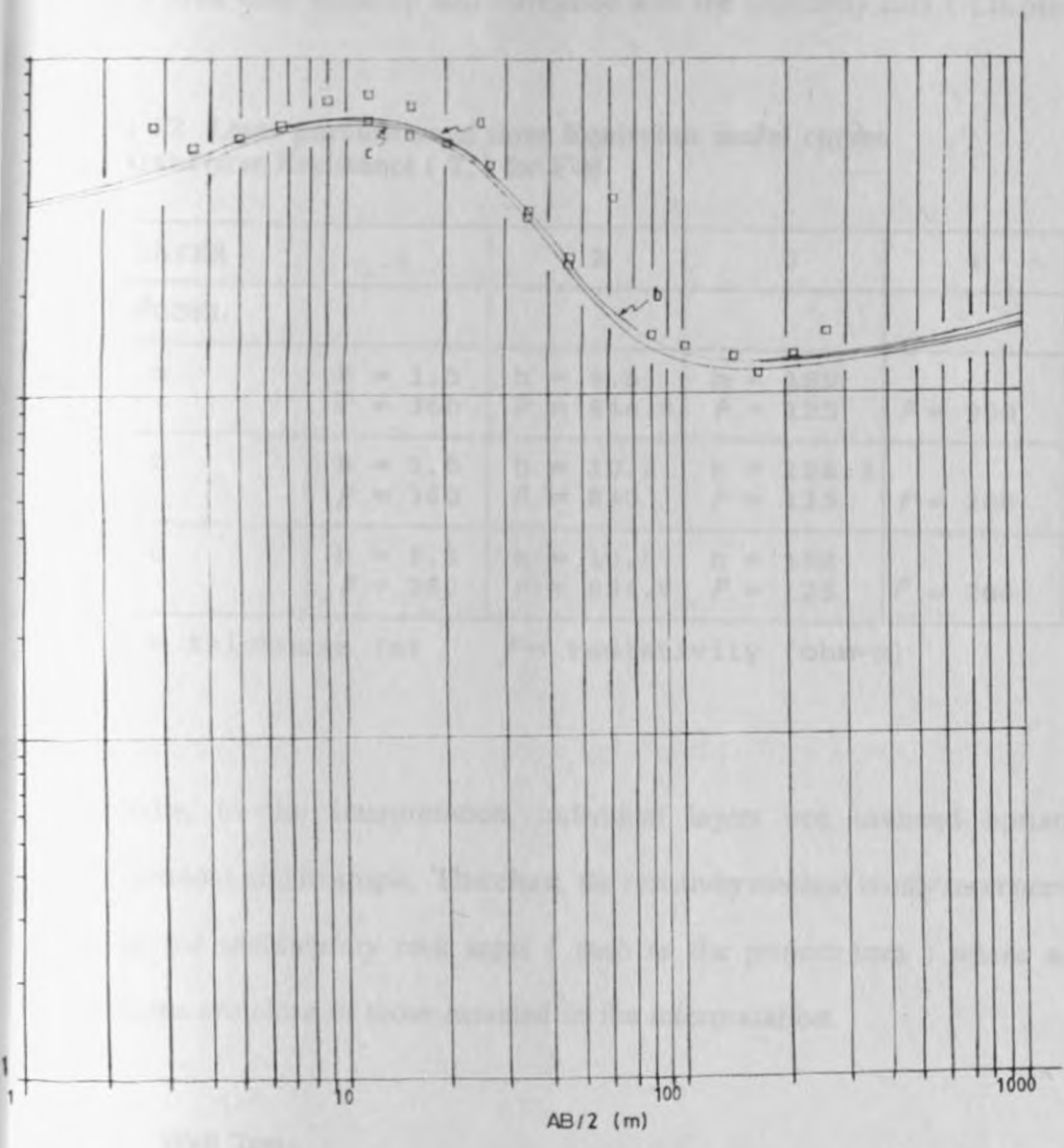


Fig. 4.5 MODELLED CURVES SHOWING EQUIVALENCE BY TRANSVERSE RESISTANCE (T) OF F40.

conditions, supplementary data such as those from logged boreholes within the project area were required and correlated with the resistivity data (Chapter 5).

Table 4.2 Layer parameters of three Equivalent model curves by Transverse Resistance (T_r) for F40

LAYER	1	2	3	4
MODEL				
a	$h = 1.5$ $\rho = 360$	$h = 9.5$ $\rho = 944.8$	$h = 189$ $\rho = 125$	$\rho = 200$
b	$h = 1.5$ $\rho = 360$	$h = 10.2$ $\rho = 880$	$h = 188.3$ $\rho = 125$	$\rho = 200$
c	$h = 1.5$ $\rho = 360$	$h = 10.5$ $\rho = 854.9$	$h = 188$ $\rho = 125$	$\rho = 200$

h = thickness (m) ρ = resistivity (ohm-m)

Generally, in the interpretation, individual layers are assumed horizontal, homogeneous and isotropic. Therefore, the resistivity method is only most accurate enough for sedimentary rock areas (such as the project area) where actual conditions are close to those assumed in the interpretation.

4.2 Well Tests

4.2.1 General Principles

Generally, the method applied for the analysis of the well test data is based on the basic analytical well flow equation first described by Theis (1935). This method is based on the following highly idealised assumptions and conditions:

- (i) the aquifer system has a seemingly infinite areal extent,
- (ii) the aquifer system is homogeneous, isotopic and of uniform

thickness over the area influenced by the test,

- (iii) prior to pumping, the hydraulic head is nearly horizontal over the area influenced by the test,
- (iv) the aquifer is pumped at a constant discharge rate,
- (v) the well penetrates the entire thickness of the aquifer and thus receives water by horizontal flow,
- (vi) the aquifer system can be treated as confined,
- (vii) the flow of the well is unsteady.

Equation 4.1 relates the drawdown (S_d) as observed in an observation well at a distance (r) from the pumped well, to the rate of discharge, Q ,

$$S_d = \frac{Q}{4\pi T} \int_u^{\infty} \frac{e^{-u}}{U} du \quad (\text{Eqn 4.1})$$

where U is defined as

$$U = \frac{r^2 S}{4 T t} \quad \text{Eqn 4.2}$$

where T = Transmissivity,

t = Time since pumping started,

r = Distance from the pumping borehole,

S = Storativity.

The integral in equation 4.1, called the exponential integral, is known as the *well function*, $W(U)$ (Freeze and Cherry, 1979). Hence, equation 4.1 becomes

$$S_d = \frac{Q}{4\pi T} \int_u^{\infty} \frac{e^{-u}}{U} du = \frac{Q}{4\pi T} W(U) \quad \text{Eqn 4.3}$$

However, the well function, $W(U)$, in equations 4.1 and 4.2 can be represented by an infinite series

$$\int_u^{\infty} \frac{e^{-u}}{U} du = W(U) = -0.5772 - \ln U + U - \frac{U^2}{2 \cdot 2!} + \frac{U^3}{3 \cdot 3!} + \dots \quad \text{Eqn 4.4}$$

Thus, This solution becomes

$$S_d = \frac{Q}{4\pi T} \left(-0.5772 - \ln U + U - \frac{U^2}{2 \cdot 2!} + \frac{U^3}{3 \cdot 3!} \right) \quad \text{Eqn 4.5}$$

From equation 4.2, it is evident that U decreases as time (t) of pumping increases and the distance (r) of the well decreases. Accordingly, Jacob (1963) provided a logarithmic approximation method, where for small values of drawdown observations made in the vicinity of the well after sufficient time of pumping has passed, the well function converges towards the sum of its first two terms. Therefore, for small values of U ($U < 0.01$), the drawdown can be approximated by

$$S_d = \frac{Q}{4\pi T} (-0.5772 - \ln U) \quad \text{Eqn 4.6}$$

Subsuming the numerical constant into the logarithmic terms and replacing the natural logarithm by the decimal logarithm, eqn 4.2 yields, if

$U < 0.01$,

$$S_d = \frac{2.303}{4\pi T} Q \log_{10} \frac{2.25 T t}{r^2 S} \quad \text{Eqn 4.7}$$

where Q = discharge rate

T = transmissivity

S = storativity

t = time since pump was started

S_d = drawdown

r = distance from pumped well

Equation 4.7 above is the Jacob's modified approximation method.

4.2.2 Recovery Test

In this project, Jacobs approximation method was utilized for the evaluation of the well characteristics by using data from the recovery test (Fig 4.6) of a single borehole. For this test, stoppage of pumping is represented mathematically by the assumption that the borehole continues to be pumped indefinitely at a constant rate and that, from a time of stoppage onwards, injection of water is carried out into the same borehole at an equal rate, so that the net pumpage from this moment is zero.

Equation 4.7 gives the drawdown due to pumping while the drawdown due to injection is given in the following expression:

$$S_d = -\frac{2.303}{4\pi T} Q \log_{10} \frac{2.25Tt'}{r^2 S} \quad \text{Eqn 4.8}$$

where t' = time since injection started

and $t' < t$

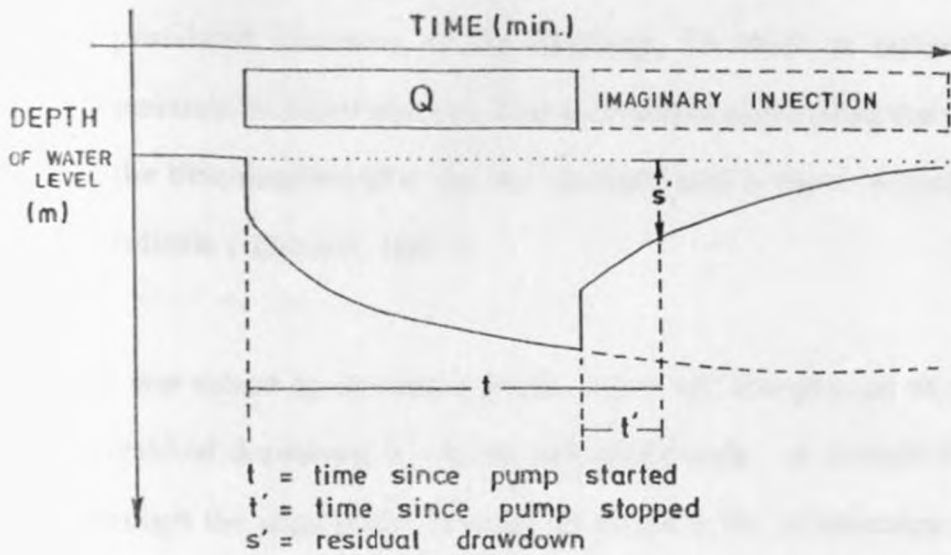


Fig 4.6 Single Borehole Recovery Test

By addition of equations 4.7 and 4.8, the residual drawdown, S_r , is given by

$$S_r = \frac{2.303}{4\pi T} Q \log_{10} \frac{t}{t'} \quad \text{Eqn 4.9}$$

This equation 4.9 has also been given by Bouwer (1978).

4.2.2.1 Advantages of Using Recovery Test Data

Recovery test data were preferred for use in the aquifer analysis to the pumping ones for the following reasons:-

- (i) during the recovery test, water level measurements were taken without being affected by the pumping vibrations noise,
- (ii) water level measurements were also not affected by momentary variations of the pumping rate as the personnel were well conversant with the measuring techniques,
- (iii) there was no need to correct the observed drawdown data for the well losses,

- (iv) usually in a pumping borehole the drawdown is very sensitive to the postulated constancy of the discharge, Q which is rather difficult to maintain in actual practice. This was unnecessary during the recovery test,
- (v) the time-recovery plot for the pumped well is more accurate and reliable (Driscoll, 1986).

Eqn 4.7 was solved by drawing a graph where t/t' was plotted on the log scale against residual drawdown, S_r , on the arithmetic scale. A straight line was then fitted through the data points in order to establish the relationship between the residual drawdown and the ratio t/t' . The slope ΔS_r , of this line was found to be:

$$\Delta S_r = \frac{2.303}{4\pi T} Q \tag{Eqn 4.10}$$

Thus, by rearranging Eqn 4.10, T can be calculated as shown below:-

$$T = \frac{2.303}{4\pi \Delta S_r} Q \tag{Eqn 4.11}$$

$$T = \frac{0.183Q}{\Delta S_r} \tag{Eqn 4.12}$$

where,

S_r is the change in residual drawdown over one log cycle t/t' .

Only well test data from three boreholes (nos. 6673, 6721, and 7097) within the Magarini sands and five boreholes (nos. 7087, 7090, 7267, 7934, and 8221) drilled

within the Mazeras sandstones (Appendix C) were used. This is because of the fact that during the pumping test of these boreholes, the discharge rates were well controlled and were not as adversely affected like in the other cases. Thus, the results are fairly reliable for these boreholes. The specific capacity was calculated by noting the final drawdown in the pumped well and multiplying its reciprocal with the discharge rate of a given borehole.

A summary of the hydraulic aquifer characteristics of some representative wells/boreholes in the project area is presented in Table 4.3.

4.3 Water Quality

Various analytical techniques were used to determine the concentration of various parameters that were required to determine the quality of the water collected from the boreholes in various geological formations. These parameters included total dissolved solids (TDS), dominant anions such as the bicarbonates/carbonates, sulphates, chlorides and fluorides and the major cations - sodium, calcium, magnesium, potassium, silicon and iron.

The choice of the analytical techniques was influenced by the standard of accuracy and precision required. According to Gaciri (1980), accuracy and precision are influenced by the concentration of the elements sought both in absolute terms and in relation to the other constituents of the sample.

For the analysis of dominant cations, Varian Techtron Atomic Absorption Spectroscopy machine, model AA6, was used with different detection limits

Table 4.3 Aquifer Characteristics in Magarini sands and Mazeras sandstones Formation in Kidiani Area, Kwale.

1 AQUIFER	2 B/H No C	3 Total Depth (m)	4 WSL (m)	5 WRL (m)	6 Q m ³ /hr	7 T m ² /hr	8 Total Drawdown s, (m)	9 Q/S m ² /hr
MAGARINI SANDS	6673	50.0	43.0	12.6	3.3	0.196	10.43	0.316
	6721	40.0	24.0	0.8	3.3	0.209	9.92	0.333
	7097	70.0	50.0	20.0	3.2	0.233	17.99	0.178
MAZERAS SANDSTONES	7087	58.0	36.0	27.4	2.80	0.043	24.34	0.115
	7090	61.0	47.0	23.7	2.93	0.062	25.30	0.116
	7267	54.0	33.0	17.9	2.84	-	31.10	0.091
	7934	70.0	22.3	15.1	1.20	0.026	20.75	0.058
	8221	40.0	18.0	7.4	1.16	-	9.29	0.125

NOTES:

- Value not calculated
- 1 Type of Aquifer Formation
- 2 Identifying serial number
- 3 Total depth to which the borehole was drilled
- 4 Water struck level: level in borehole at which water was encountered (in metres below ground level)
- 5 Water rest level: level to which water rises in borehole (in metres below ground level)
- 6 Tested yield at commissioning pumping test (in m³/hr)
- 7 Transmissivity values calculated using Recovery test method
- 8 Total drawdown: final water level at the end of pumping phase
- 9 Specific Capacity: calculated as Q/S in m²/hr

(Table 4.4) of each element. Before carrying out the above analysis, two standards of each element were used to calibrate the machine. The sources of error(s) during this analysis have adequately been discussed by Maina (1983). This technique was chosen because it relatively lacked interferences (Maina, 1983; Ediger, 1976) and generally required minimum manipulation (Rawlings & Greaves, 1960).

The determination of the anions concentration-sulphates, fluoride, bicarbonates/carbonate and chlorides- was done using the standard procedures described by the Kenya Bureau of Standards (KBS, parts 2 and 5, 1985) for the specifications of drinking water in Kenya.

Table 4.4 Detection Limits of AAS Varian Techtron machine

Element	Wavelength (nm)	DL (PPM)
Ca	422.7	0.0005
K	766.5	0.003
Na	589.0	0.0003
Mg	285.2	0.0003
Si	251.4	0.3
Fe	386.0	0.005

(DL - Detection Limit)

(nm - nanometer)

Total dissolved solids (TDS) in all the samples were determined by evaporating each filtered sample in a weighed platinum/nickel dish on a steam bath. The residue was then dried in an oven to a constant weight at 180° C. The increase in weight over that of the empty dish represents the weight of the total dissolved solids.

For the analysis of the dominant ions in the water samples, trilinear diagram method (Piper, 1944; Maina, 1983; Mailu, 1983) was employed. Various types of water from both the Magarini sands and Mazeras sandstone formations were distinguished.

The distribution of the sampling sites is shown in Fig 3.2. The results of the chemical analysis of the water samples from boreholes in different formations are shown in Table 4.5.

Table 4.5 Chemical Characteristics of Groundwater in Magarini sands and Mazaras sandstones in Kidiani Area, Kwale District Between 1987 - 1989

Sample	Na ppm	K ppm	Ca ppm	Mg ppm	Fe ppm	Si ppm	SO ₄ ppm	F ppm	Cl ppm	HCO ₃ ppm	CO ₃ ppm	TDS ppm	Cond µS/cm	pH	B/H C-
Ms-1	12.0	3.0	3.2	1.9	0	24	7.6	0	40	60	0	73	110	6.0	5556
Ms-2	15.0	4.0	100.0	14.4	0	16	13.6	0.1	20	165	0	217	330	6.8	5559
Ms-3	85.0	10.0	17.6	20.5	0	40	5.0	0.1	224	28	0	443	600	6.3	5764
Ms-4	132.0	13.5	52.8	82.1	0	66.7	39.4	0.1	286	434	0	882	1300	7.1	6673
Ms-5	10.5	1.5	1.6	3.8	0	26.7	3.5	0.1	28	10	0	49	85	6.9	7268
Ms-6	60.0	9.0	21.6	18.8	0	30	15.0	0	42	172	0	253	320	8.0	7361
Ms-7	21.0	2.0	2.4	2.4	0	20	5.3	0.1	15	35	0	80	123	6.7	7362
Ms-8	45.0	5.5	10.4	10.1	0	100	70.0	0.8	40	124	0	200	300	6.9	7610
Mzs-1	123.0	10.0	42.4	22.6	0	60.0	33.8	0.1	92	372	0	512	700	7.3	6672
Mzs-2	11.5	4.0	1.6	3.4	0	40.0	5.1	0	28	22	0	50	80	7.0	7088
Mzs-3	70.0	4.0	9.6	16.3	0	80.0	28.0	0.2	32	92	0	264	290	7.2	7270
Mzs-4	80.0	10.0	26.4	7.2	0	40.0	30.0	0.1	81	280	0	471	650	7.6	7280
Mzs-5	73.0	6.0	22.4	37.9	0	50.0	24.0	0.4	54	316	0	474	606	7.1	7281
Mzs-6	30.0	4.5	18.4	11.0	0	40.0	12.0	0.2	34	106	0	176	270	6.5	7283
Mzs-7	67.0	8.0	17.4	15.8	0	50.0	25.0	0.1	68	160	0	284	420	6.5	7594
Mzs-8	22.0	6.0	6.0	8.4	0	40.0	11.0	0.2	38	55	0	115	190	6.9	7932
Mzs-9	53.0	7.5	64.0	24.0	0	60.0	0	0	40	322	0	408	500	8.0	7933
Mzs-10	788.0	150.0	8.0	25.2	0	20.0	0	0.5	1475	985	0	3434	4500	7.8	8218

CHAPTER 5

INTERPRETATION OF RESULTS AND DISCUSSIONS

5.1 General Introduction

As already highlighted in Chapter 4, the analysis comprised three different types of data, namely, resistivity, well test and water quality data. Qualitative analysis of the VES data yielded results which to a certain extent were speculative. As such, quantitative interpretations of the said data in terms of horizontally stratified layers of definite thicknesses and resistivities were necessary. However, this could not be meaningful without control by reliable lithological and hydrogeological information. Consequently, a correlation between VES data and the stratigraphy information from the borehole logs was carried out. Also apparent resistivities presented in form of iso - resistivity maps at various depths have been interpreted related to groundwater flow and groundwater potential distribution. Lateral variation of the electrical properties of the subsurface material at these depths has also been evaluated. This chapter focuses on the interpretations of the results and their subsequent discussions.

5.1.1 Description and Interpretation of Apparent Resistivity Maps

As has already been observed in chapter 4, qualitative interpretation of the electrical sounding data should, normally, precede the subsequent quantitative interpretation. In this project, apparent resistivity maps were prepared by plotting the apparent resistivity values, as registered on the sounding curves, at given electrode spacings ($AB/2 = 13, 50$ and 100 m), common to all soundings, and contouring the results using the method described by Bishop (1960).

Zohdy, et. al. (1980) remark that these apparent resistivity maps do not represent the areal variation of resistivity at a depth equal to that electrode spacing. Instead, they merely indicate the general lateral variation in the electrical properties at that spacing.

Fig 5.1 shows apparent resistivity values at AB/2 spacing of 13 m. From it, highest apparent values ($\rho_a > 1500$ ohm-m) are within the Magarini sands. At the same depth, the corresponding value for Mazeras sandstone area does not exceed 1000 ohm-m. Resistivity values decrease in various directions suggesting the variation of the low resistivity anomalous zones.

At an AB/2 spacing of 50 m (Fig 5.2), the apparent resistivity values are generally lower compared to those ones at AB/2 = 13 m. From the geo-electric sections, this depth represents the conductive zone. Within the Mazeras sandstones, the anomalous areas are found towards the south-western and western parts. The resistivity "high" corresponds to the hilly parts of the project area. Towards the north-east, the contours are close suggesting a rapid drop of the water quality. Areas covered by the Magarini sands have their contours afar showing relatively low gradient suggesting stable waters. The decrease in the contour resistivity values suggest that the anomalous parts are the southern, eastern and south-eastern.

Fig 5.3 represents the apparent resistivity values at AB/2 = 100 m. This depth generally represents a non-conductive "electrical basement" zone. Like in the other two maps (Figs 5.1 and 5.2), the anomalous zones with lower resistivity values are towards the eastern, southern and south-eastern parts. However, for the zone

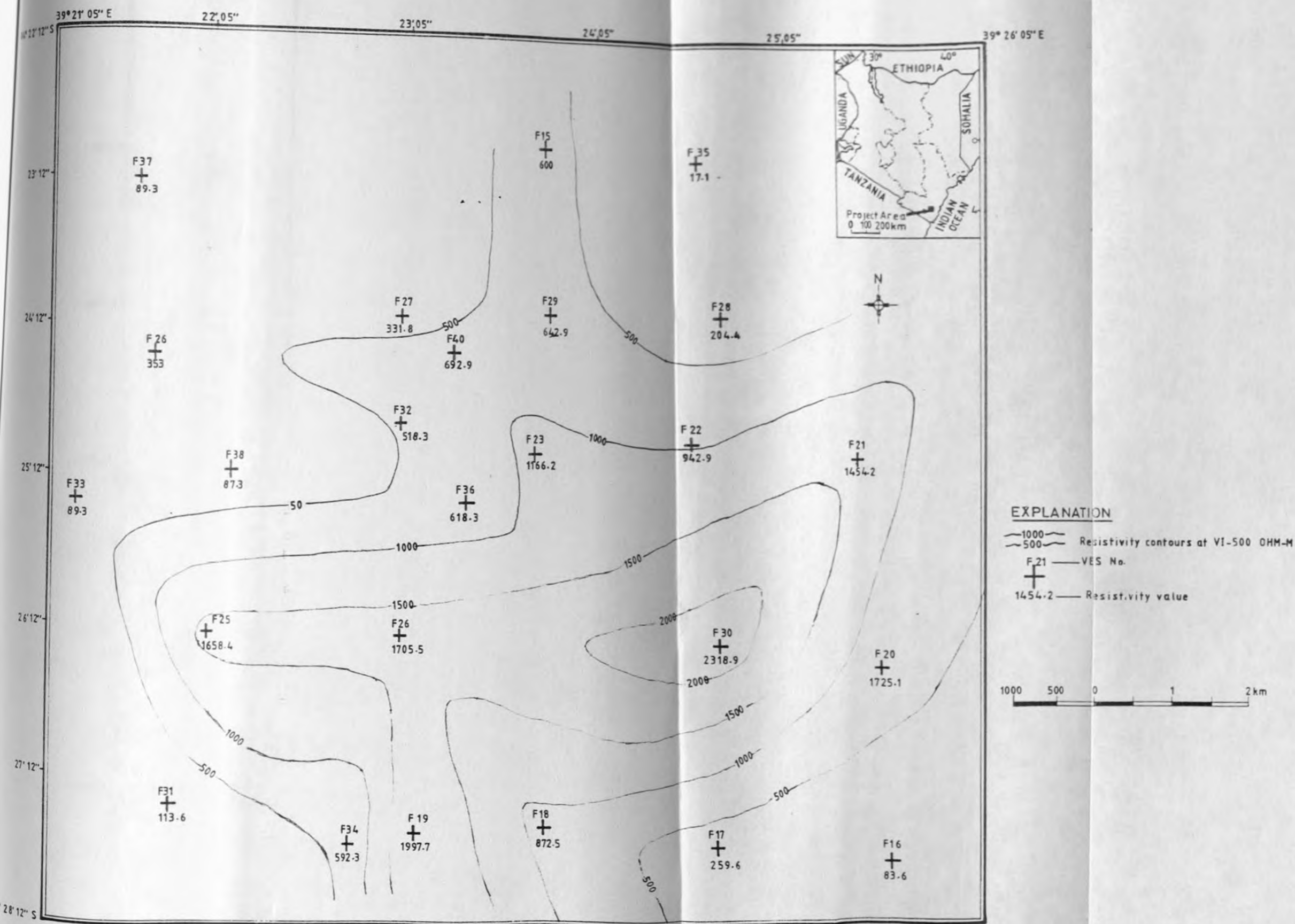


Fig 5.1 APPARENT RESISTIVITY MAP AT AB/2 SPACING = 13m

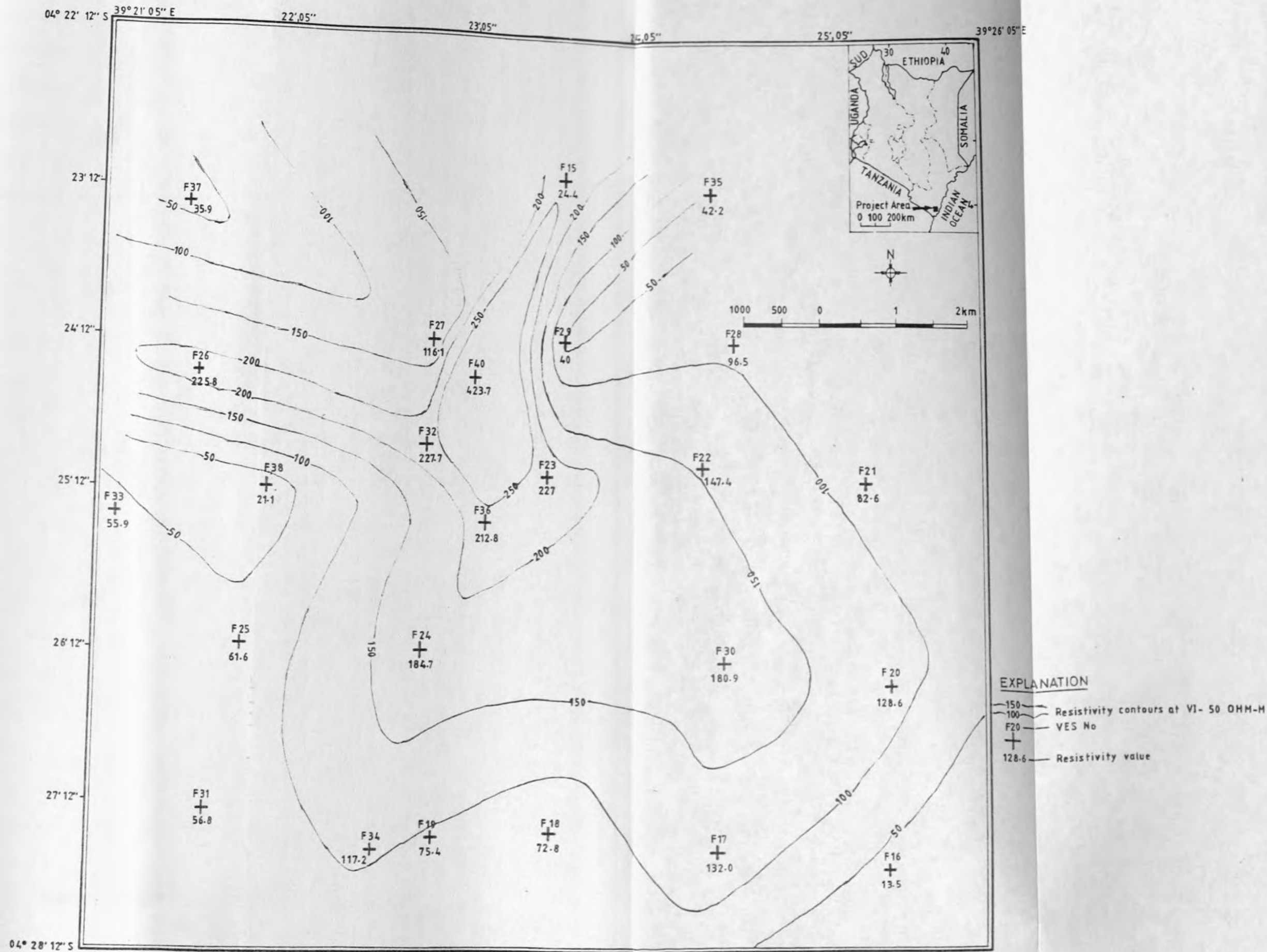


Fig. 5.2 APPARENT RESISTIVITY MAP AT AB/2 SPACING = 50m

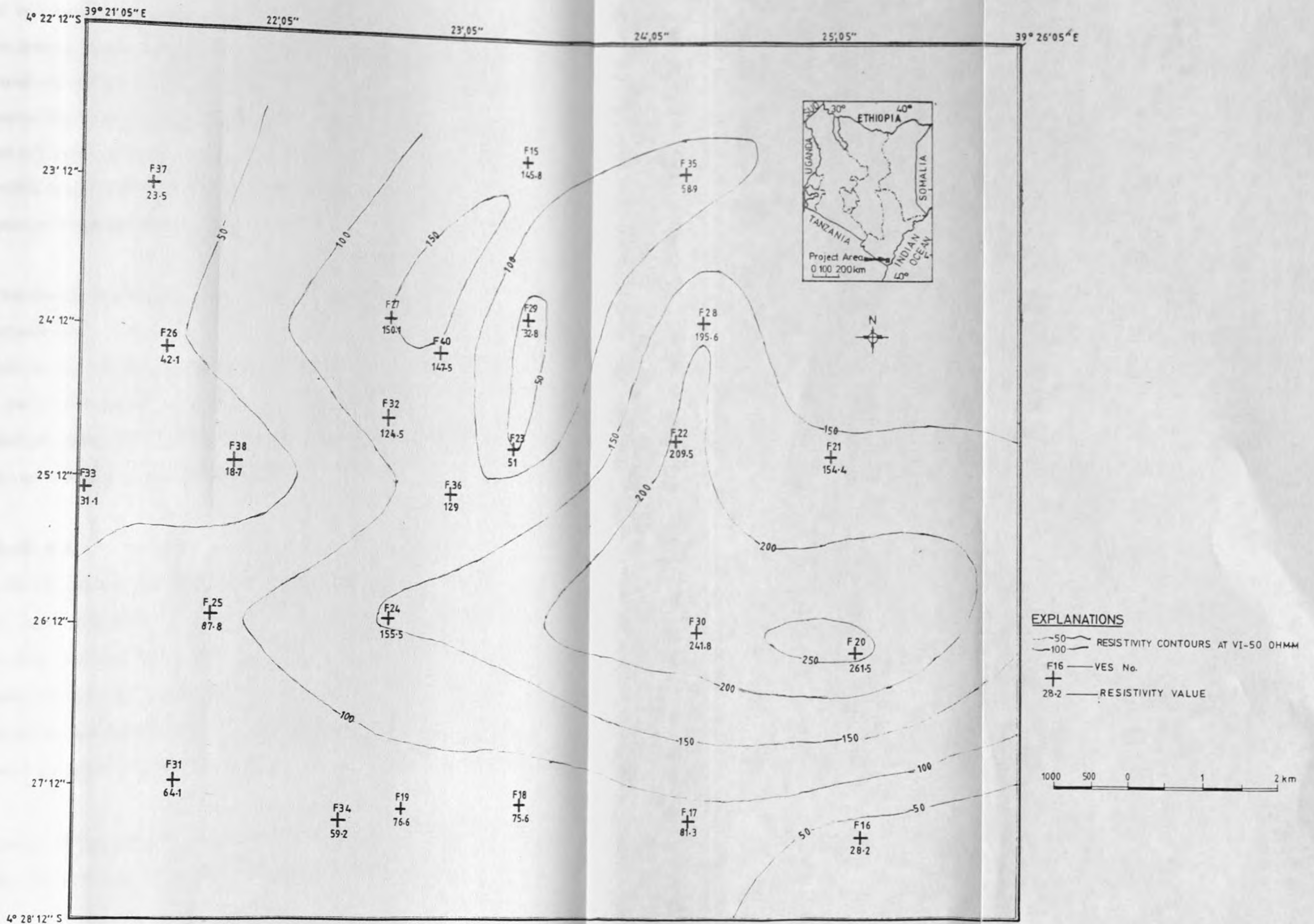


Fig. 5-3 APPARENT RESISTIVITY MAP AT AB/2 SPACING=100m

covered by Mazeras sandstone, an interesting situation emerges. A zone of "internal drainage" with anomalous values of between 50 to 100 ohm-m is clearly demarcated, spreading in a north-south direction. Drilling results from a borehole at Mivumoni Primary School, where sounding F23 was done, indicate the presence of gravel within the conductive zone. It is evident from Fig 5.3 that resistivity "highs" within the Mazeras sandstones correspond yet again to the hilly parts of the project area as observed at F27 and F40.

5.2 Interpreted Geo-Electric Cross-Sections and Stratigraphical Correlation

The results of the VES data are hereby presented in three geo-electric cross-sections along cross-sectional lines B-B', T-T' and X-X'(Fig 3.2). It must be emphasized yet again that these profiles were decided upon after grouping the sounding curves (chapter 4) into different Types.

5.2.1 Profile B-B'

This is a SW-NE profile mainly through soundings done on the Mazeras sandstones (Fig 3.2). As already shown in section 4.1.1, the sounding curves indicate the presence of at least four layers in the subsurface. This observation is further highlighted on the geo-electric cross-section shown in Fig. 5.4. The layers appear to be thinning out and become shallower towards the north-west end of the profile. A few micro-geo-electric layers form lenses within the major ones.

Interpreted resistivities (Fig 5.5a) suggest that the top layer is composed of dry, red, sandy soils often intercalated with some clayey materials. This top layer

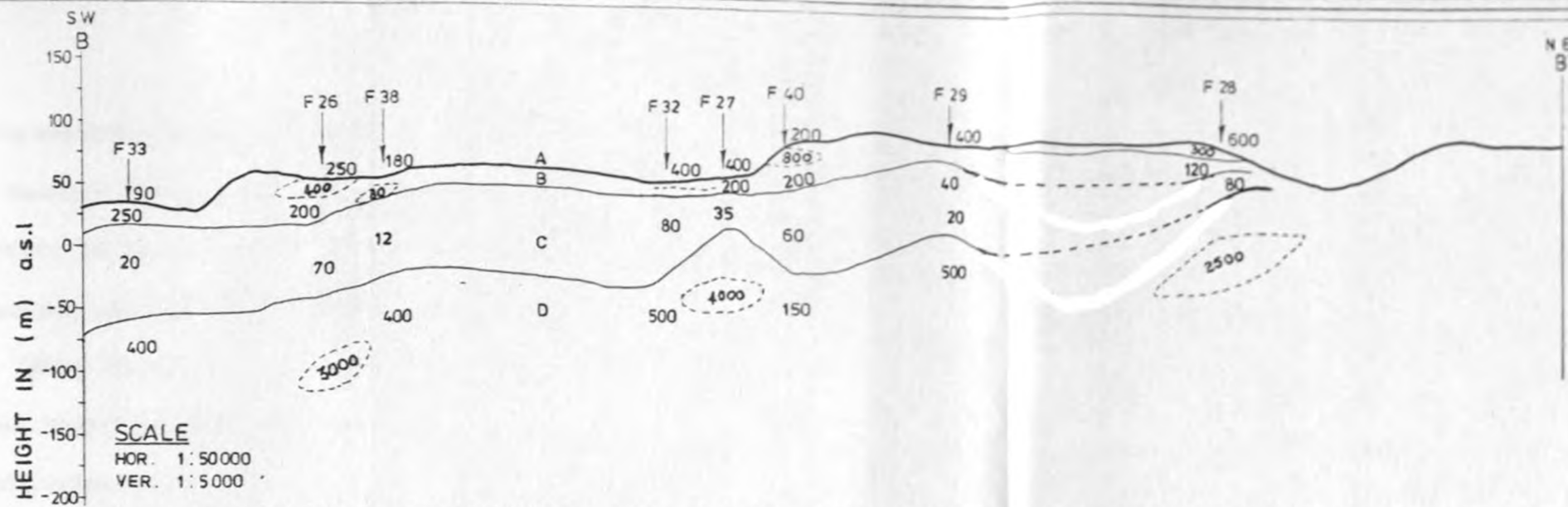


Fig. 5.4 INTERPRETED GEOELECTRIC CROSS-SECTION ALONG PROFILE B-B' IN THE KIDIANI AREA, KWALE.

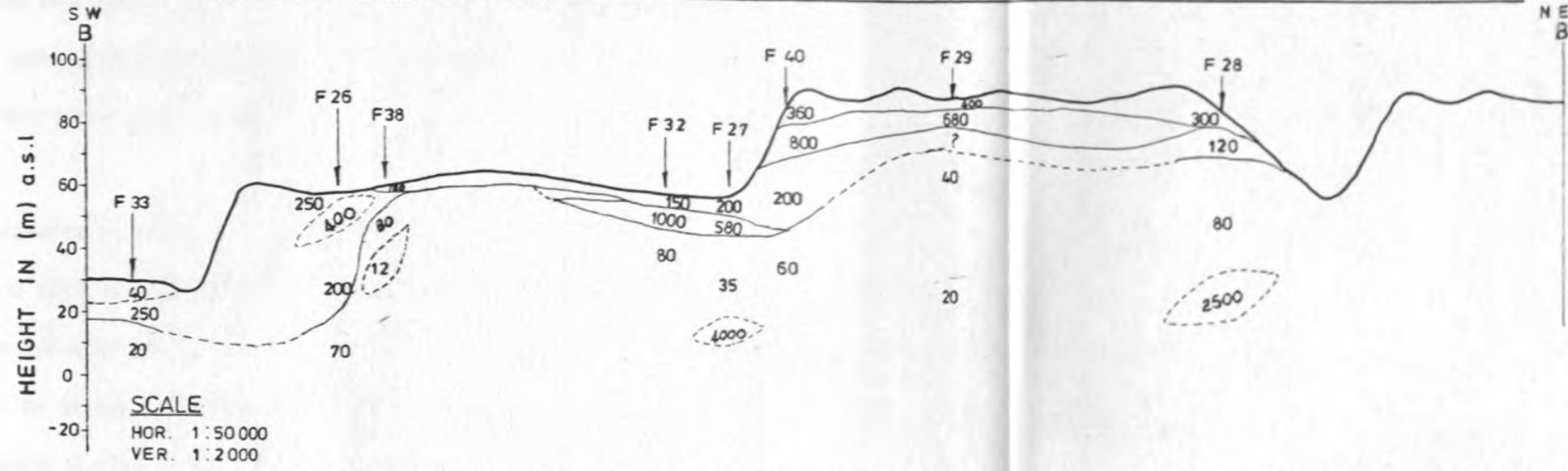


Fig. 5.5 (a) INTERPRETED GEOELECTRIC CROSS-SECTION ALONG PROFILE B-B' IN THE KIDIANI AREA, KWALE UPTO 100 m.

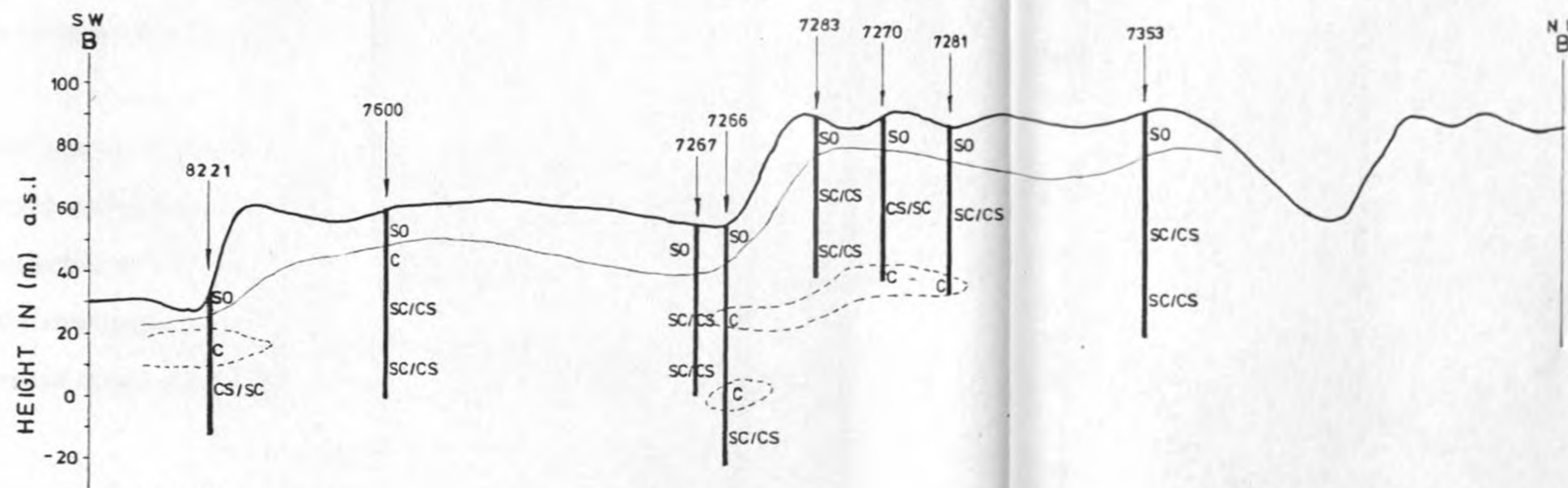


Fig. 5.5 (b) BOREHOLE LOGS STRATIGRAPHIC CORRELATION ALONG PROFILE B-B' IN KIDIANI AREA, KWALE

RESISTIVITY INTERVAL RANGES	INTERPRETED THICKNESS RANGES (m)
LAYER A = 100 - 500 $\mu\Omega \cdot m$	0 - 2.0
" B = 120 - 280 "	5.0 - 60.0
" C = 10 - 80 "	20.0 - 155.0
" D = 200 - 500 "	∞

EXPLANATION

- RESISTIVITY VALUE ($\Omega \cdot m$) AT THE BOUNDED GEOELECTRIC LAYER
- EXTRAPOLATED VES LOCATION ON THE PROFILE LINE
- VES LOCATION ON THE PROFILE LINE
- B-B' RESISTIVITY PROFILE IN Fig. 3.2

- SO = TOP SANDY SOIL
- CS = CLAYEY SANDS
- SC = SANDY CLAYS
- C = CLAYS

EXPLANATION

- EXTRAPOLATED BOREHOLE LOG & No. ON THE PROFILE LINE
- BOREHOLE ON THE PROFILE LINE
- B-B' PROFILE ALONG WHICH THE BOREHOLE LOGS HAVE BEEN CORRELATED IN Fig. 3.2
- OBSERVED LITHOSTRATIGRAPHICAL BOUNDARY
- INFERRED LITHOSTRATIGRAPHICAL BOUNDARY

attains a maximum thickness of about 2.0 m. Apparently, the thickness of these top layer materials seem to be topographically controlled. Where there are depressions, the layer is often thicker than in other areas. The resistivities of the top layer may also reflect variations in the soil moisture due to infiltration of rain water. Often, these values signify geological variation of the surface layer. For example, in both soundings F33 and F38 done on a rainy day, the top layer resistivity values are relatively low compared to others (F27,F32) which were made on a hot and sunny day (Appendix B). Also, where this layer was composed of white, loose and dry sands (F18), the resistivity values were high compared to areas where the layer comprised red, compact soils (F37).

The second layer attains a maximum thickness of about 60 m and resistivity values between 120 and 600 ohm-m. However, it is observed that there are numerous geo-electric layer lenses with a variety of resistivity values from as low as 40 ohm-m to as high as 1000 ohm-m. Borehole logs shown in the stratigraphic correlation section (Fig 5.5b) suggest that this layer is essentially composed of either clayey sands or sandy clays. The various formation lenses comprise clays, sands and often quartzitic sands. This stratigraphic section, therefore, reveals the rapidly, variable and often complex geological nature of the subsurface.

The third layer is characterised by low resistivity values ranging from 12 to 80 ohm-m and a thickness of about 80m. This actually forms the conductive zone in the geo-electric section (Fig 5.4) and forms part of the un-limited layer in Fig 5.5a. From the stratigraphic section (Fig 5.5b), it is suggested that this layer is largely composed of clayey sands / sandy formations and to some extent shales/mudstone

which occur as intercalations within the sandstones. It is within this zone that water was struck in most boreholes within the project area.

Interestingly, it was noted that often water was struck earlier at shallower depth(s) in some boreholes not necessarily within the conductive zones. From Fig 5.5b, the shallower water levels can be associated with the presence of perched aquifers formed by the impervious clayey layers above the water bearing sandy formations.

Fig 5.4 reveals that resistivity values between 50 and 80 ohm-m of the conductive zone occur for boreholes sited on elevated ground such as at sites F26, F32, F36, F28, and F29 which correspond to boreholes nosC- 7931, 7267, 7283, 7592, and 7280, respectively. The conductive zone, however, seems to contain water with different qualities as implied by different resistivity values. Thus, by comparison, the (20 ohm-m) resistivity value of the conductive zone, may suggest the presence of relatively poor quality water than the 50 to 80 ohm-m resistivity values. Thus, there seems to be a loose correlation between the topography and the distribution of the saturated layers in the project area.

The conductive zone appears to be thin at F27. This is not unexpected since the sounding was done on a slopy site where erosional processes had removed most of the overlying material, thus, rendering the conductive zone shallower than in other areas. Generally, this conductive zone has a thickness ranging between 30 m, at F27, and 115 m at F36 with an average thickness of about 80 m.

Underlying the conductive zone is a non-conductive "electrical basement" layer with relatively high resistivity values. These values suggest that the layer is composed of slightly weathered and less fractured sandstones. They, therefore, contain little or no water. Unfortunately, no very deep boreholes have been sunk in the project area and, consequently, no logs are available for comparing and calibrating the resistivity sounding data.

Using information from Figs 5.4 and 5.5a and 5.5b, a correlation between resistivity values and formation/stratigraphic characteristics in the Mazeras sandstones (Table 5.1) is established as presented below.

TABLE 5.1 CORRELATION BETWEEN RESISTIVITY AND FORMATION CHARACTERISTICS OF MAZERAS SANDSTONES OF KIDIANI AREA, KWALE

Depth (m)	Resistivity (Ω m)	Formation Characteristics
0-2	100-600	Top dry sandy soils often with clayey content
2-60	120-280	weathered sandstone; clayey sands and sandy clays and quartzitic clays forming intercalations
60-215	12-80	very highly decomposed sandstone saturated with water. Often clays may be present.
>215	200-300	slightly weathered sandstone less fractured; often shale/mudstone form intercalations

5.2.2 Profile T-T'

This is also a SW-NE profile, but traversing through areas where Magarini sands predominate. The resistivity sounding interpretation (Fig 5.6) suggests that four geo-electric layers can be demarcated. However, in the central part of this profile a fifth low resistivity layer is evident.

The first layer has resistivity values varying from 200 to 10,000 ohm-m with a maximum thickness of about 16 m (Figs. 5.7a and 5.7b). The resistivity range clearly indicates the variation of the wetness of this layer as well as its geological nature. The 200 ohm-m value on F17 indicates red, compacted wet Magarini sands while the 10,000 ohm-m value on F30 represents dry, loose, white Magarini sands. Comparing and contrasting with the stratigraphic correlation section (Fig 5.7b), it is apparent that this layer represents the top sandy soils. Generally, it has resistivity values between 200 and 10,000 ohm-m, the high values indicating the dry characteristics of the sands.

In Figs 5.6 and 5.7a there is resistivity "low" indicating the rapid grading of the dry sands into moist, clayey layer. This forms an intermediate layer between the top, dry sands and the conductive zone below. Often, it comprises the geo-electric layer lenses with resistivity values between 130 and 270 ohm-m and a maximum thickness of about 15 m. From the stratigraphic correlation section (Fig 5.7b), this layer is associated with clayey sandy lenses. Often, this layer may also form perched aquifer(s) as evidenced on sounding F34 where borehole no. 5557 has been drilled.

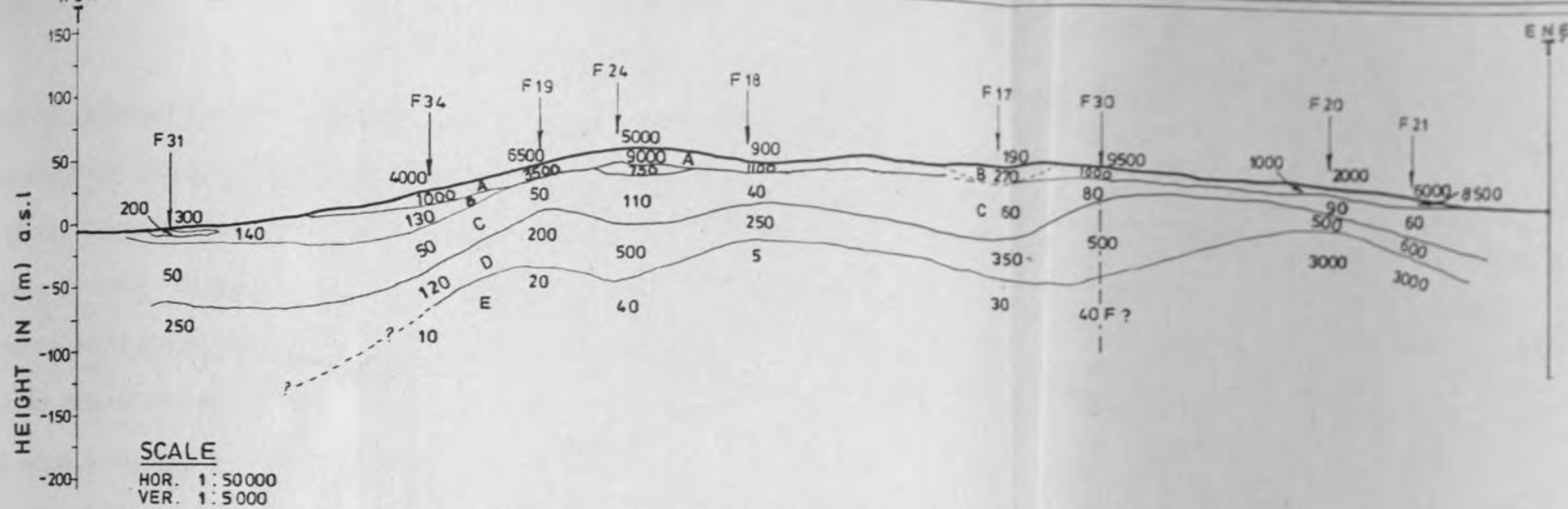


Fig. 5.6 INTERPRETED GEOELECTRIC CROSS-SECTION ALONG PROFILE T-T' IN KIDIANI AREA, KWALE

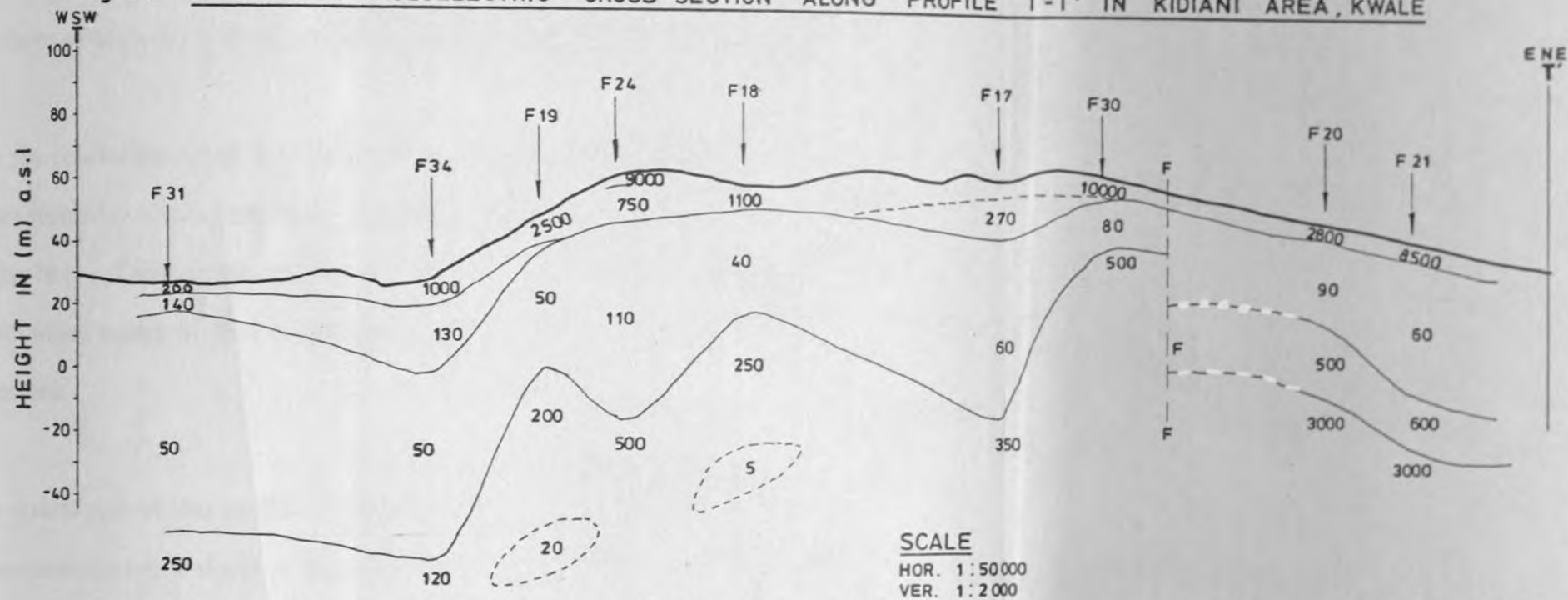


Fig. 5.7(a) INTERPRETED GEOELECTRIC CROSS-SECTION ALONG PROFILE T-T' IN KIDIANI AREA, KWALE UPTO 100 m.

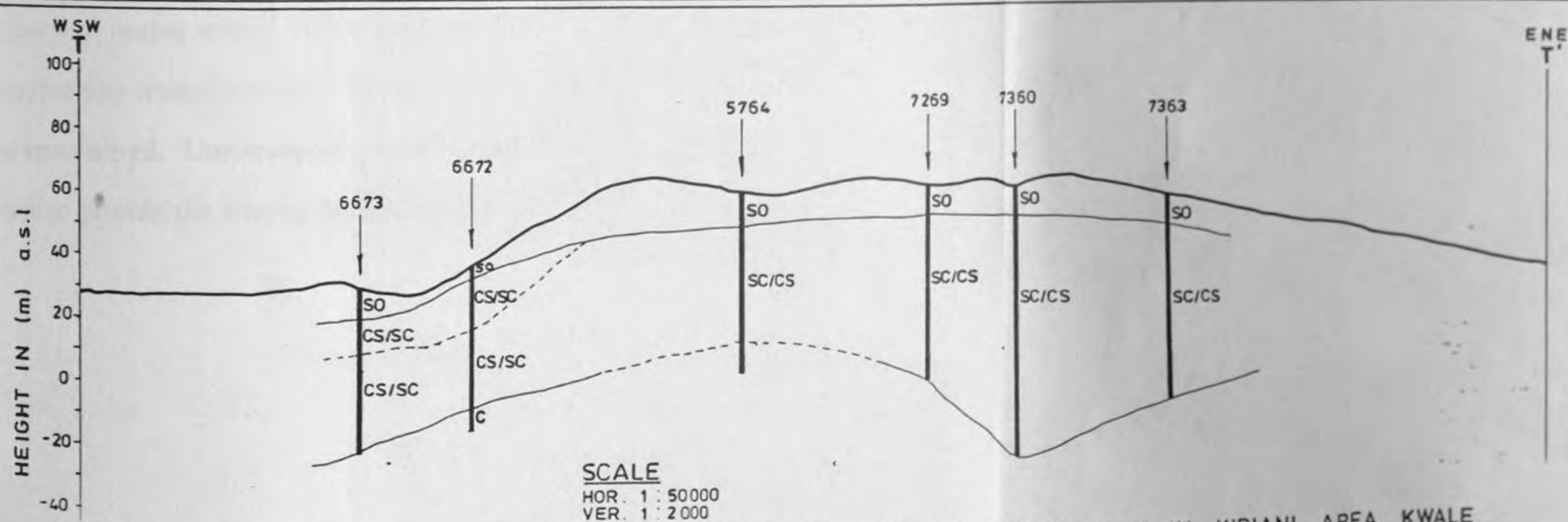


Fig. 5.7 (b) BOREHOLE LOGS STRATIGRAPHIC CORRELATION ALONG PROFILE T-T' IN KIDIANI AREA, KWALE

RESISTIVITY INTERVAL RANGES	INTERPRETED THICKNESS RANGES (m)
LAYER A = 150 - 10000 $\mu\Omega$ m	0 - 10.0
B = 130 - 270 "	5.0 - 15.0
C = 40 - 110 "	10.0 - 70.0
D = 150 - 500 "	15.0 - 70.0
E = 10 - 40 "	central zone
F = 500 - 3000 "	western zone near Mombweni

EXPLANATION

- 110 RESISTIVITY VALUE ($\mu\Omega$ m) OF THE BOUNDED GEOELECTRIC LAYER
- F 30 VES ON THE PROFILE LINE
- F 31 EXTRAPOLATED VES SITE ON THE PROFILE LINE
- T - T' RESISTIVITY PROFILE IN Fig. 3.2
- F - F INFERRED FAULT

- SO = TOP SANDY SOIL
- CS = CLAYEY SOIL
- SC = SANDY CLAY
- C = CLAY
- S = SANDS/HIGHLY WEATHERED SANDSTONES

EXPLANATION

- T - T' PROFILE ALONG WHICH BOREHOLE LOGS HAVE BEEN CORRELATED IN Fig. 3.2
- 6672 EXTRAPOLATED BOREHOLE LOG & No. ON PROFILE LINE
- INFERRED LITHOSTRATIGRAPHICAL BOUNDARY
- OBSERVED LITHOSTRATIGRAPHICAL BOUNDARY

The second major geo-electric layer is the conductive zone. Generally, this layer has low resistivity values between 40 and 110 ohm-m and a maximum thickness of about 65 m. From the stratigraphic correlation section (Fig 5.7b), it is apparent that water in most boreholes was struck within this zone. For example, in borehole no. 6673 at F24 water was struck at 45 m while for borehole no.7602 at F18, water struck level was at 38 m. This, therefore, confirms that the conductive zone is actually saturated. Further, interpretation of the geological stratigraphic section (Fig 5.7b) reveals that this layer is essentially composed of sandy clays/clayey sands with several thin layers of clays forming a multi-aquifer system.

Below the conductive zone is a non-conductive layer characterised by relatively medium resistivity values between 300 and 600 ohm-m with a maximum thickness of about 70 m. These resistivity values may indicate the presence of more sandy material which could, in fact, be saturated. Small amounts of clay may, however, be expected.

In the central part of this profile, a less extensive, low resistivity geo-electric layer is encountered after a depth of approximately 150 m. Even though its thickness has not been determined, its resistivity values of between 5 to 40 ohm-m, suggest that it has poor quality water. Values up to 10 ohm-m may indicate the presence of saline/brackish waters while the 40 ohm-m value suggests that clayey material may be encountered. Unfortunately, no deep boreholes have been drilled in this formation to provide the missing corroborative information.

10-14	Very loose sand
14-18	Well-sorted, clean sand
18-22	Sandy and gravelly sand
22-25	Medially sorted, clean sand

It is noteworthy that towards the north-east of the profile, there is a relatively very high resistivity layer at about 50 m below the sandy surface. This is rather unexpected. Even though only shallow boreholes have been drilled in this part, available logs indicate that this high resistivity layer could be due to coral limestones. The well log of one such borehole drilled at Kidzumbani (Table 5.2) provides evidence that coral limestones underlie the Kilindini sands. The 100 to 600 ohm-m intermediate layer (Fig 5.6) is most probably due to weathered and fractured coral limestone. Fig 5.7a clearly suggests the presence of a fault between the corals and the Tertiary sands.

Table 5.3 gives a generalised correlation between the resistivity values and the Magarini sands formation characteristics in Kidiani Area.

5.2.3 Profile X-X'

This is a NNW-SSE profile. Towards the north it shows general thinning-out of the geo-electric layers. However, the same layers are thicker in the middle and towards the south of the profile, becoming noticeably thinner again in parts underlain by the coral limestones (at F20 and F21).

Table 5.2 Well log for Borehole no 5767, Kidzumbani.

Depth (m)	Formation Characteristics
0-4	Greyish sandy soils with limestone pebbles
4-6	Beach sands plus some limestone pebbles
6-10	Highly weathered limestone
10-16	Fine beach sands
16-18	Weathered limestone
18-22	Sands and clayey sands
22-25	Weathered coral limestone

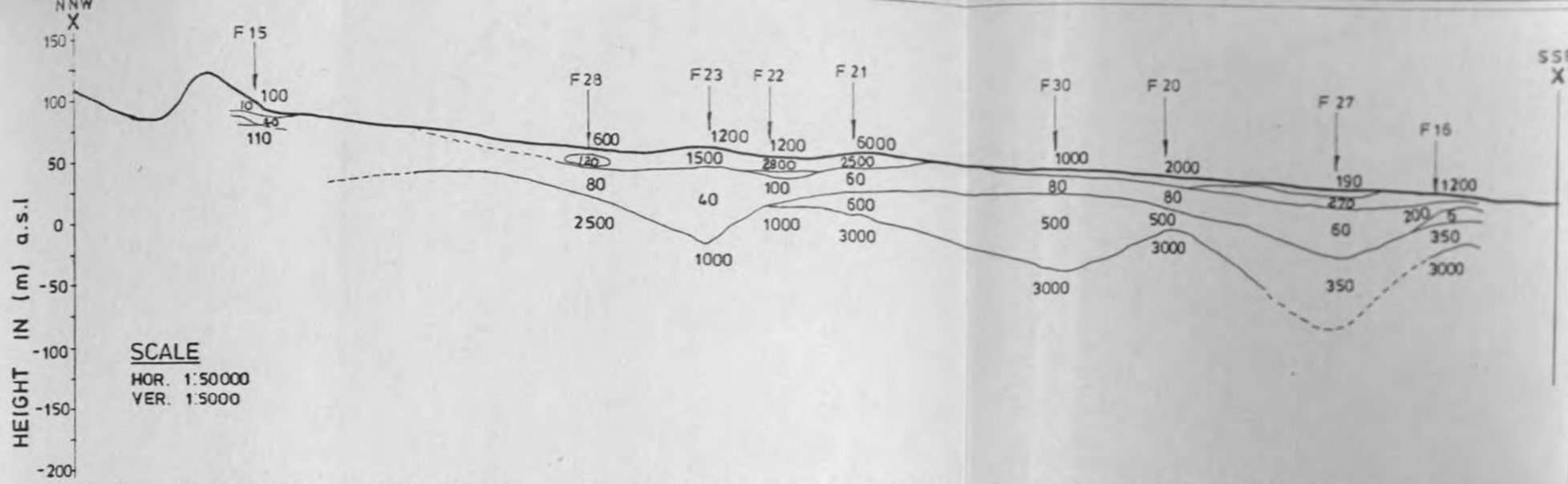
Table 5.3 Correlation between resistivity and formation characteristics of Magarini sands in Kidiani Area, Kwale

Depth (m)	Resistivity (Ω m)	Formation Characteristics
0-10	200-10000	red, compacted and white loose Magarini sands intercalations
10-25	130-270	moist, clayey sands or sandy clays
25-90	40-110	sandy clays/ clayey sands saturated
90-160	150-600	moist sands
>160	10-40	clayey formation, probably saline water
>160	600-3000	moderately to unweathered coral limestone

From the geo-electric section (Fig 5.8), at least four layers can be observed. Like in the other sections (Figs 5.4 and 5.6), the top layer is thin with a maximum depth of about 10 m with resistivity values ranging between 100 and 6,000 Ω m. This layer is essentially composed of dry and loose sands. Where the sands are compacted and moist, for example at F17, the resistivity values are generally low.

The second layer comprises geo-electric lenses of variable thicknesses (5-10 m) and resistivity values in between 120 and 500 ohm-m (Fig 5.9a).

Below is a conductive zone with resistivity values from 40 to 100 ohm-m and a maximum thickness of about 100 m. This layer is essentially composed of sandy beds with little clay content (Fig 5.9b). Often, thin gravel beds (for example, at F23) were encountered where they form the aquifer zone.



LAYER	RESISTIVITY INTERVAL RANGES	INTERPRETED THICKNESS RANGES (m)
A	200 - 5000 $\Omega \cdot m$	0 - 2.0
B	120 - 500 "	5.0 - 10.0
C	40 - 100 "	10.0 - 65.0
D	350 - 600 "	15.0 - 65.0
E	1000 - 3000 "	∞

EXPLANATION

- RESISTIVITY VALUE ($\Omega \cdot m$) OF THE BOUNDED GEOELECTRIC LAYER
- VES ON THE PROFILE LINE
- EXTRAPOLATED VES SITE ON THE PROFILE LINE
- INFERRED LITHOSTRATIGRAPHICAL BOUNDARY
- X-X' RESISTIVITY PROFILE IN Fig. 3.2

Fig. 5.8 INTERPRETED GEOELECTRIC CROSS-SECTION ALONG PROFILE X-X' IN KIDIANI AREA, KWALE

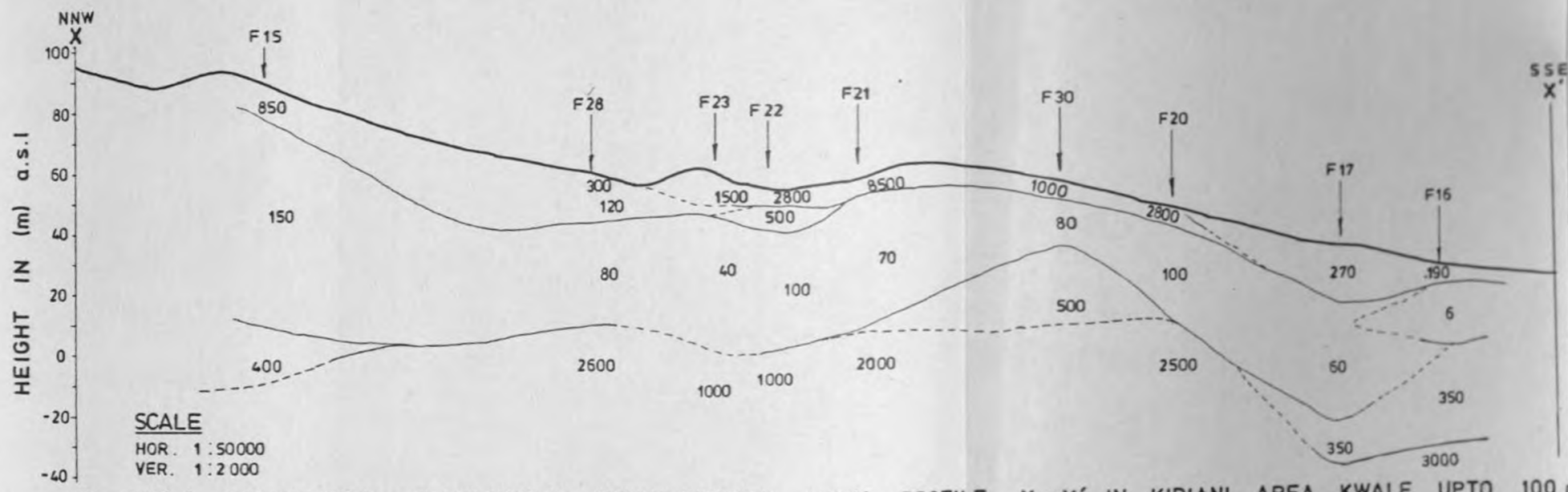
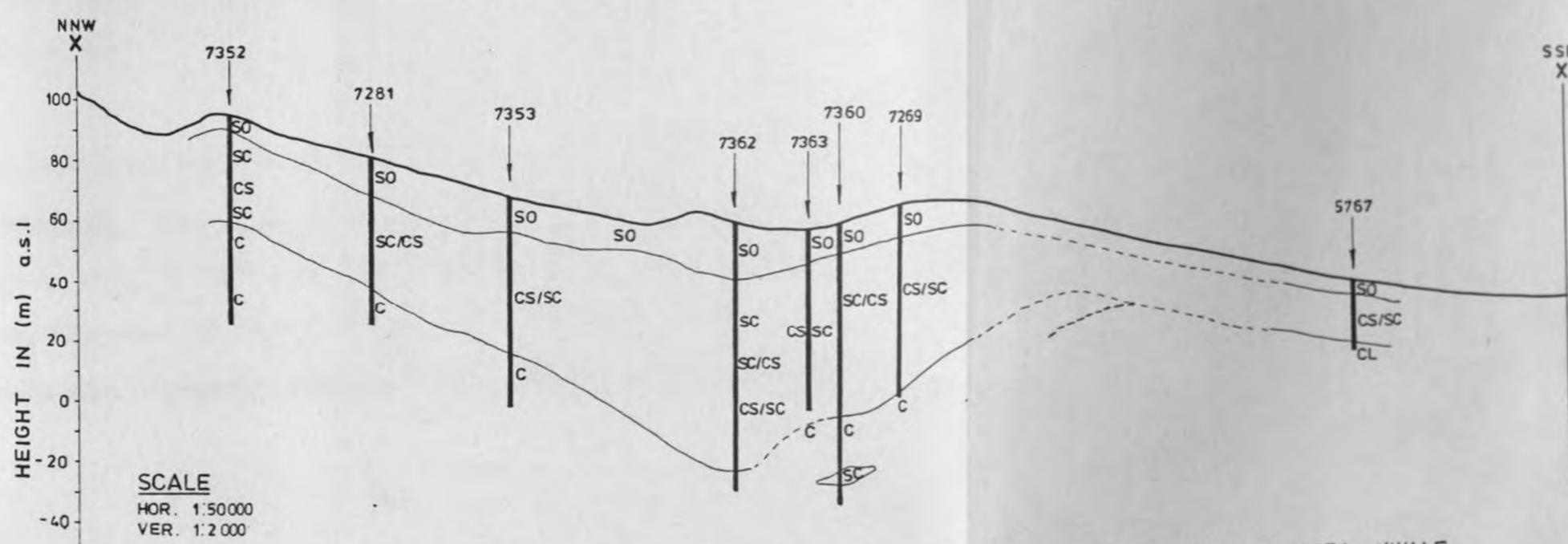


Fig. 5.9 (a) INTERPRETED GEOELECTRIC CROSS-SECTION ALONG PROFILE X-X' IN KIDIANI AREA, KWALE UPTO 100 m.



- SO = TOP SANDY SOILS
- CS = CLAYEY SANDS
- SC = SANDY CLAYS
- C = CLAYS
- M = MUDSTONE/SHALE
- CL = CORAL LIMESTONE

EXPLANATION

- PROFILE LINE ALONG WHICH THE BOREHOLE LOGS HAVE BEEN CORRELATED IN Fig. 3.2
- 7353 EXTRAPOLATED BOREHOLE LOG & No.
- OBSERVED LITHOSTRATIGRAPHICAL BOUNDARY

Fig. 5.9 (b) BOREHOLE LOGS STRATIGRAPHIC CORRELATION ALONG PROFILE X-X' IN KIDIANI AREA, KWALE

Below the conductive zone, is the 350-600 ohm-m geo-electric layer. This layer is not extensive and is only encountered in parts underlain by the coral limestones and has a thickness ranging from 20m to about 60 m. It represents the moderately weathered and possibly fractured coral limestone zone below which is a highly resistive unfractured, fresh coral limestone formation.

The boundary between the 3000 ohm-m layer and another one of 1000 ohm-m (Fig 5.8) is not clear, thus, the zig-zag line separating them. This possibly implies the inter-fingering (fault?) of the Kilindini sands and the coral limestones in the eastern part of the project area.

5.2.4 Discussions on the VES Data Results

From the interpretations of the electro-stratigraphy presented above, it is apparent that comparison of the resistivity values and the stratigraphic correlation as observed from the borehole logs is fair. However, the greatest limitation is the lack of deep, well-logged boreholes with which all the resistivity values acquired could be calibrated as the deepest borehole in the project area is about 100 m deep while the vertical electrical soundings were made to a maximum AB/2 separation of 250 m.

Mwangi (1981) concentrated his work around Msambweni, an area underlain by coral limestones. The corals were saturated with sea water although he encountered lenses of fresh water. The saline water generally lowered the resistivity of the corals. In this project, high resistivity values ($\rho > 2500$ ohm-m) are observed at areas covered by the Kilindini sands. Although the effects of the top

sandy layer cannot be underestimated, they, nevertheless, cannot be entirely associated with the high resistivity values of the subsurface layers. Well log data (Table 5.2) provide evidence that the coral limestones are at a relatively shallow depth. Their presence, therefore, may partially be attributed to the observed high resistivity values.

The variation and often complex nature of the subsurface is exemplified by the presence of several clayey layers occurring in between the sandy formations. These layers hydrogeologically sub-divide the aquifer, especially within the Magarini sands, into a multi-aquifer system. The presence of these thin clayey beds cannot be detected using the resistivity method as their effects are geo-electrically suppressed (Flathe, 1955, 1976). This also could lead to the enhancement of the principle of equivalence (section 4.1.2.3).

The geo-electric sections (Figs 5.4, 5.6, 5.8) provide a rather simplified situation of the subsurface. Several smaller and undetectable layers are usually lumped together to form one broad geo-electric layer. The sharp contrast in resistivity between the conductive zone and the non-conductive zone, either below or above it, is probably indicative of a dry/saturated interface rather than a lithostratigraphical or geological boundary. The same effect could also result from the conductive layers brought about by tropical chemical weathering of lithology since the transition between the weathered conductive layer (saprolite) and the underlying bedrock is usually sharp.

A comparison between the observations made from the apparent resistivity maps and the flow direction (Fig 5.10) suggest that the flow direction of groundwater in the project area is not uniform and unidirectional. It is mainly either ESE, (in the Magarini sands) or SSW (in the Mazeras sandstones). This observation clearly and faithfully agrees with the observations made from the apparent resistivity maps. This too, corresponds to the topography and the drainage pattern of the area. The elevated parts form the recharge zone while the lower parts are the discharge zones. The hilly parts are part of the Shimba Hills, a major catchment zone for the project area.

The hilly parts of the Magarini sands formation appear to have been caused by some structural features. Measurements of the dip angles at some outcrops along the Nguluku-Msambweni road suggest the possibility of a minor anticline. Hence, it appears that the drainage of this area has been modified by the geologic structures. The many lineaments (Fig 2 b) show a clear control of groundwater flow direction.

Qualitatively, the aquifer material in Kidiani Area was gauged by mapping its transverse resistance, T_r , values (thickness x resistivity of the aquifer) as presented in Fig 5.11. Generally, the higher the value of transverse resistance (T_r) the better the aquifer (Al-Ruwaih and Ali, (1986). Low values of T_r are usually due to thin aquifer, high clay content or possibly saline water or a combination of all these factors. Accordingly, the best areas for groundwater prospecting are the elevated ones, especially within the Mazeras sandstones where the values of T_r are between 4000-9000 ohm-m². This is further supported by the fact that the present

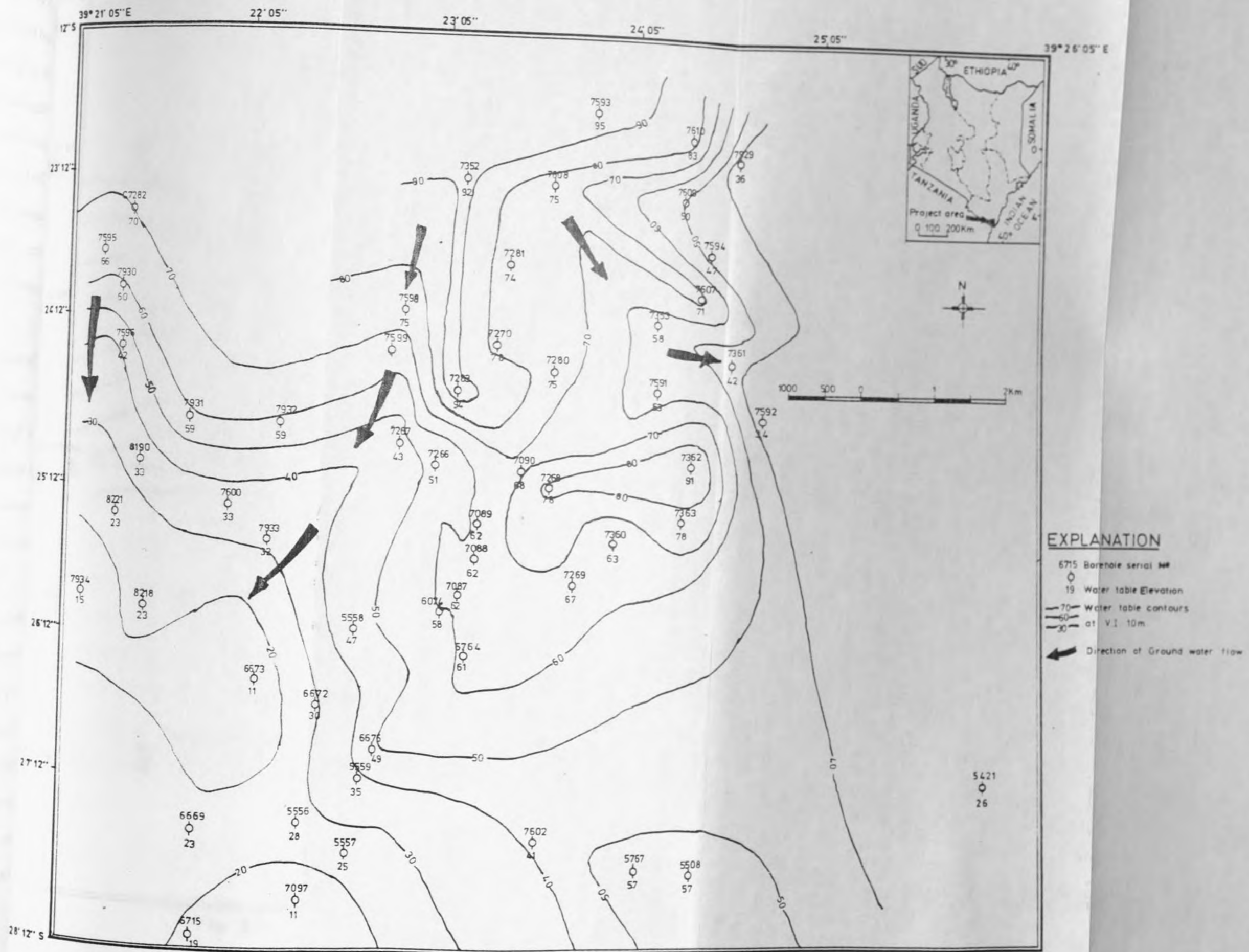


Fig. 5.10 MAP SHOWING THE RECHARGE AND DISCHARGE AREAS FOR KIDIANI AREA, KWALE.

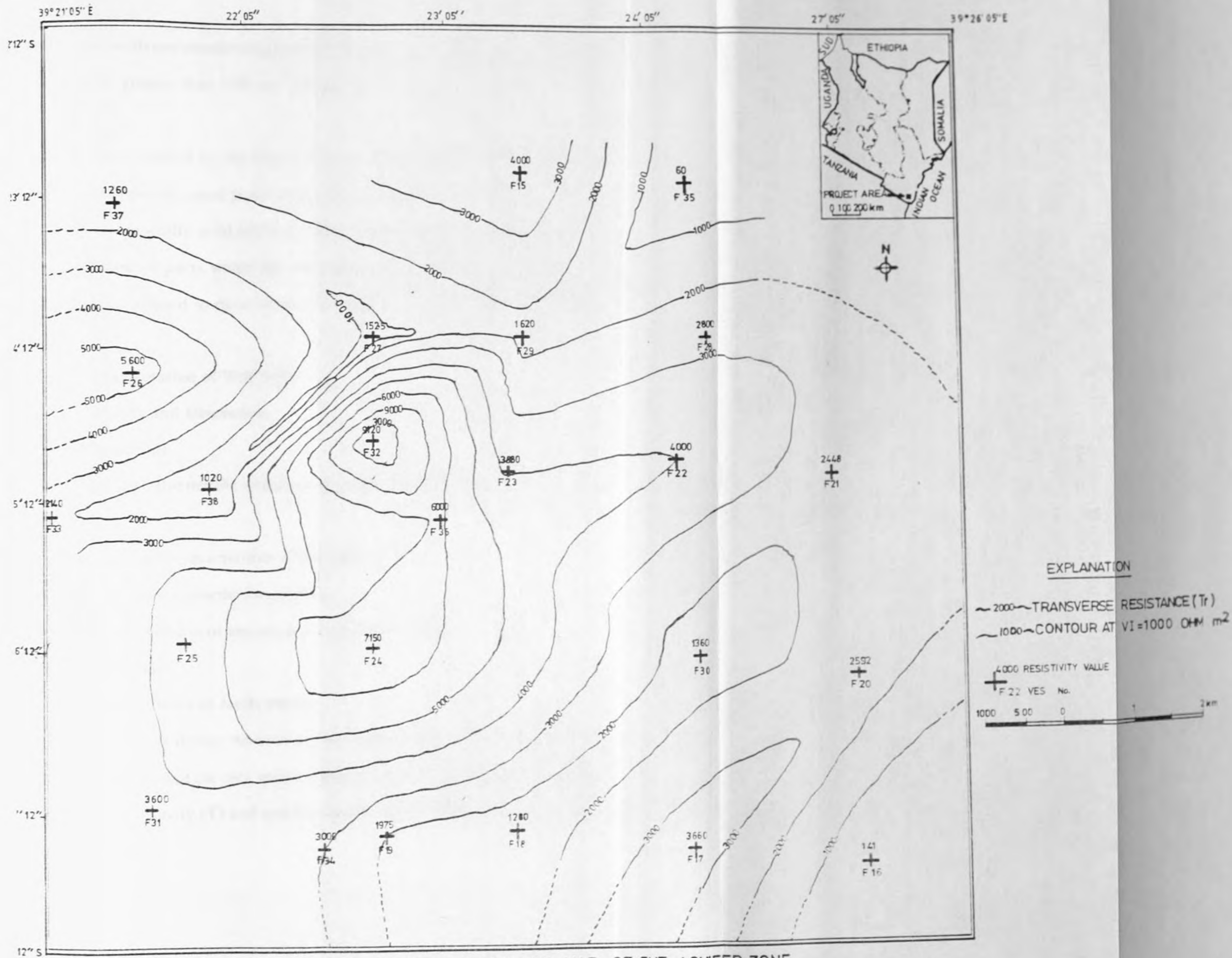


Fig 5.11 TRANSVERSE RESISTANCE MAP OF THE AQUIFER ZONE IN KIDIANI AREA, KWALE.

production wells are concentrated within this zone. Generally, it can be taken that values of T , greater than $3000 \Omega m^2$ provide the best prospecting sites.

For the areas covered by the Magarini sands, values of T , greater than $2000 \Omega m^2$ will normally provide good prospecting sites. All the wells drilled within this range of T , values generally yield sufficient water. Values of T , of about $1000 \Omega m^2$ seem to occur in parts where the clay layers are evident. Such T , values are, therefore, considered to occur in zones unsuitable for groundwater prospecting.

5.3 Interpretation of Well Tests:

Results and Discussions

5.3.1 Introduction

Several factors influence the interpretation of the pumping test data. Among them are:-

- (a) hydrogeologic characteristics of the aquifer,
- (b) errors in data collection/acquisition,
- (c) potential omission of important environmental impacts,
- (d) pumping rates,
- (e) theoretical limits of Jacob theory.

The method of analyzing the recovery test data used in this interpretation gives limited results in that the only aquifer characteristics which were fairly determined include transmissivity (T) and specific capacity (Q/S) values but not the storage coefficient (S).

5.3.2 Effects of some Hydrogeologic Factors on the Interpreted Results

Provided the aquifer conforms to the earlier stated assumptions (chapter 4), the residual-drawdown curve, when extended to the left of drawn graph, should pass through the zero-drawdown point where the ratio t/t' reaches 1. However, it was observed that not always did the curves pass through this point. This, therefore, meant that the aquifer did not conform to the assumed idealised conditions.

Several hydrogeologic factors may be held responsible for this effect on the recovery data. Such factors have been given by Driscoll (1986); Groundwater Manual (1981) and Kruseman and De Ridder (1976, 1983); Boswinkel (1983) and Nilsson (1983). However, all these authors agree that, despite these limitations, the Theis-Jacob straight line approximation method of analysis for single borehole pumping tests remains valid anyway. Driscoll (1986) has given a very elaborate graphical analysis of these hydrogeological factors of which a similar treatise is given below.

The plot of the residual drawdown against the ratio t/t' for borehole 7087 (Fig 5.12) reveals that the zero-point drawdown occurs at a t/t' ratio equal to 4. According to Driscoll (1986) and Groundwater Manual (1981), if the graph indicates zero drawdown at t/t' value of 2 or more, then some recharge water must have reached the aquifer during the pumping phase, thus, bringing about full recovery to the original static level within a relatively short recovery period before t/t' approaches unity.

This observation is collaborated by a time-drawdown curve (Fig 5.13) plotted for the same borehole. From this figure, apparent actual recharge is indicated by the

Borehole N^oC7087

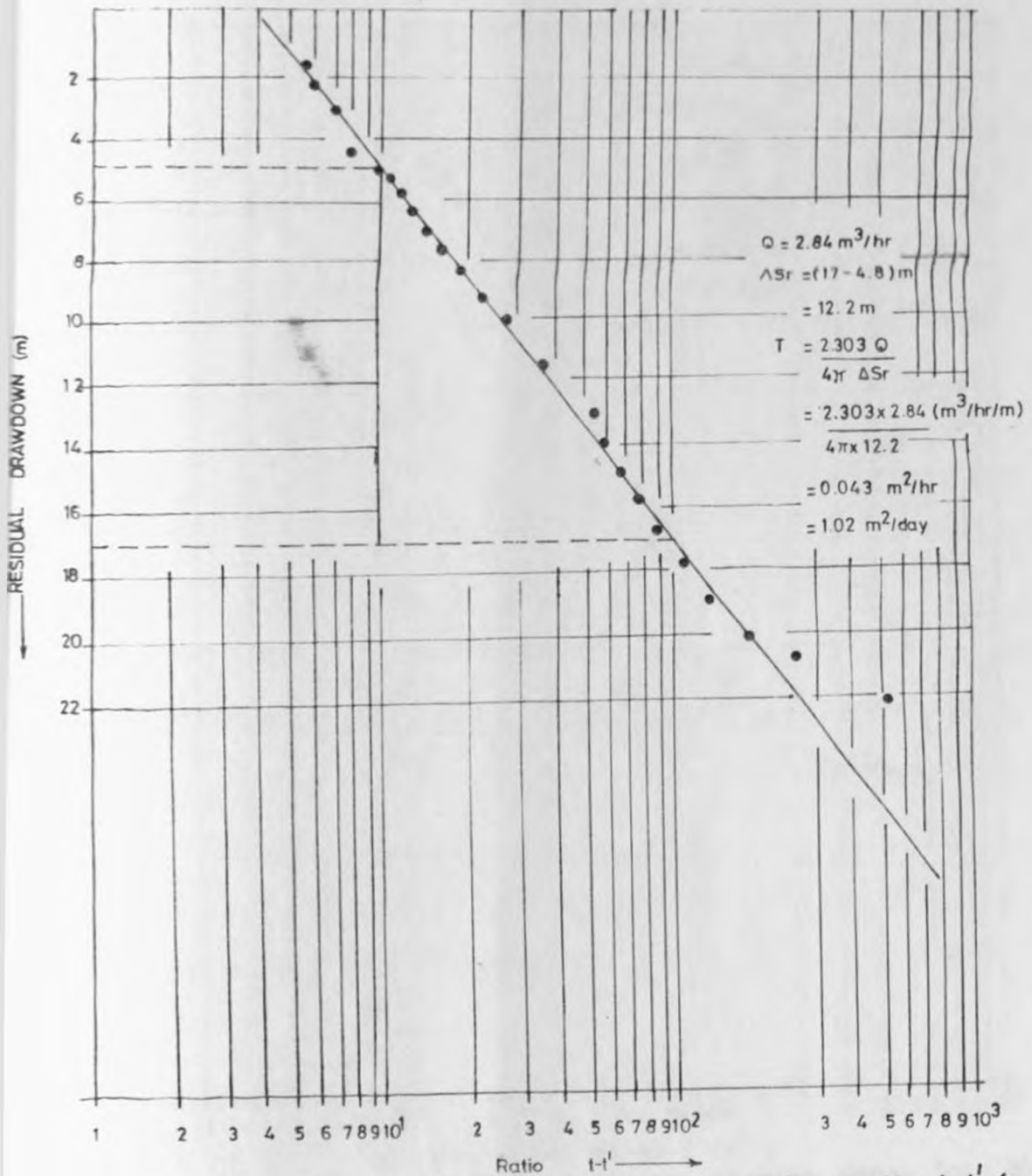


Fig. 5.12: Residual Drawdown curve against ratio $t-t'$ for C7087

Borehole No. C 7087

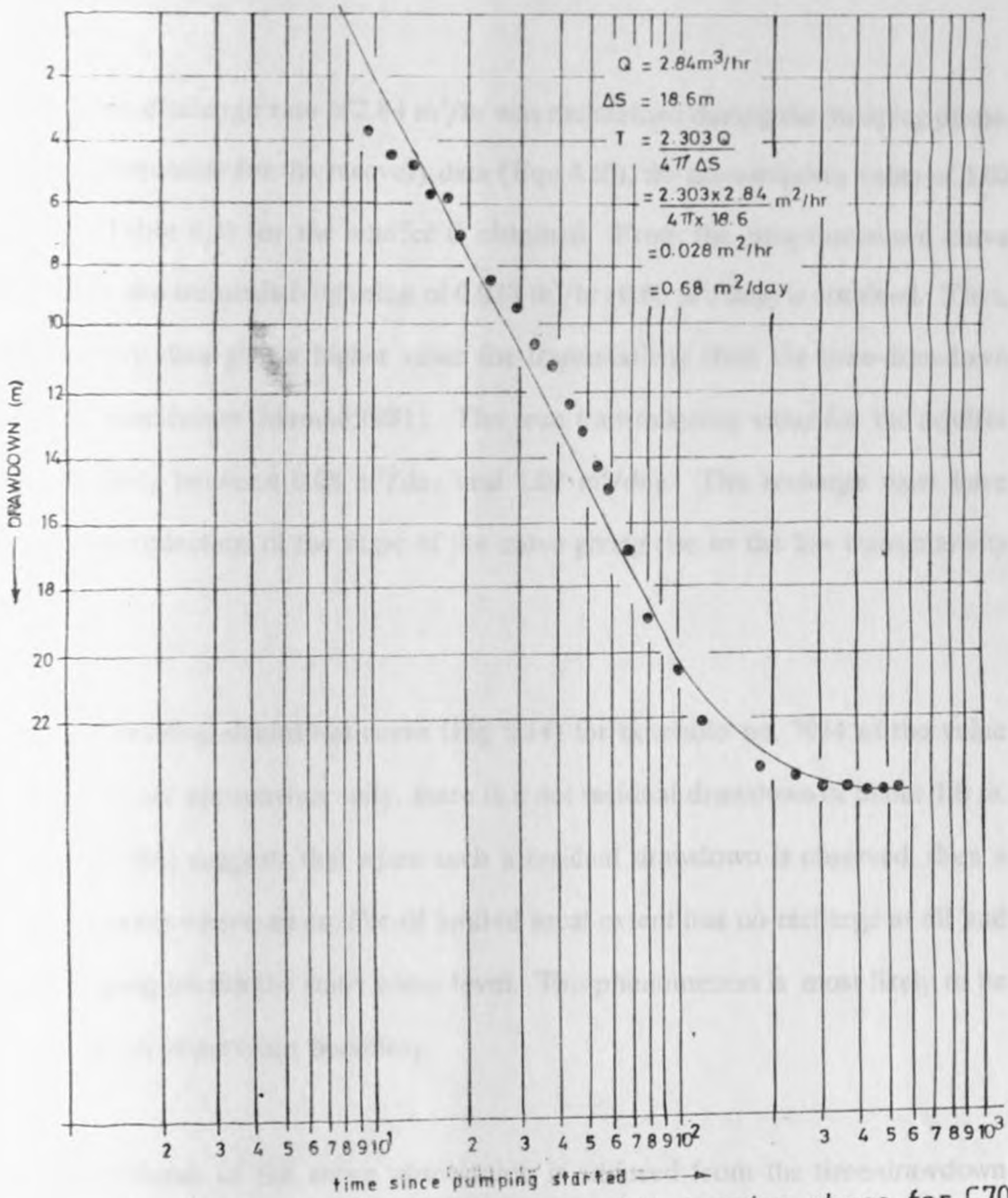


Fig.5.13. Time Drawdown curve for pumping phase for C7087

flattening of the slope of the curve. Since the second part of the curve is not horizontal, then the rate of recharge is slower than the pumping rate of the borehole.

An average discharge rate of $2.84 \text{ m}^3/\text{hr}$ was maintained during the pumping phase. Using the equation for the recovery data (Eqn 4.10), the transmissivity value of $1.02 \text{ m}^2/\text{day}$ (Table 4.3) for the aquifer is obtained. From the time-drawdown curve (Fig 5.13), the transmissivity value of $0.028 \text{ m}^2/\text{hr}$ ($0.68 \text{ m}^2/\text{day}$) is obtained. Thus, the recovery data give a higher value for transmissivity than the time-drawdown curve (Groundwater Manual, 1981). The true transmissivity value for the aquifer is most likely between $0.68 \text{ m}^2/\text{day}$ and $1.02 \text{ m}^2/\text{day}$. The recharge must have caused the reduction of the slope of the curve giving rise to the low transmissivity value.

From the residual-drawdown curve (Fig 5.14) for borehole no. 7934 as the value of the ratio t/t' approaches unity, there is a net residual drawdown of about 1.0 m. Driscoll (1986) suggests that when such a residual drawdown is observed, then a situation exists where an aquifer of limited areal extent has no recharge at all and only pumping lowers the static water level. This phenomenon is most likely to be caused by an impervious boundary.

Further evidence of the above observation is adduced from the time-drawdown curve (Fig 5.15). The boundary causes the slope of the drawdown plot to steepen instead of flattening. This is because the expanding cone of depression must deepen more rapidly in other directions in order to maintain the same yield. Only

Borehole No C 7934

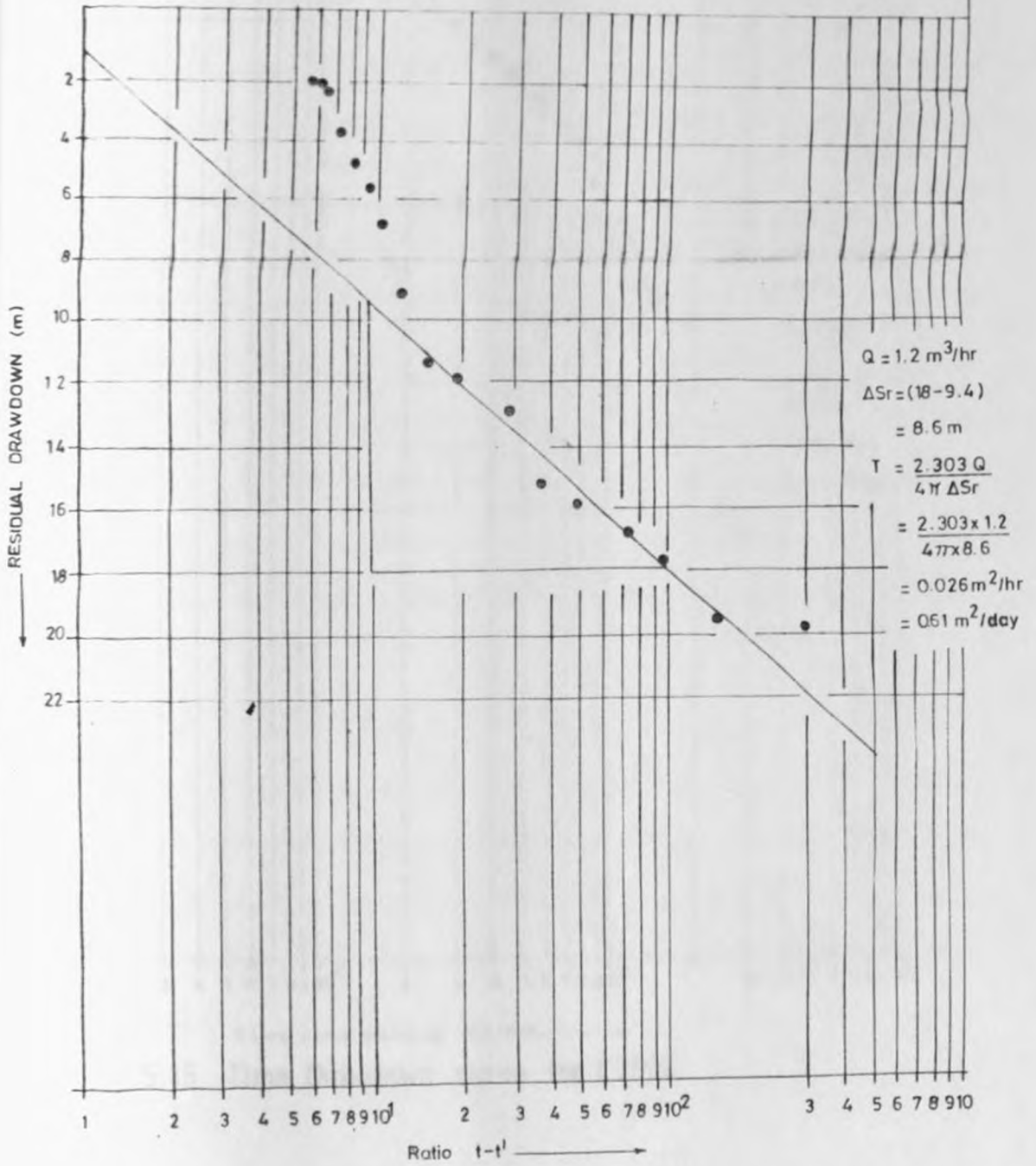


Fig. 5.14 Residual Drawdown curve against ratio $t-t'$ for C7934

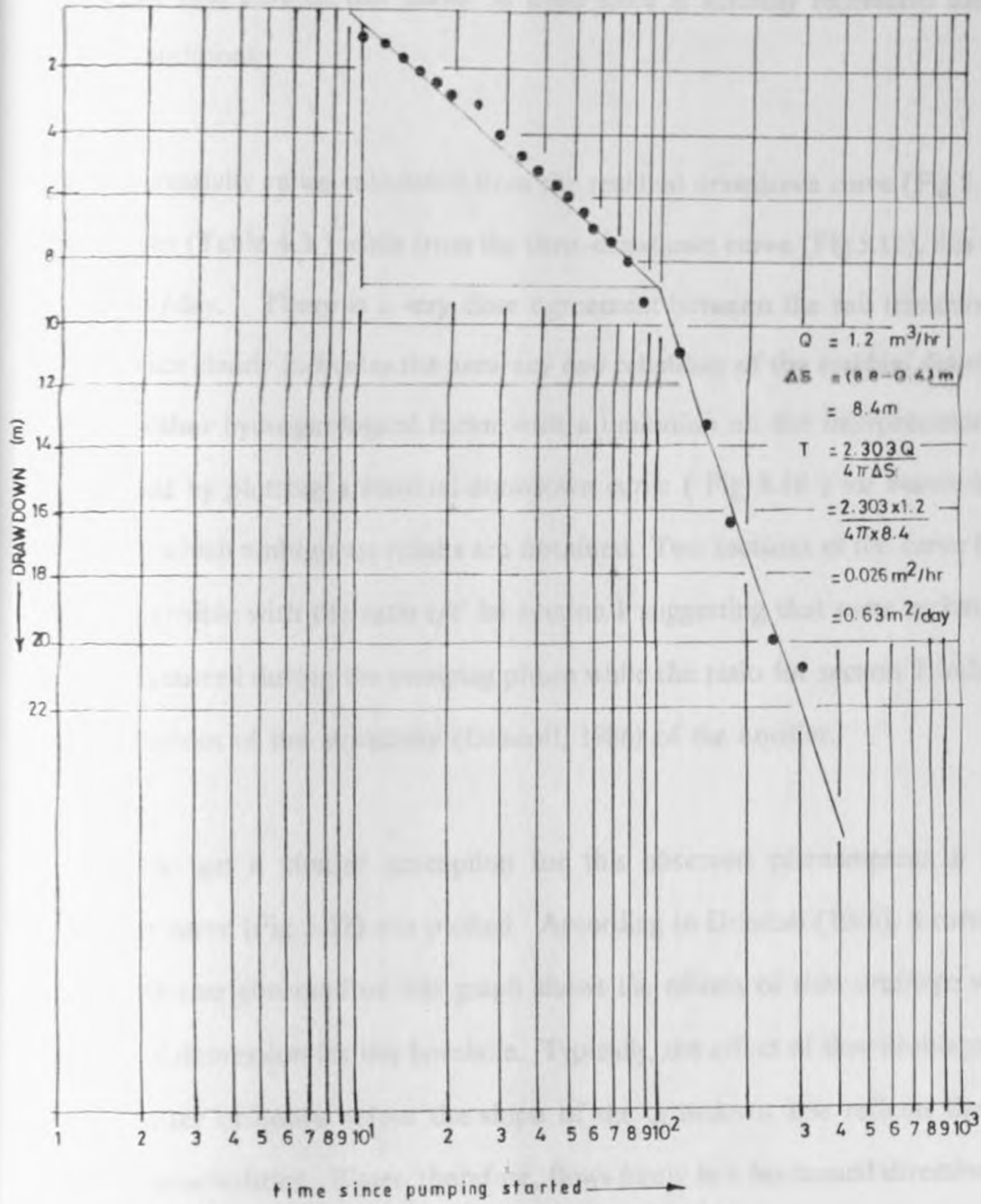


Fig. 5.15 Time Drawdown curve for C7934

the initial, first part of this curve is used since it actually represents the true aquifer conditions.

The transmissivity value calculated from the residual drawdown curve (Fig 5.14) is $0.61 \text{ m}^2/\text{day}$ (Table 4.3) while from the time-drawdown curve (Fig 5.15), this value is $0.63 \text{ m}^2/\text{day}$. There is a very close agreement between the two transmissivity values which clearly indicates the accuracy and reliability of the residual drawdown data. Another hydrogeological factor with a limitation on the interpretation was investigated by plotting a residual-drawdown curve (Fig 5.16) for borehole no. 8221 from which ambiguous results are obtained. Two sections of the curve P and T are discernible with the ratio t/t' for section P suggesting that some recharge to the well occurred during the pumping phase while the ratio for section T indicates some variations of the storativity (Driscoll, 1986) of the aquifer.

In order to get a clearer perception for this observed phenomenon, a time-drawdown curve (Fig 5.17) was plotted. According to Driscoll (1986), a curvature such as the one observed on this graph shows the effects of slow drainage within the cone of depression for this borehole. Typically, the effect of slow drainage lasts only a matter of hours before the slope of the drawdown line reflects the true aquifer characteristics. Water, therefore, flows freely in a horizontal direction, but vertical flow is greatly retarded.

No true transmissivity values can be calculated from these curves as to do so, several hours of pumping would have to pass. In this particular test, pumping was done for only 400 minutes and the resulting drawdown of only 9 metres was

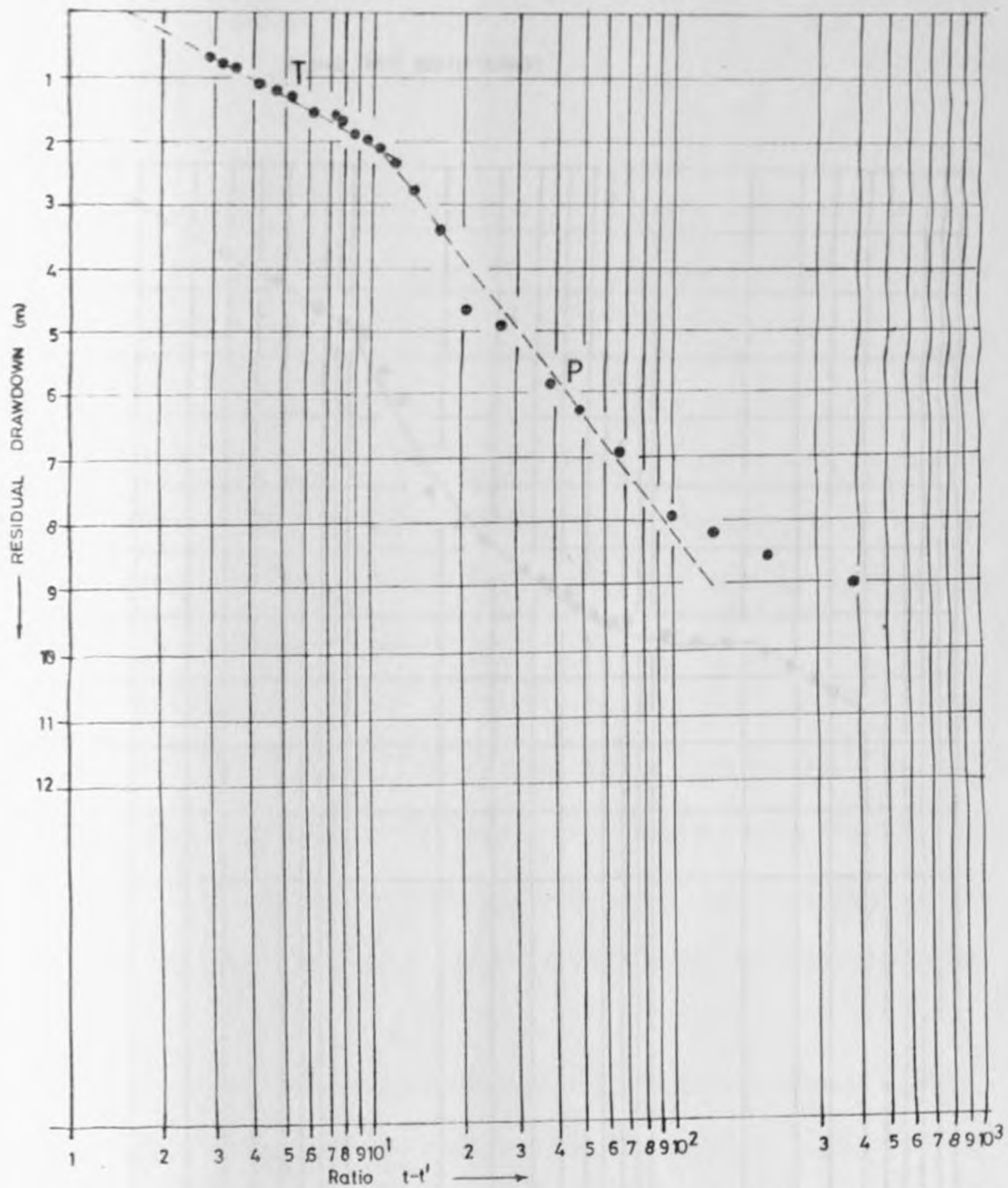


Fig. 5.16 Residual Drawdown curve against ratio $t-t'$ for C8221

Fig. 5.17 Residual Drawdown curve for C8221

Borehole N°C 8221(FUOMBI)

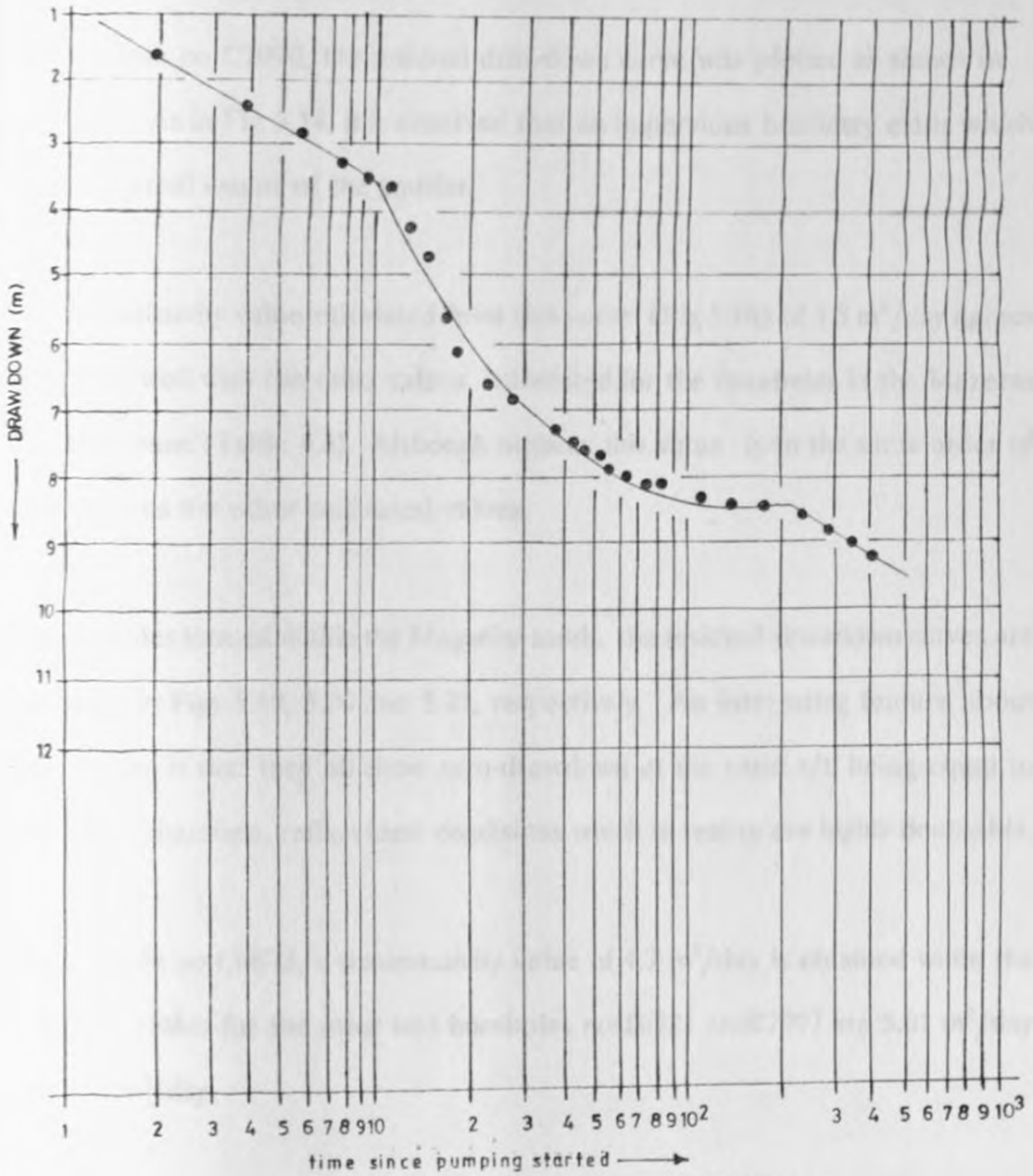


Fig.5.17 Time Drawdown curve for C8221

relatively small compared to other cases considered before. However, the possibility of the presence of an impervious layer in the vicinity of the borehole hindering flow cannot be underestimated.

For borehole no C7090, the residual drawdown curve was plotted as shown in Fig 5.18. As in Fig 5.14, it is observed that an impervious boundary exists which limits the areal extent of the aquifer.

The transmissivity value calculated from this curve (Fig 5.18) of $1.5 \text{ m}^2/\text{day}$ agrees favourably well with the other values calculated for the boreholes in the Mazeras sandstone zone (Table 4.3). Although highest, this value is in the same order of magnitude as the other calculated values.

For boreholes located within the Magarini sands, the residual-drawdown curves are presented in Figs 5.19, 5.20 and 5.21, respectively. An interesting feature about these curves is that they all show zero-drawdown at the ratio t/t' being equal to one. They, therefore, reflect ideal conditions which in reality are highly doubtful.

For borehole no C6673, a transmissivity value of $4.7 \text{ m}^2/\text{day}$ is obtained while the respective values for the other two boreholes nos. C6721 and C7097 are $5.01 \text{ m}^2/\text{day}$ and $5.59 \text{ m}^2/\text{day}$.

5.3.3 Discussions of the Recovery Test Results

In general, the average transmissivity value for aquifer(s) within the Mazeras sandstones is $1.048 \text{ m}^2/\text{day}$ while that of the Magarini sands aquifer(s) is

Borehole N° C 7090

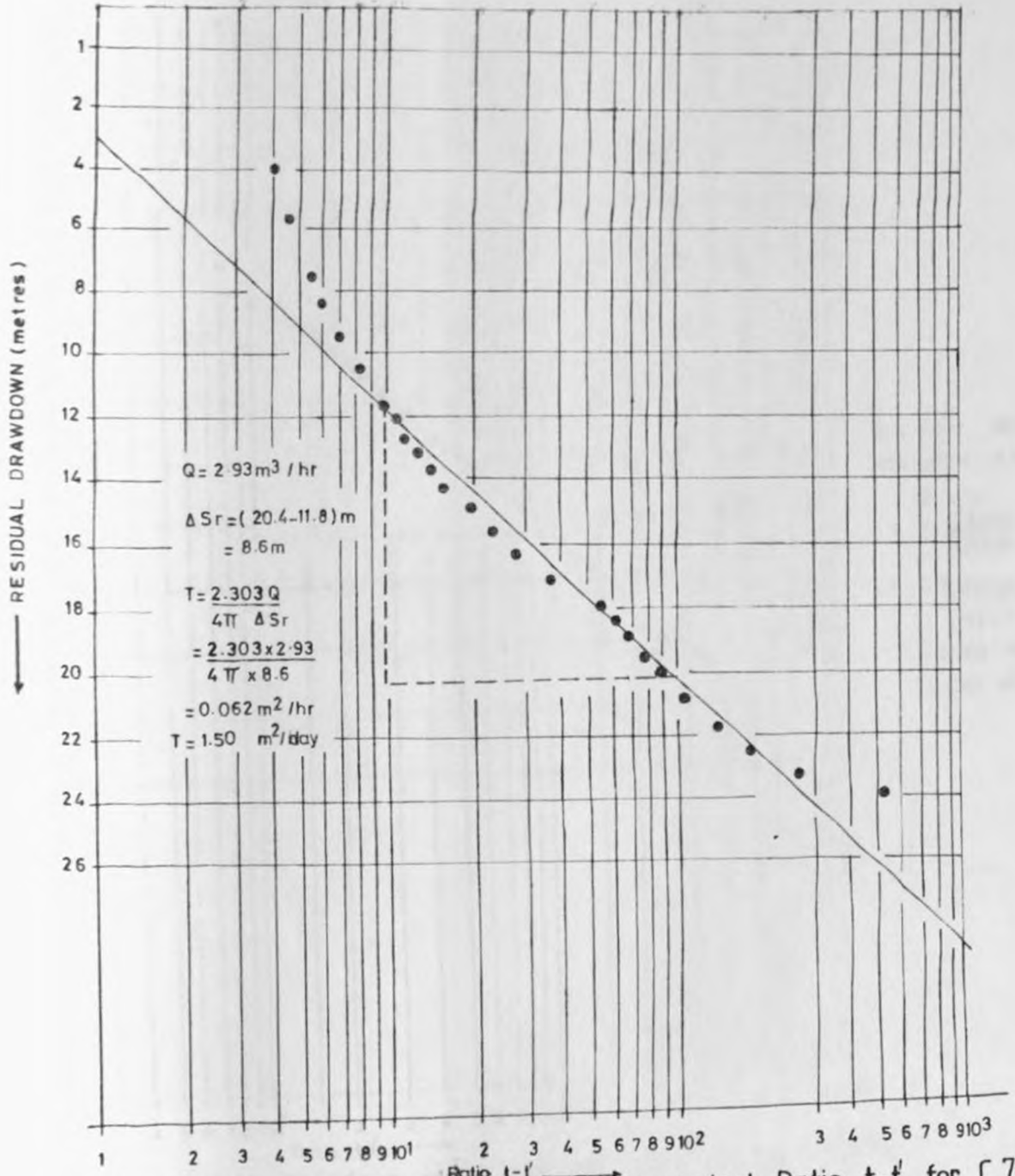
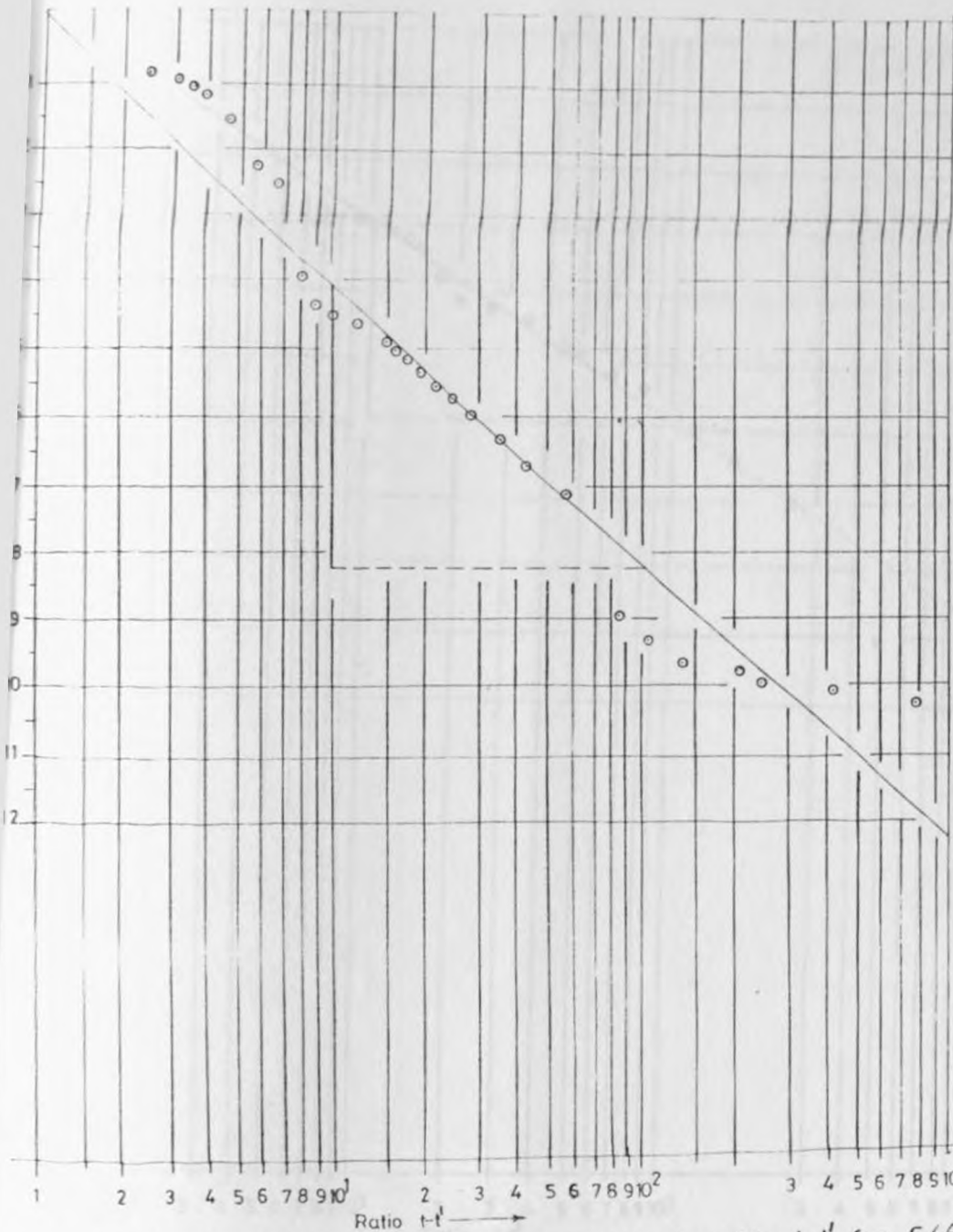


Fig. 5.18 Residual-Drawdown Curve against Ratio $t-t'$ for C 7090

Borehole No 6673



$$\begin{aligned}
 Q &= 4.5 \text{ m}^3/\text{hr} \\
 \Delta S_r &= (8.2 - 4.1) \text{ m} \\
 &= 4.1 \text{ m} \\
 &= \frac{2.303 Q}{4 \pi T \Delta S_r} \\
 &= \frac{2.303 \times 4.5}{4 \pi \times 4.1} \text{ m}^2/\text{hr} \\
 &= 0.201 \text{ m}^2/\text{hr} \\
 &= 4.83 \text{ m}^2/\text{day}
 \end{aligned}$$

Fig. 5.19 Residual Drawdown curve against ratio $t-t'$ for C6673

Borehole N° C 6721

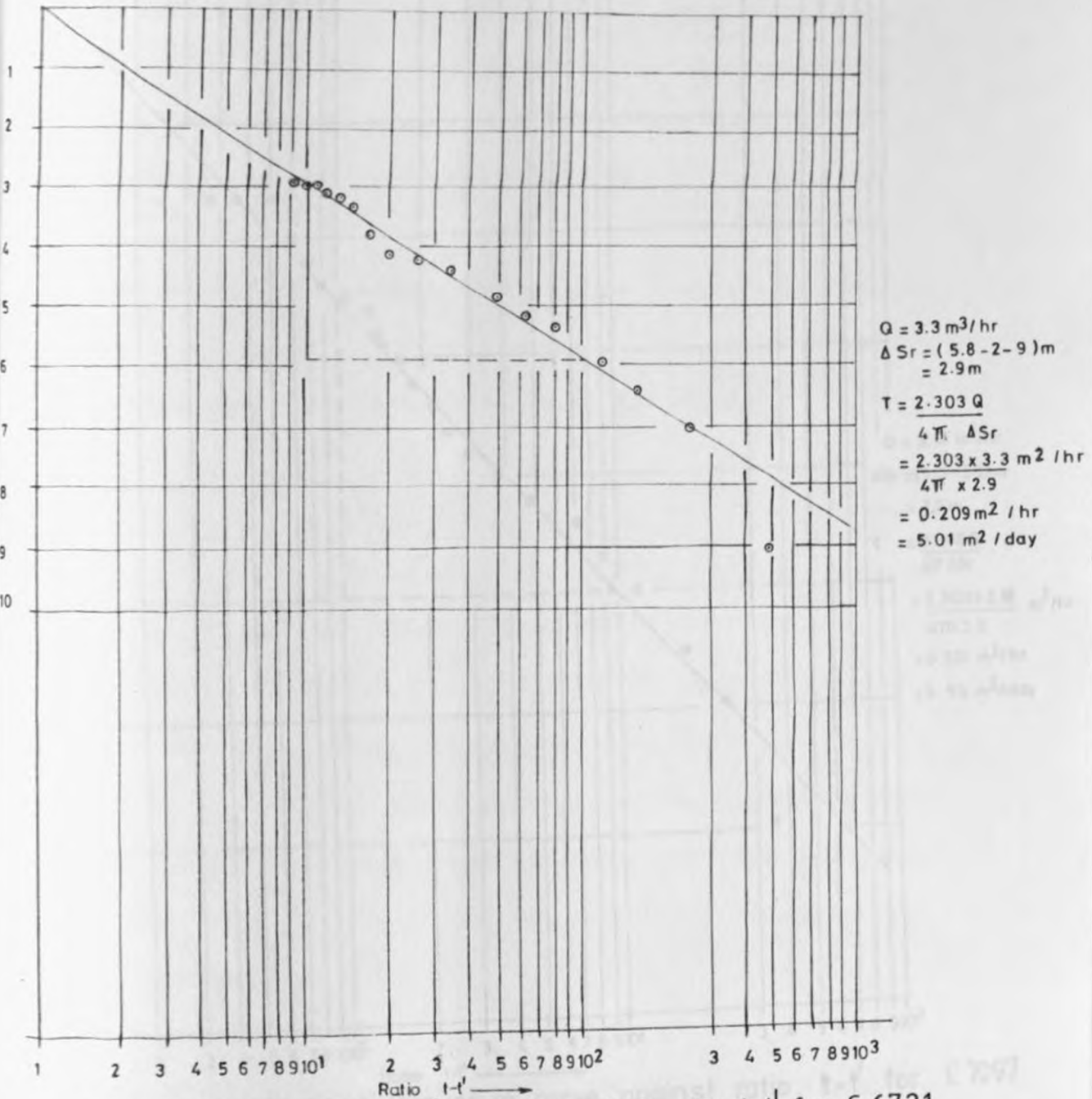


Fig. 5.20 Residual Drawdown curve against ratio $t-t'$ for C 6721

Borehole NEC 7097

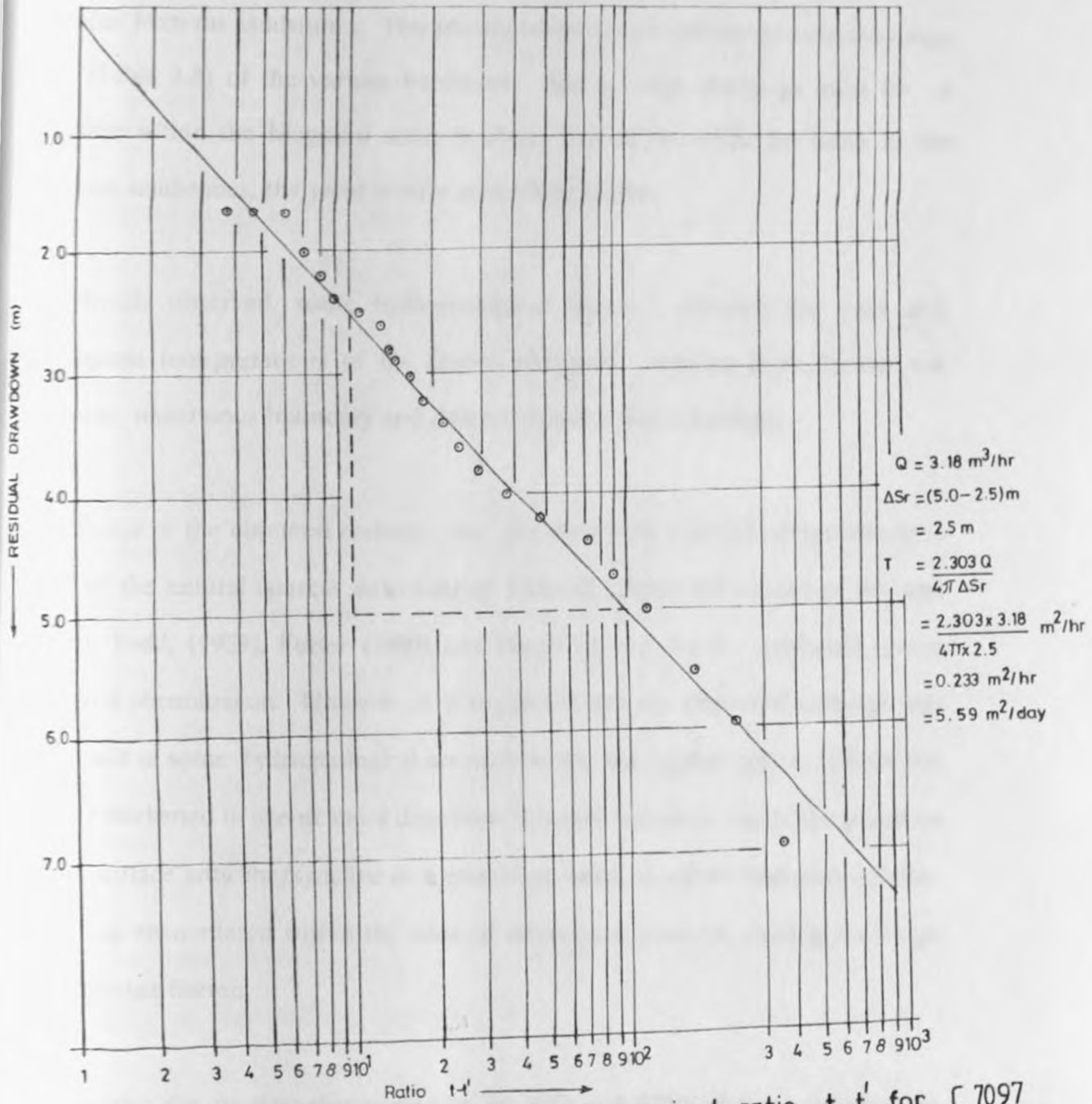


Fig. 5.21 Residual Drawdown curve against ratio $t-t'$ for C 7097

5.104 m³/day. This is as anticipated as the Magarini sands are less consolidated and, therefore, more permeable and any recharge water is transmitted into the groundwater storage more readily than in the compacted, highly cemented and less pervious Mazeras sandstones. This phenomenon is well reflected in the discharge rate (Table 4.3) of the various boreholes. The average discharge rates for a borehole within the Magarini sands is about 3.67 m³/hr while for those in the Mazeras sandstones, the yield is only about 2.32 m³/hr.

As already observed, some hydrogeological factors affected the data and subsequent interpretations of the results obtained. Among those factors are recharge, impervious boundary and delayed yields / slow drainage.

The source of the observed recharge was not clear from the field observations as none of the natural sources described by Driscoll (1986), Groundwater Manual (1981), Todd, (1959), Fetter (1980) and Hazel (1975) can be attributed to the observed phenomenon. However, it is suggested that the observed recharge was as a result of some hydrogeological anomaly within the aquifer system. Either the aquifer thickened in one or more directions from the borehole due to the presence of sub-surface anticline/syncline or a zone/formation of higher hydraulic conductivity was encountered within the cone of depression, thereby, causing the slope to somewhat flatten.

Clays within the stratigraphic sections (Figs 5.5b and 5.7b) of the boreholes are impervious by nature. Therefore, they provide poor paths for water from the storage of the aquifer. The clays may be inclined within the subsurface and may

be of limited lateral extent.

Silty clay layers and some fine grained sands inhibit the vertical flow of water and only readily permit limited horizontal flow. This causes the aquifers to have delayed yields for some time before the aquifer conditions stabilize, thus, displaying the observed phenomenon (Fig 5.17).

The aquifer within the Magarini sands has higher specific capacity values ranging from $0.178 \text{ m}^2/\text{hr}$ to $0.333 \text{ m}^2/\text{hr}$ (Table 4.3) with an average value of $0.276 \text{ m}^2/\text{hr}$ while the corresponding values for compacted Mazeris sandstone aquifer are $0.058 \text{ m}^2/\text{hr}$ to a maximum of $0.125 \text{ m}^2/\text{hr}$ with a mean of $0.101 \text{ m}^2/\text{hr}$.

The relatively thick and laterally extensive saturated Magarini sands aquifers suffer very little drawdown after releasing large volumes of water, thus, showing high specific capacities; whereas the unsaturated or thin and laterally restricted Mazeris sandstones aquifers suffer considerable drawdown even when small volumes of water are abstracted. Hence, their specific capacities are low. Generally, therefore, the higher the specific capacity, the greater the available groundwater resources.

The two parameters also appear to be a reflection of the geological nature of the respective aquifers with the Magarini sands being more permeable since they are unconsolidated and the Mazeris sandstones having low porosity due to their high compaction.

The specific capacity values (Table 4.3) can also be used to evaluate the relative well efficiency. Generally, the well efficiency depends not only on the nature of the aquifer itself but also on either the design or construction factors.

In the project area, boreholes, both in the Magarini sands and Mazeras sandstones, were similarly designed with similar types of screens (usually slotted PVC). Thus, any variation in the specific capacity values could only occur either due to the construction method or the nature of the aquifer system. Either the boreholes were inadequately developed whereby some drilling fluid (Bentonite) was left around the screen (such fluid was only used where caving in the borehole occurred) or the screens were improperly emplaced resulting in partial penetration of the aquifer. However, great care was always taken during this exercise and it is hoped that this problem was greatly minimised.

Otherwise, lower specific capacity values seem to suggest that the aquifer within the Mazeras sandstones is "less efficient" than that of the Magarini sands.

5.3.4 Comparison Between the Interpreted VES and Well Test Analyses Results

The results of both the resistivity survey and the recovery test provide a basis for comparison between the different aquifer systems within the project area.

Comparatively, the aquifer system in the Tertiary Magarini sands is at a depth range of about 25 - 90 m (Table 4.3). The traverse resistance value (Fig 5.11) of the conductive zone within the Magarini sands is low, about 1000 - 4000 Ωm^2 . However, analysis of the recovery test data gives results showing that the aquifer

has higher transmissivity and specific capacity values of 0.276 m²/hr and 0.213 m²/hr, respectively (Table 4.3). Quantitatively, therefore, Magarini sands aquifer yields higher amounts of water (3.67 m³/hr) at relatively shallower depths.

On the other hand, the aquifer within the Mazerias sandstones shows a slightly different trend. The depth range of this aquifer is from about 60 to 125 m (Table 4.3) and has higher transverse resistance values (Fig 5.11) of up to 9000 Ωm². The corresponding results from the hydraulic tests indicate that this aquifer has relatively lower transmissivity and specific capacity values of 0.044 m²/hr and 0.101 m²/hr, respectively. Consequently, the average output from the boreholes of this aquifer is lower (2.32 m³/hr) than that of boreholes in the Magarini sands.

It is, therefore, apparent that from the above comparison, the Mazerias sandstone aquifer is generally "poorer" than that of the Magarini sands both in output and relative depth. However, more water may be obtained from the Mazerias sandstone aquifer if the boreholes are drilled where structural features (Fig 2b) are evident. Such features enhance the recharge into the groundwater storage system, thereby boosting the outputs. This seems to be the situation in the project area, especially where the sites are on elevated ground.

5.4 Interpretation of Water Quality Analysis

Results and Discussions

In order to fully appreciate the groundwater potential in the project area, the chemical characteristics (Table 4.5) of the water samples collected and analyzed as previously described (Chapters 3 and 4) were determined so as to evaluate the

water quality and its possible use.

5.4.1 Dominant Ions

For the analysis of the dominant ions (sodium, potassium, magnesium, sulphate, chloride, and bicarbonate/carbonate), a trilinear diagram method (Piper, 1944; Maina, 1983; Mailu, 1983) was employed. Using this method, various types of water from the aquifers within Magarini sands and Mazeras sandstones were distinguished.

From Fig 5.22 (with ion concentration in epm) , most of the waters from boreholes within the Mazeras sandstones have sodium cation present in appreciable amounts. About 70 per cent of the water samples form a cluster, indicating the presence of 50 per cent and above, of sodium cations. Therefore, they are sodium type of waters. From the anion triangle, about 70 per cent of the borehole water samples have the bicarbonate as the dominant anion. However, 20 per cent of the remaining waters have chloride ions as the dominant anion (over 60 %). Hence, the waters from the Mazeras sandstone aquifer can be classified as sodium bicarbonate or sodium chloride water types.

From the same Fig 5.22, samples of borehole water from Magarini sands have sodium as the dominant cation (over 75 per cent) while both bicarbonate and chloride (50 per cent each) form the anions. Consequently, the waters are either sodium bicarbonate or sodium chloride types.

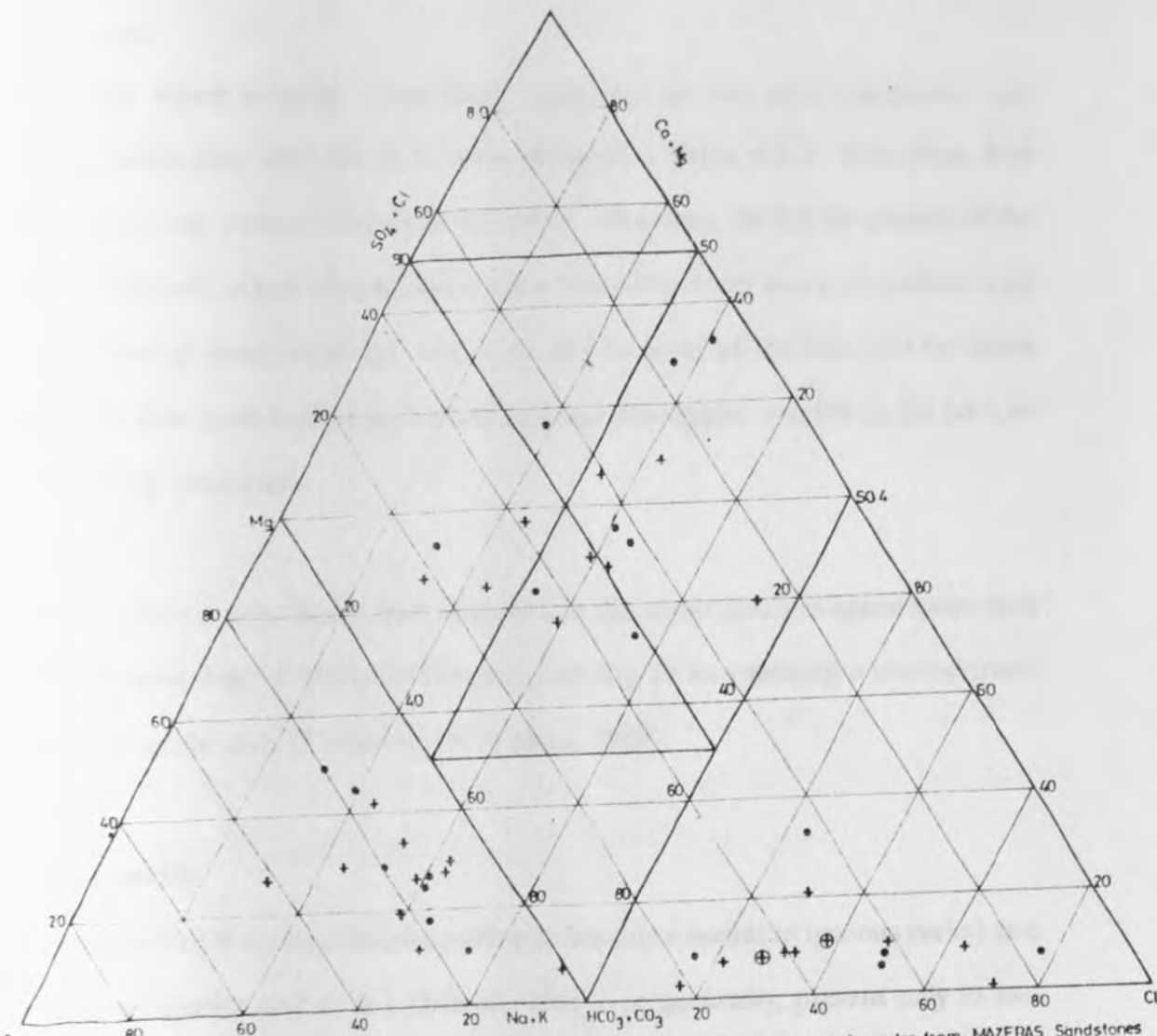


Fig 5. 22 TRILINEAR DIAGRAMS

- + Concentration Values (in epm) of borehole water from MAZERAS Sandstones
- Concentration Values (in epm) of borehole water from MAGARINI Sands
- ⊕ Concentration Values (in epm) of borehole water from both Formation

5.4.2 Minor Ions

Iron (Fe), silica (Si), fluoride (F) and pH constitute minor chemical characteristics in this project.

5.4.2.1 Iron

For all the water samples, both from boreholes in Mazeras sandstones and Magarini sands, iron only occurs in trace amounts (Table 4.5). Therefore, iron does not pose any serious hazards to the water. However, during the course of the author's fieldwork, water samples from some boreholes were found to contain a lot of rust. Most of those boreholes had been idle for most of the time and the users complained that upon boiling such water, a black precipitate was left at the bottom of the boiling containers.

The minute/trace amounts of iron observed in the water analysis agree quite well with the observations of Mailu (1983) and generally, fit a commonly observed trend for most groundwaters (Levinson, 1974; Hem, 1959).

5.4.2.2 Fluoride

Fluoride, derived from fluorite (the principal fluoride mineral in igneous rocks) and the minerals apatite and mica (Driscoll, 1986), is, generally, present only in low concentrations in groundwater since its solubility is low (Hem, 1959).

In the project area, borehole water samples from within the Mazeras sandstone aquifer have fluoride content ranging from 0.00 to 0.50 ppm with a mean value of 0.17 ppm while those within the Magarini sand have their fluoride values in the

range of 0.00 to 0.80 ppm with a mean of 0.16 ppm.

5.4.2.3 Silica

Silicon, the second most abundant element in the Earth's crust after oxygen (Driscoll, 1986), forms a broad range of rock forming minerals. It is not readily dissolved by water but, nevertheless, warm water sometimes contains as much as 100 ppm silica; and silica concentrations of 20 ppm are common (Driscoll, 1986).

In this project, water samples from boreholes within the Mazeras sandstone aquifer have silicon amounts ranging from 20 to 80 ppm (Table 4.5) with a mean value of 48 ppm. Those water samples from boreholes within the Magarini sands have amounts of silica in the range of 16 to 100 ppm with a mean value of 40.4 ppm.

5.4.2.4 PH

The pH values are important in groundwater investigations since they assist in the evaluation of the reactivity of the waters. Waters with low pH tend to be corrosive. Freeze and Cherry (1979) remark that the tendency for adsorption of cations or anions plus the cation exchange capacity all depend on the pH.

The pH values for water samples from boreholes within the Mazeras sandstone aquifer range from 6.5 to 8.0 ppm with a mean of 7.23 ppm. Those samples in the Magarini sands aquifer have pH values in the range of 6.0 to 8.0 ppm and a mean value of 6.89 ppm. Thus, waters in the two aquifer systems are essentially neutral. The pH values for these waters in the project area are within the "normal" 6 - 9 range (Freeze and Cherry, 1979) for groundwater.

5.4.2.5 Specific Conductance and Total Dissolved Solids (TDS)

Driscoll (1986) and Hem (1970) remark that pure liquid water has very low electrical conductance. However, the presence of charged ionic species in solution makes it conductive. Since natural waters contain a variety of both ionic and uncharged species in various amounts and proportions, then, determinations of the conductance cannot be used to obtain accurate estimates of ionic concentrations or total dissolved solid. However, specific conductance values are often useful as a general indication of the total dissolved solids.

Freeze and Cherry (1979) and Driscoll (1986) have given a conversion relationship between conductance values and TDS as shown below:

$$\text{TDS} = A \times C$$

where,

C is the conductance in $\mu\text{S}/\text{cm}$, **TDS** is expressed in ppm and

A is a conversion factor.

Estimation of total dissolved solids from conductivity measurements is convenient because conductivity can be determined quickly in the field using rather simple equipment and procedures. Examination of the TDS and specific conductance values (Table 4.5) gives an average conversion factor (**C**) for borehole waters within the Mazeras sandstones of **0.69** while the value for those samples in Magarini sands is **0.62**. These values fall within the **0.55 - 0.75** range given by both Driscoll (1986) and Freeze and Cherry (1979).

A simple but widely used scheme for categorizing groundwater based on TDS is given in Table 5.4.

Table 5.4 Categorization of Groundwater based on TDS

CATEGORY	TOTAL DISSOLVED SOLIDS (PPM)
Freshwater	0 - 1000
Brackishwater	1000 - 10,000
Saline water	10,000 - 100,000
Brine water	more than 100,000

SOURCE: FREEZE & CHERRY (1979)

Using this categorization, it is apparent that all the borehole water samples within the project area (except one sample, no. 8218) are freshwaters.

5.4.3 Discussions on the Water Analysis

5.4.3.1 Water Quality and Use

The primary purpose of a water analysis is to determine the suitability of water for a proposed use as groundwater quality is of nearly equal importance to quantity (Walton, 1970; Todd, 1959). The three main classes of use are domestic, agricultural and industrial.

5.4.3.1.1 Domestic Use

Various water standards have been recommended and formulated for use for domestic purposes by re-known organisations such as World Health Organisation, W.H.O.,(1984) and Kenya Bureau of Standards (K.B.S.) specifications, part "a", (1985) as shown in Table 5.5. The express purpose of regulating the water usage is to minimise hazards that such waters may otherwise cause.

By these standards, it is evident that all the waters within the entire project area, except for those near borehole no. 8218 (Table 4.5) are generally potable and fit for domestic human consumption and use.

5.4.3.1.2 Industrial Use

The quality requirements for industrial waters vary widely according to the potential use. For most industrial purposes, water must be of much higher quality. Municipal supplies are generally good enough to satisfy the quality requirements of most processes. Often, groundwater may be desirable for particular uses due to its low relatively constant temperature.

In the project area, only a few factories are found reflecting low economic productivity. These factories process such agricultural products as bixa, cashewnuts and coconuts. The now defunct Ramisi sugar factory is also found within the project area. The groundwater supplies in this area are suitable for these processes with only a little treatment.

Table 5.5 Drinking Water Specifications, Kenya Standards (K.B.S.), (1985)

Substance or Characteristic	Unit	Guideline Value	Highest desirable level	Maximum permissible level	Maximum admissible conc.
Fluoride	ppm	1.5	0.9	1.7	1.5
Chlorine	ppm	250	200	600	-
Sulphate	ppm	400	200	400	250
Sodium	ppm	200	-	-	175
Potassium	ppm	-	-	-	12
Magnesium	ppm	-	30	150	50
Calcium	ppm	-	75	200	-
Iron	ppm	0.30	0.10	1.0	0.20
TDS	ppm	1000	500	1500	1500
pH	pH	6.5-8.5	7.0-8.5	6.5-9.2	7.5

5.4.3.1.3 Irrigation Use

Water quality problems in irrigation include salinity and toxicity. Excessive salinity may occur when the soil permeability is significantly reduced by the build up of salts in the top soils. Consequently, crop production is limited since sufficient water cannot reach the root zone. Toxicity is also another problem in maintaining good yields. Some common toxic substances include sodium, boron and chloride (Driscoll, 1986).

Sodium, a soluble product during weathering of plagioclase feldspars (Davis and Dewiest, 1966), has far-reaching effects on soils. Because of this importance, a method to measure the effect of its ions has been adopted by McLaughlin (1966), Mailu (1983) and Driscoll (1986). This method measures the sodium adsorption ratio (SAR) which is calculated by using the following equation:-

$$SAR = \frac{Na}{\sqrt{\left(\frac{Ca+Mg}{2}\right)}} \quad \text{Eqn 5.1}$$

where,

sodium, calcium and magnesium are in ppm (Table 4.5).

Table 5.6 gives the calculated values of SAR for all the borehole water samples in the project area. From this table, except for borehole no.8218 with an SAR value of 30.82, the other samples within the Mazeras sandstones have low SAR values between the range of 1.185 and 3.795 with a mean value of 2.320. For those within the Magarini sands, the SAR values are in the range of 0.711 to 3.265 and a mean of 1.991.

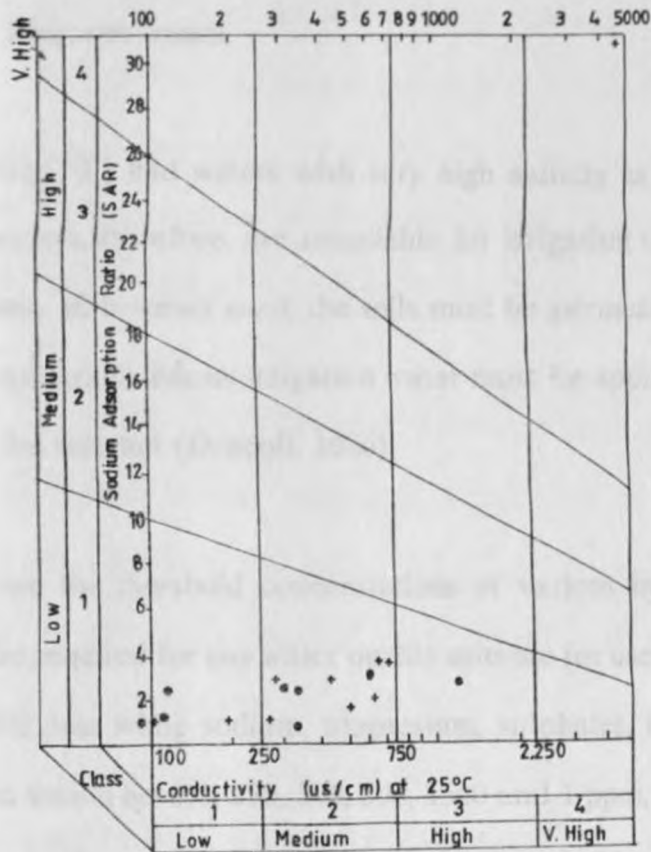
Most of the water samples have very low SAR values and are, therefore, suitable for irrigating most crops. Since the SAR values are less than 10, a value far much less than the critical SAR value of 18, (Driscoll, 1986) then they pose little danger of the sodium problem. Fig 5.23 drawn using the SAR values in Table 5.6 has been used to classify the borehole waters in the project area based on the salinity hazard indicated by the electrical conductivity of the water and the sodium or alkali hazard, (SAR).

Water samples from the boreholes within the Mazeras sandstones have low to medium salinities and also sodium toxicity (Fig 5.23). Consequently, they can be used for irrigating most crops with little likelihood that soil salinity will develop.

TABLE 5.6 SAR VALUES FOR BOREHOLE WATER SAMPLES IN MAGARINI SANDS AND MAZERAS SANDSTONES IN KIDIANI AREA KWALE

MAZERAS SANDSTONES			MAGARINI SANDS		
SAMPLE	No.	SAR	SAMPLE	No.	SAR
Mzs-1		3.795	Ms-1		1.313
Mzs-2		1.185	Ms-2		0.711
Mzs-3		3.193	Ms-3		3.265
Mzs-4		3.562	Ms-4		2.651
Mzs-5		2.182	Ms-5		1.031
Mzs-6		1.367	Ms-6		2.279
Mzs-7		2.799	Ms-7		2.293
Mzs-8		1.360	Ms-8		2.382
Mzs-9		1.434			
Mzs-10		30.817			

However, sodium sensitive crops such as avocados may accumulate injurious sodium concentrations. According to Driscoll (1986), most of these waters are hazardous



- + Water samples from Mazeras sandstones.
- Water samples from Magarini sands.

Fig. 5.23 Classification of irrigation waters based on SAR and conductivity [Adapted from Driscoll (1986)]

to use on fine-textured soils with high cation exchange capacity. They, however, may be used on coarse-textured organic soils with good permeability, qualities of the soils prevalent in the project area. The same can be said for those waters from boreholes within the Magarini sands.

Only one sample (Mzs-10) had waters with very high salinity as well as high sodium toxicity. Its waters, therefore, are unsuitable for irrigation under normal and ordinary conditions. If, however used, the soils must be permeable, drainage must be adequate, considerable excess irrigation water must be applied, and very tolerant crops should be selected (Driscoll, 1986).

Maina (1983) has given the threshold concentrations of various hydrochemical parameters that may be required for any water quality suitable for use by livestock. Calcium should be 500 ppm while sodium, magnesium, sulphates, bicarbonates, chlorides and fluorides should be 100, 250, 500, 500, 1500 and 1 ppm, respectively. Therefore, the waters in the project area are obviously suitable for livestock consumption.

5.4.3.2 Relation to Geology

From the interpretation given earlier, the waters in the entire project area are of mixed types, i.e., they are either sodium bicarbonate or sodium chloride waters. This could probably be associated with the environment in which such waters were formed. It could also be a reflection of some geographic factors such as rainfall and temperatures. According to Driscoll (1986), rainwater in coastal regions, generally, contains more chlorides than it does further inland. He further remarks

that atmospheric chlorides contribute about 0.4 ppm to the total chloride content of inland surface waters. Since the rainfall in this area is relatively high (about 1000 mm p.a.), then high amounts of chlorides are dissolved in it. Due to high temperatures (average of 27° C) prevalent in this area, the water evaporates leaving behind chloride and other dissolved salts as evaporites. These, then, tend to leach into the surrounding rock formations and may be trapped as groundwater. This probably explains the high content of the chloride and other dissolved salts in borehole no. 8218 and others near its vicinity.

Maina (1983) and Ongweny (1973) observed that the chemical components of groundwater are not only as a result of geographic factors (climatic, hydrologic, biologic and chemical processes) but also geological processes (mineralogical composition, structure and texture of specific rock types). Todd (1959) has shown that the concentration of salts in water depends on the environment, movement and source of groundwater. He has further indicated that the supply of ions in groundwater is provided by the solution of rocks or soils through which the water has travelled. This is what Freeze and Cherry (1979) refer to as "the order of encounter".

Various factors seem to have contributed greatly to the chemistry of groundwater in this area. However, geological factors have had a greater effect as can be observed from the analysis. The relatively high amounts of silicon noted in these waters are indicative of the vast amounts of silica (quartz in sands) that are found in this area. Chemical weathering of silicate minerals due to high temperatures and rainfall result in the dissolution of silica.

Only little amounts of sulphates are observed in these waters. Their origin may not entirely be evaporite. Their presence may be associated with galena and possibly pyrite (Du Bois, 1970) due to oxidation processes. Caswell (1953) and Miller (1952) have explained the presence of sulphates in ground waters within Taru grits and Maji-ya-Chumvi beds as being due to formation of evaporites in the land-locked basins. These evaporites are marine in origin. However, Mazeras sandstones, Magarini sands and Kilindini sands are continental in origin. This, therefore, explains the minute amounts of the sulphates present.

It is for the same reason that the TDS are lower for these waters than would be expected for groundwaters within marine sediments. Marine sediments, according to Bredehoeft (1963), are associated with connate water. Thus, the water samples have more TDS than water derived from continental sediments. High potential evaporation in this area could, however, increase the TDS.

Fluoride in these waters is associated with the presence of micas within the predominant rock formations, especially the flaggy sandstones. The fluoride concentration is less than the recommended 1.5 ppm by W.H.O.(1973, 1984) and may be helpful in preventing tooth decay.

There is little iron in the aquifers themselves. However, the high amounts often detected in some boreholes essentially originate from secondary sources such as piping, screens and pump parts which have decayed and disintegrated into the groundwater system, thereby resulting in bacteriological contamination (Mlengu, 1983).

The pH values indicate that these waters are basically neutral. Consequently, they are not corrosive.

Other parameters in these waters are as expected. Their relative concentrations seem to agree with what other researchers have observed (Driscoll, 1986; Freeze and Cherry, 1979; Maina, 1983; Mailu, 1983). However, modification of these parameter concentrations by various geographic factors cannot be underestimated.

In this area, the groundwater flow is generally either easterly or southerly. Therefore, boreholes found towards these discharge zones should have higher concentrations of dissolved salts (TDS). However, this does not seem to be the case. Therefore, it is suggested that the groundwater quality is dependent on the ambient geological conditions prevalent in a particular locality.

Previous researchers have expressed fear of sea-water intrusion (Bestow, 1958; Caswell, 1953; Gentle, 1968). However, their data on which they based their recommendation was limited. From the present results, this does not seem to be a problem. Mwangi (1981) delineated the sea-fresh water boundary to be about 6 km from the coastline and Majanga (1987) remarked that the depth to the salt water seems to increase from the coastline towards the inland. Hence, it is suggested that the presence of a coral ridge parallel to the coastline provides a barrier to the subsurface invasion by sea-water.

5.4.4 Correlation Between Aquifer Resistivity and Salinity

In order to interpret the aquifer resistivity determined from the model curves of the vertical electrical sounding (VES) data (Appendix B) in terms of the water quality, the formation factor of the rock formations (Al-Ruwaih and Ali, 1986 and Mathiez and Huot, 1966) was assumed to be constant throughout the entire area covered by the same geological formation. Thus, any variations in the aquifer resistivity reflect changes in the water quality. However, such an assumption is greatly subjective since it ignores the effects of porosity, cementation factor and, to a lesser extent, the temperature of groundwater. (Archie, 1942 in Al Ruwaih and Ali, 1986).

The correlation between the aquifer resistivity and the groundwater salinity, measured in terms of TDS (ppm) and compared with the specific conductance (Table 4.5), is shown in Fig 5.24 .

A summary of the determined aquifer resistivity values and the salinity of the borehole waters within Mazeras sandstone formation is presented in Table 5.7 below.

Table 5.7 Salinity and Aquifer Resistivity of some Boreholes in Mazeras sandstones in Kidiani Area, Kwale.

Borehole Number	Conductivity ($\mu\text{S}/\text{cm}$)	TDS ppm	Aquifer Resistivity (Ωm)
7282	750	517.5	14
7280	650	449	20
7281	340	235	35
7283	140	97	80
7932	220	152	70

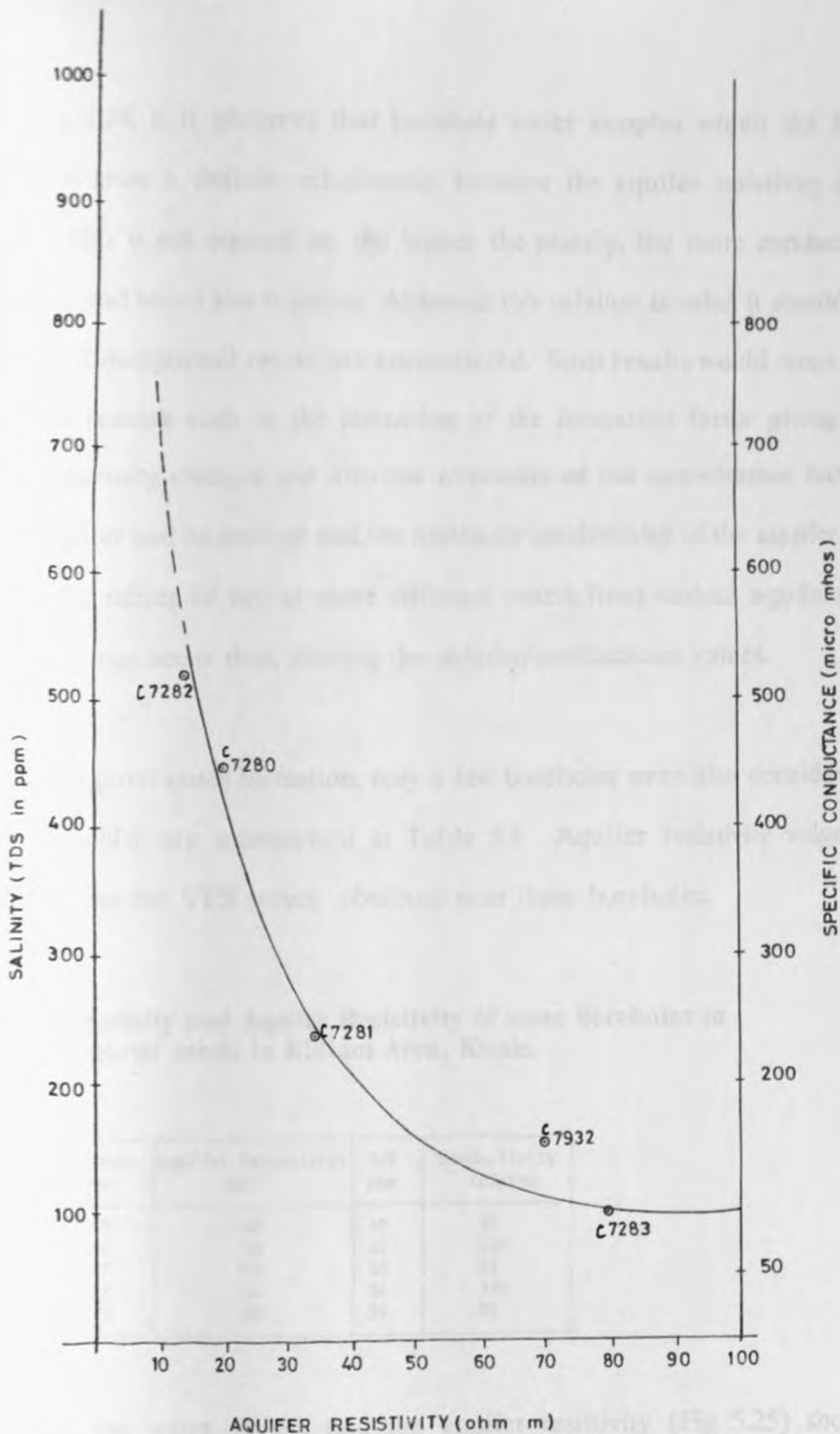


Fig. 5.24 Comparison between aquifer resistivity and groundwater salinity in Mazeras sandstones in Kidiani area Kwale.

From Fig 5.24, it is observed that borehole water samples within the Mazeras sandstones show a definite relationship between the aquifer resistivity and the salinity. This is not unusual as the higher the salinity, the more conductive the waters are and hence less resistive. Although this relation is valid, it should not be surprising if exceptional results are encountered. Such results would come up due to several reasons such as the alteration of the formation factor giving rise to different porosity changes and also the alteration of the cementation factor, the type of aquifer and its geology and the hydraulic conductivity of the aquifer. More importantly, mixing of two or more different waters from various aquifers within a borehole may occur thus, altering the salinity/conductance values.

For the Magarini sands formation, only a few boreholes were also considered, the results of which are summarised in Table 5.8. Aquifer resistivity values were obtained from the VES curves obtained near these boreholes.

Table 5.8 Salinity and Aquifer Resistivity of some Boreholes in Magarini sands in Kidiani Area, Kwale.

Borehole Number	Aquifer Resistivity (Ωm)	TDS ppm	Conductivity ($\mu\text{S}/\text{cm}$)
7363	40	49	85
6669	50	62	100
5557	60	50	81
7602	40	84	136
6673	80	59	95

A plot of the water salinity and the aquifer resistivity (Fig 5.25) shows the relationship between the salinity and the aquifer resistivity. As observed in Fig 5.24, this plot yet again shows a rather agreeable relationship; that as the salinity

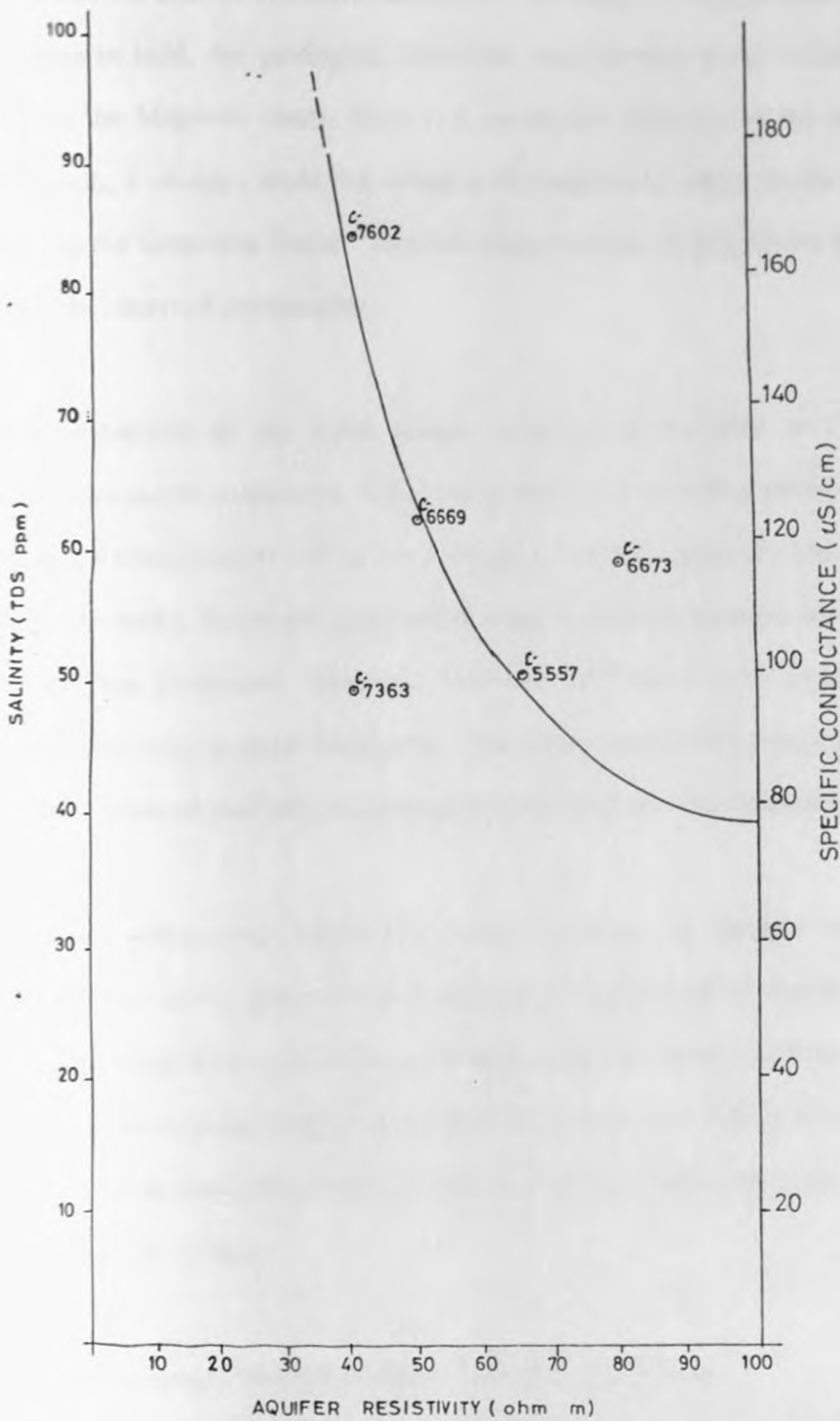


Fig. 5.25 Comparison between aquifer resistivity and groundwater salinity in Magarini sands in Kidiani area Kwale.

increases the aquifer resistivity decreases. It should be emphasized that, for this relation to hold, the geological formation must remain more or less the same. Within the Magarini sands, there is a noticeable variation of the surface layer. Generally, it changes from red, compact formation to a white, sandy one, thereby altering the formation factor. The following example clearly shows this deviation from the observed relationship.

The conductivity of the water sample collected at borehole no C7592 is 250 microsiemens per centimetre. This value gives a corresponding salinity value of 155 ppm (250×0.62 , where 0.62 is the average conversion factor for boreholes within Magarini sands). From the graph in Fig 5.25, the expected aquifer resistivity would be less than 20 ohm-m. However, from the VES curve, it is apparent that the aquifer resistivity is about 80 ohm-m. This clearly shows the variation of Magarini sands in terms of porosity, cementation factor and the clay content present.

Thus, the relationship established above between the aquifer resistivity and groundwater salinity within the two different geological formations should only be used where and when it has been established that the formation characteristics are similar to those of the project area where the above observations were made. Any variations and alterations in the formations will only negate from this relationship and reduce its validity.

5.4.5 Groundwater Potential Distribution in Kidiani Area

The groundwater potential in the different aquifers in the project area was evaluated by considering such factors as the amount of available recharge,

hydrogeological characteristics of the aquifers and other geological factors.

5.4.5.1 Rainfall/Recharge

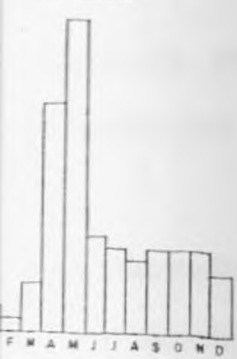
To study the recharge potential, analysis of rainfall distribution patterns and its variation in time is considered. Rainfall distribution in both time and space is given in Table 1. From this table, the highlands in the northwest of the project area exclusively covered by the Mazeras sandstones receive good rainfall amounts as indicated by rainfall stations at Shimba Hills Settlement and Kikoneni Agriculture Station (Fig 5.26). From the same figure, a not dissimilar pattern of rainfall distribution is observed in the central parts of Kidiani Area covered by Magarini sands as indicated by the rainfall station at Kwale (Buda) Forest Station.

A similar observation is made in the eastern part of the project area which is covered by the Kilindini sands formation. This is clearly indicated by the data recorded at the rainfall stations at Tiwi Chief's Camp and Msambweni District Office.

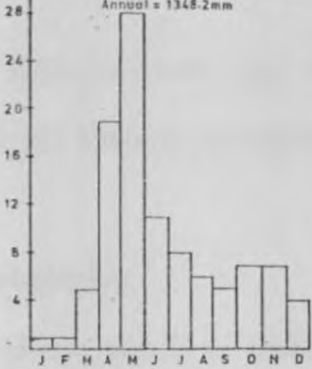
It is apparent that, in the regions covered by the Mazeras sandstones, over 64% of the average annual precipitation (> 1140 mm) falls during the long and the short rainy seasons in the months of April-June and October-November, respectively. However, in the areas covered by the Magarini sands, only about 61% of the annual precipitation (> 1215 mm) falls within the same period while in areas where the Kilindini sands are dominant, about 70% of the average annual precipitation (> 1270 mm) falls during the same period.

KILINDINI SANDS

TCC - TIWI CHIEFS CAMP
Annual = 1190.9mm

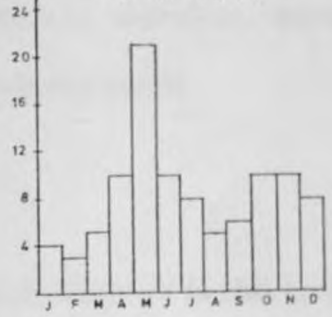


MDO - MSAMBWENI DISTRICT OFFICE
Annual = 1348.2mm



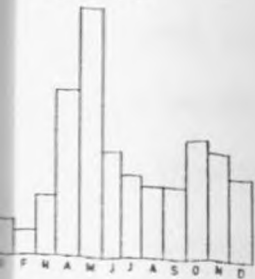
MAGARINI SANDS

KFS - KWALE FOREST STATION
Annual = 1215.7mm

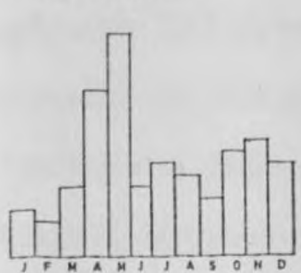


MAZERAS SANDSTONES

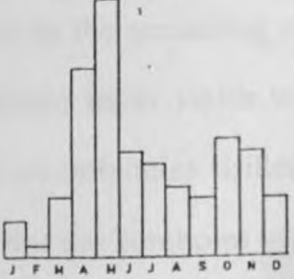
KAS - KWALE AGRIC STATION
Annual = 1088.3mm



NCO - NDAYAYA CHIEFS CAMP
Annual = 846.5mm



SHS - SHIMBA HILLS SETTLEMENT
Annual = 1311.5mm



KKS - KIKOHENI AGRIC STATION
Annual = 1304.6mm

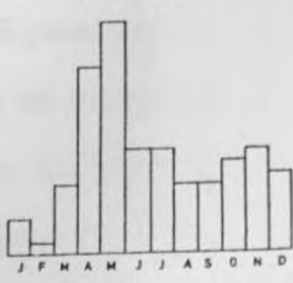


Fig. 5.26 Mean monthly rainfall distribution patterns

5.4.5.2 Well Characteristics

From the aquifer characteristics data (Table 4.3), it is apparent that the Mazeras sandstones aquifer is less pervious (average $Q/S = 0.101 \text{ m}^2/\text{hr}$, $T = 1.048 \text{ m}^2/\text{day}$) than the aquifer within the more porous Magarini sands (average $Q/S = 0.178 \text{ m}^2/\text{hr}$; $T = 5.104 \text{ m}^2/\text{day}$). According to Thambu (1987), the Kilindini sands at the south-coast have very high transmissivity values and also high specific capacity values.

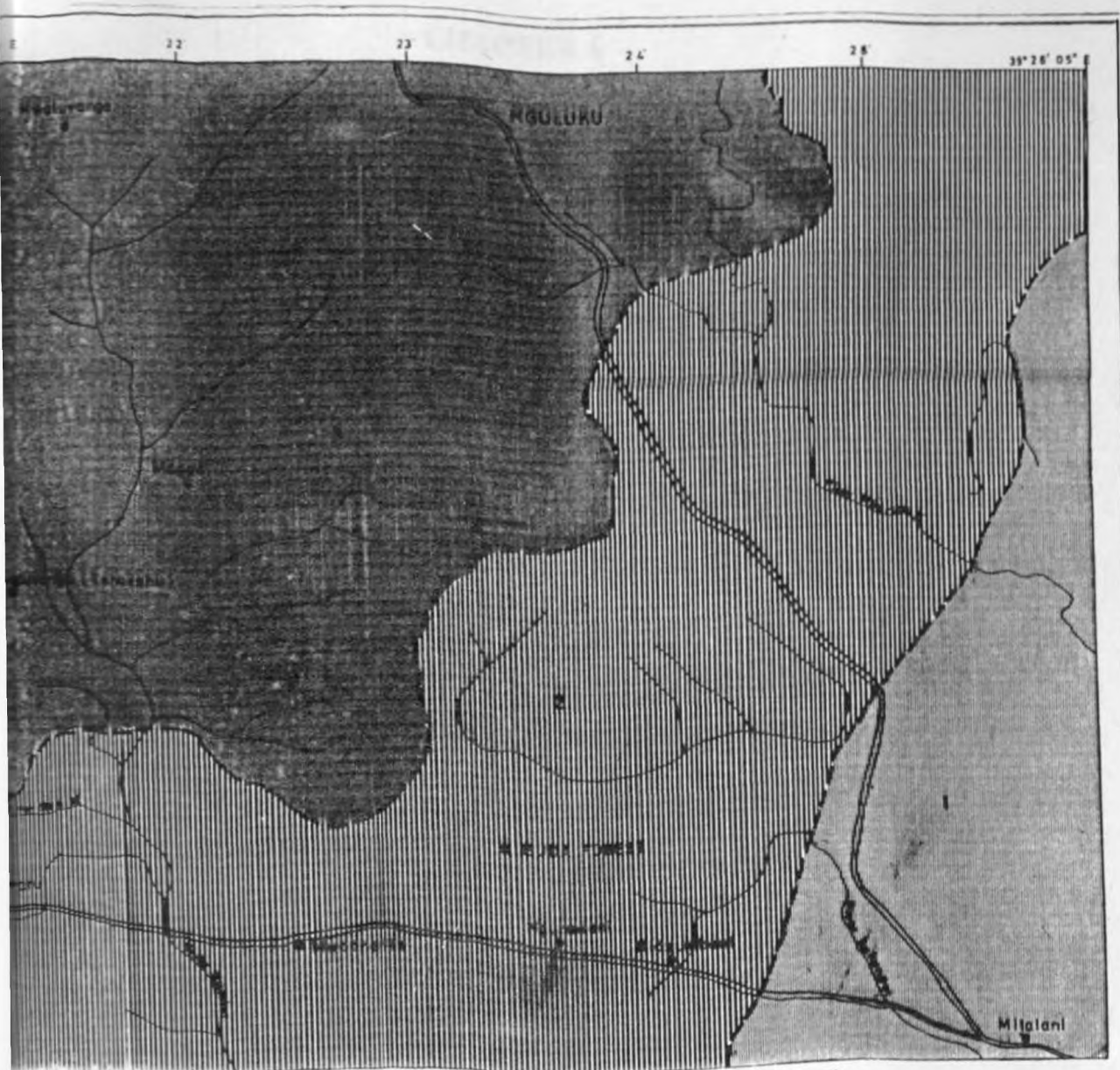
Geologically, these Kilindini sands are well sorted and are, therefore, more permeable than both the Mazeras sandstones and the Magarini sands.

5.4.5.3 Boreholes Distribution

Further assessment of the general groundwater potential distribution in this area can be made from the analysis of the distribution of boreholes already drilled. 60% of these boreholes penetrate the Magarini sands aquifer and have relatively higher yields averaging about $3.67 \text{ m}^3/\text{hr}$ while the remaining 40% penetrate the Mazeras sandstones aquifer and have generally lower yields with an average of about $2.32 \text{ m}^3/\text{hr}$. In this area, there are no boreholes drilled in the Kilindini sands. However, Thambu (1987) observed that the boreholes which penetrate this aquifer have very high yields of about $20 \text{ m}^3/\text{hr}$ at very shallow depths.

Thus, by combining the precipitation/recharge data, the hydraulic characteristics of the different aquifers and the information obtained from the piezometric map (Fig 5.10), it is concluded that the aquifer within the Kilindini sands has high groundwater potential while the Magarini sands aquifer has intermediate

groundwater potential. The Mazeras sandstones aquifer has, relatively, the lowest groundwater potential than the other two types of aquifers. This analysis is summarised in the groundwater potential distribution map in Figure 5.27.



LEGEND			
	HIGH POTENTIAL	MEDIUM POTENTIAL	MODERATE / LOW POTENTIAL
Type of Aquifer	Kilindini sands	Magarini sands	Mazeras sandstones
Permeability (T)	0.445 m ³ /hr /m	0.276 m ³ /hr /m	0.044 m ³ /hr /m
Water Capacity (Q ₁₅)	0.608 m ² /hr	0.213 m ² /hr	0.101 m ² /hr
Large Test Well Yield/Quality	6.00 m ³ /hr (Good)	3.67 m ³ /hr (Good)	2.32 m ³ /hr (Good although it could be saline)
Annual Rainfall (average-indicative recharge)	1270 mm	1216 mm	1138 mm

Fig. 5.27 Groundwater potential distribution map

CHAPTER 6

CONCLUSIONS AND RECOMMENDATIONS

6.1 Vertical Electrical Soundings (VES)

The main objective of this study was to determine the applicability of the vertical electrical sounding in relation to exploration and evaluation of groundwater potential in Kidiani area with special emphasis on the demarcation of water quality interfaces. This objective was achieved by making twenty five (25) geo-electrical vertical sounding measurements in Kidiani area where already some hydrogeological information was available.

6.1.1 Conclusions

From the analysis and interpretation of the VES data, it is concluded that the use of the computer curve modelling technique to interpret the VES data permitted rather accurate delineation of conductive/non- conductive zones and recognition of hydro-lithostratigraphical units. Since, within the conductive zone, salinity controls resistivity changes both vertically and laterally, then geoelectric layers were only interpreted in terms of water quality horizons.

The presence of thin clay layers observed from the borehole logs hydrogeologically subdivide the saturated zone into a multi-aquifer system. However, due to their small relative thicknesses, these layers could not be resolved by conventional VES measurements.

The last high resistivity layer underlying the Mazeras sandstones is due to the fresh, relatively unfractured sandstone rock. In the areas covered by the Kilindini sands, inter-fingering of these sands with the coral limestone was suggested with the high resistivity values being associated with the unweathered and unsaturated coral limestone formation.

A generalised graphical empirical relationship has been established between the aquifer resistivity and the water salinity (TDS). Some correlation, however loose, between the transverse resistance (T_r) and the best area(s) for groundwater prospecting has also been suggested whereby T_r values of more than 3000 ohm-m² (for Mazeras sandstones) and 2000 ohm-m² (for Magarini sands) occur at the most promising sites. However, it must be emphasized that this correlation must be cautiously applied since it is only applicable where the geological formation and other formation parameters are similar to those of the project area.

Finally, correlation between the resistivity values and formation characteristics from the borehole stratigraphic sections is fairly good, up to a depth of 50 metres for Magarini sands and 70 metres for Mazeras sandstone. However, lack of deep boreholes in this area inhibited accurate resistivity correlation at greater depth of probe.

6.1.2 Recommendations

According to Dindi (1983), two deep NE-SW trending faults are passing under the project area. However, they were not detected since the resistivity soundings were done to a maximum AB/2 spacing of only 250 m. It is a well accepted fact that

faults are excellent groundwater reservoirs. Consequently, only deep soundings (AB/2 spacing of 1000 m) will be able to map these faults, thereby enhancing the groundwater potential in the area. Therefore, deeper well-logged boreholes, even if they may be for exploratory purposes only, should be drilled within both the Tertiary Magarini sands and the Triassic Mazeras sediments so as to calibrate the resistivity data obtained with large AB/2 spacing.

Further, it has been established that there is a strong structural control of groundwater resource in this area. It is therefore, recommended that resistivity surveys should be concentrated in areas where structural features are discernable. This would increase the prospects of striking huge quantities of groundwater.

To supplement this method of investigation, reflection seismic method should be applied to corroborate deeper soundings and also sufficiently map the structural nature of the subsurface. Similar work carried out in north - eastern Tanzania gave encouraging results.

From the resistivity soundings, therefore, productive boreholes are expected at the zone of "internal drainage" demarcated on the apparent resistivity map with AB/2 spacing of 1000 m. This is the best site for prospecting for groundwater within the Mazeras sandstones. As such, a borehole should be drilled within this zone to confirm this observation.

The experience of the author during the course of fieldwork tends to suggest that, for best results, any resistivity soundings in this area should be done just after a

rainfall. If done during the dry weather, then it is recommended that elaborate precautions should be taken to improve the surface contacts of the current electrodes. One way of doing so would be to wet the current electrodes. Otherwise, the dry nature of the surface soil would increase the contact resistance at the current electrodes, thus making current penetration a major problem.

6.2 Well Tests

Jacob's straight line approximation method was applied to the recovery data obtained from a few representative boreholes in the project area. The recovery data were preferred as they were free from interference by pumping vibration noise. Further, there was no momentary alteration of the pumping rates by the personnel and no well losses needed to be corrected for. Consequently, fair and reliable results were obtained from the analysis of these data leading to the following conclusions and recommendations.

6.2.1 Conclusions

From the interpretation of the recovery data, three major hydrogeological factors were deduced to have affected the test. These are:-

- (a) recharge possibly due to thickening of the aquifer during the course of pumping or an increase of the hydraulic conductivity of the aquifer material,
- (b) impervious boundaries mainly due to the presence of thick clay beds within the aquifer(s) and
- (c) delayed yields/ slow drainage arising from the presence of fine silty clayey layers which inhibited vertical flow of water in the aquifer.

It is further concluded that Magarini sands aquifer has higher transmissivity ($5.104 \text{ m}^2/\text{day}$) and specific capacity ($0.276 \text{ m}^2/\text{hr}$) values than the Mazeras sandstones aquifer with respective values of $1.048 \text{ m}^2/\text{day}$ and $0.101 \text{ m}^2/\text{hr}$. Thus, the aquifer within the Magarini sands is more productive ($3.67 \text{ m}^3/\text{hr}$) than the one in the Mazeras sandstone formation with an average output of $2.32 \text{ m}^3/\text{hr}$.

6.2.2 Recommendations

On the basis of the above conclusions, it is recommended that full and detailed pumping test with observation borehole(s) should be carried out. Such a test will provide data from which not only the principal factors of the aquifer performance - transmissivity and storage coefficient, but also the performance characteristics of the aquifer will be well determined.

It is further recommended that during the performance of this test, effects on the drawdown by changes in barometric pressures, nearby stream levels and tidal oscillations should be given due attention. This will help in determining and planning of long term groundwater resources in the area. Should this prove expensive, as is usually the case, then step-drawdown well tests should be carried out. Such tests not only yield the above evaluated aquifer parameters, but will also give others such as the well losses.

Care should be taken not only in the designing of the boreholes but, also in the construction and final development of these boreholes. Where and when drilling fluids are used, the boreholes should be well developed in order to increase the permeability. This would improve the well efficiency and thus enhance the

productive capacity of the completed boreholes.

6.3 Water Quality

The boreholes from which samples were taken are spread throughout the entire area and, although the sample size is small, it is nevertheless representative.

6.3.1 Conclusions

From the results and discussions (Chapter 5), it is concluded that the waters found both in Mazeras sandstones and Magarini sands are either sodium bicarbonate or sodium chloride water. These waters are potable and generally useful for most purposes such as domestic, livestock and irrigation. They may also be useful for industrial purposes but require only a little treatment.

The chemistry of these ground waters seems to reflect the geological environment in which they were formed. However, improvement by geographic factors, especially rainfall and evaporation (temperatures) together with the "order of encounter" of these waters, is also suggested.

6.3.2 Recommendations

Since the sample size for analysis was relatively small, it is, therefore, recommended that more water samples should be collected. A complete chemical analysis of these samples, to incorporate both bacteriological and trace constituents determination, should be done.

The iron content in some boreholes should constantly be monitored and investigated. Where it is found to be excessive, its main sources, i.e., decayed and disintegrated or re-active metals appertaining to pump parts, piping systems and screens, should be replaced with others that do not react with water such as stainless steel equipment. However, steel is expensive. Thus, plastic equipment should be adopted in this area.

Further, continuous monitoring of the hydro-chemical characteristics is recommended in order to check the level of contamination of these waters. Encroachment of salt water into the subsurface groundwater storage should always be monitored and appropriate remedial measures taken accordingly.

In this project, evaluation of groundwater balance would have been very important in order to determine the amount of water available for recharge and safe harvesting as suggested by Heath and Trainer (1968), McCann (1974) and Ward (1967). This would require a lot of data such as precipitation, temperatures, infiltration, evapotranspiration and effects of the vegetation cover. However, most of these data were not available during the execution of this project. It is, therefore, recommended that, for future investigations, most, if not all, of these data should be collected and evaluated for water balance. Houston's (1987) suggestion of applying more than one analytical technique should also be effected in order to provide an independent check on the water balance results.

All in all, the results obtained in this "regional" hydrogeologic investigation provide sufficient preliminary information regarding the groundwater potential in the

Tertiary Magarini sands and the Triassic Mazeras sandstones in Kidiani Area. It is, therefore, concluded that the Cainozoic Kilindini and Magarini sands have a higher groundwater potential than the Mesozoic Mazeras sandstones. These results can be extended for exploration and assessment of groundwater resources in other areas of the Coast Province which are covered by the two extensive formations.

REFERENCES

1. K. and A. H. (1980). Hydrological investigations for Groundwater investigation in the Kilindini and Magarini Areas of Northern Kenya. *Journal of Hydrology*, Vol. 25, pp. 165-178. Elsevier Science Publishers, B.V., Amsterdam, The Netherlands.

2. (1980). Hydrological Investigations in the Kilindini and Magarini, South Coast Areas. *Unpublished report for Ministry of Water Development and Ministry of Environment and Natural Resources Water and Soil Dept. Nairobi.*

3. (1984). Report of the Kilindini-Magarini groundwater investigation. *Hydrology Branch, Ministry of Works Kenya* 27pp.

4. F.K. and P. (1967). Direct current electrical sounding. *Electric Association.*

5. (1963). *Soil surface Mapping*. John Wiley and Sons, Inc. New York, London.

REFERENCES

- AL-Ruwaih, F. and Ali H.O., (1986). Resistivity measurements for Groundwater investigation in the Umm - Aish Area of Northern Kuwait. *Journal of Hydrology Vol.88 pp 185-198. Elsevier Science Publishers, B.V; Amsterdam, The Netherlands.*
- Austromineral, (1980). Groundwater Exploration in the Taita Hills and Mombasa, South-Coast Areas. *Unpublished report for Ministry of Water Development and Ministry of Environment and Natural Resources. Mines and Geol. Dept: Nairobi.*
- Bestow, T.T., (1958). Report of the Malindi-Ganda groundwater investigation. *Hydraulic Branch, Ministry of Works Kenya. 27pp.*
- Bhattacharya, P.K. and Patra, H.P., (1968). Direct current electrical sounding. *Elsevier, Amsterdam.*
- Bishop, M.S., (1960). Subsurface Mapping . *John Wiley and Sons, Inc. New York, London*

- Boswinkel, J.A., (1983). Reliability and accuracy of determination of Transmissivity with Well Tests. *Groundwater Survey TNO, Deft, Proceedings International Symposium in METHODS AND INSTRUMENTATION FOR THE INVESTIGATION OF GROUNDWATER SYSTEMS. Netherlands Organization for Applied Scientific Research (TNO) and Unesco.*
- Bouwer, H., (1978). Groundwater Hydrology. *McGraw - Hill Series in Water Resources and Environmental Engineering. McGraw-Hill Book Company.*
- Bredehoeft, J.D., (1963). Possible mechanism for concentration of brines in subsurface formations. *Am. Assoc. Petroleum Geologists Bull. Vol 47 pp 257 - 269.*
- Brown, R.H., Konoplyantev, A.A., Ineson J, and Kovalevsky V.S., (1972). Groundwater Studies. *Unesco, Paris.*
- Cagniard, L., (1952). La prospection geophysique des eaux sousterrains *UNESCO, pg 184 - 190.*
- Caswell, P.V., (1953). Geology of the Mombasa-Kwale Area. *Geol. Surv, Kenya. Report No.24, 69 pp.*

- Caswell, P.V., (1956). Geology of Kilifi - Mazaras Area. *Geol. Surv. Kenya, Report No. 34, 54 pp.*
- Davis, S.N. and De Wiest R.J.M., (1966). Hydrogeology. *John Wiley and Sons, Inc. New York, London, Sydney. 463 pp.*
- Davis, S.N. and De Wiest R.J.M., (1970). Hydrogeology. *John Wiley and Sons, Inc. (3rd Ed.). New York, London, Sydney 463 pp.*
- Dindi, E.W., (1983). A gravity Survey of the Jumbo Hill area South-Coast, Kenya. *M.Sc. Thesis, University of Nairobi. (Unpublished).*
- Dobrin, M.B., (1976). Introduction to Geophysical Prospecting. *Third Edition. New York, McGraw Hill.*
- Driscoll, F.G., (1986). Groundwater Water and Wells. *2nd Edition. Johnson Division, St. Paul, Minnesota 55112.*
- Du Bois C.G.B., (1970). Minerals of Kenya. *Geol. Surv. Kenya. Bulletin no.11. Ministry of Natural Resources.*
- Ediger, R.D., (1976). The use of Atomic Absorption in Water Analysis, *Order No. AA-882; Perkin-Elmer.*

Fetter, E.W. Jnr, (1980). Applied Hydrogeology. *Charles E. Merrill Publ. Company, Columbus, Ohio.*

Flathe, H., (1955). Possibilities and limitations in applying geoelectrical methods to hydrogeological problems in the coastal areas of northwest Germany. *Geophysical Prospecting, Vol.3 pp 95-110.*

Flathe, H., (1976). The role of geologic concept in geophysical research work for solving hydrogeological problems. *Geoexploration, Vol 14: pp 195 - 206.*

Freeze, R.A. and Cherry, J.A., (1979). Groundwater. *Prentice-Hall, Inc. Englewood cliffs, N.J.*

Gaciri, S.J., (1980). A Hydrogeochemical Survey of the Isle of Man. *Ph.D Thesis. University of Sheffield. (Unpublished)*

Gentle, R.I., (1968). The Hydrogeology of the Coastal strip between Gazi and Mtwapa. Kenya Coastlands. *Water Dept, Kenya, Tech. paper No.3. Ministry of Natural Resources and Wildlife.*

Gregory, J.W., (1921). The Rift Valley and geology of East Africa. *Seeley Service and Co. Ltd; London. 479 pp.*

Groundwater Manual, (1981). A Water Resources Technical Publication. *U.S. Department of Interior, Water and Power Resources Service. United States Government Printing Office, Denver: 1981.*

Hazel, C.P., (1975). Groundwater Hydraulics. *Australian Water Resources Council. Groundwater School, Adelaide.*

Heath, R.C. and Trainer, F.W., (1968). Introduction to Groundwater Hydrology. *John Wiley and Sons, Inc. New York, London Sydney.*

Hem, J.D., (1959). Study and Interpretation of the chemical characteristics of Natural Water. *U.S. Geological Survey Water Supply Paper No. 1535 - C. 17 pp Washington, D.C.*

Hem, J.D., (1970). Study and Interpretation of the Chemical Characteristics of Natural Water. *2nd Edition, U.S. Geological Survey Water Supply Paper No. 1535 - C. 17 pp Washington, D.C.*

Homilius, J. and Mundry, E., (1979). Three-layer model curves for Geoelectrical Resistivity Measurements - Schlumberger Array, *Hannover.*

Houston, J., (1987). Groundwater Recharge Assessment, in Developing World Water. *Grosvenor Press International*

- Jacob, C.E., (1963). Recovery method for determining the coefficient of Transmissivity. *U.S. Geological Survey Water Supply Paper 15361, Washington, D.C.*
- K.A.M.E. Project, (1977). The Geology of Mombasa - Kwale Area. *Mines and Geol. Dept. Nairobi (Unpublished).*
- Kaitera, P., (1967). Reasons for long term changes in sea level. *Proc. IUGG. 14th Gen. Ass., Zurich, 1967.*
- Kaufman, A.A. and Keller, G.V., (1983). Frequency and Transient Soundings. *Elsevier, Amsterdam, Oxford, New York.*
- Keller, G.V. and Frischknecht, F.C., (1966). Electrical Methods in Geophysical Prospecting. *New York, Pergamon Press, 519 p.*
- Keller, G.V. and Frischknecht, F.C., (1970). Electrical Methods in Geophysical Prospecting. *Vol.10 Pergamon Press; Oxford, New York, Toronto, Sydney, Braunschweign.*
- Kent, P.E., Hunt, J.A., and Johnstone, D.W., (1971). The geology and geophysics of Coastal Tanzania. *Institute of Geological Sciences. Paper No.6 HMSO London.*

Kenya Bureau of Standards. (1985 a). Kenya Standard, Specification for Drinking Water. *Part 1; Requirements for Drinking Water*. KBS; Nairobi .

Kenya Bureau of Standards. (1985 b). Kenya Standard, Specification for Drinking Water. *Part 2; Physical Methods of Test for the Quality of Drinking Water*. KBS; Nairobi .

Kenya Bureau of Standards. (1985 c). Kenya Standard, Specification for Drinking Water. *Part 5; Methods for Determining Salts, Cations and Anions in Drinking Water*. KBS; Nairobi.

Kenya Meteorological Department, (1988). Climatological Statistics for Kenya. *Kenya Met. Dept. Ngong Road. Nairobi.*

Koefoed, O., (1960). A generalised Cagniard graph for interpretation of sounding data. *Geophys. Prospect. Vol. 8, pg 459 - 469.*

Koefoed, O., (1979). Geosounding Principles; 1: Resistivity Sounding Measurements. *Elsevier Scientific Publishing Company. Amsterdam, Oxford, New York; 276 p*

Kruseman, G.P. and De Ridder, N.A., (1976). Analysis and Evaluation of Pumping Test Data. *International Institute for Land Reclamation and Improvement Wageningen, The Netherlands*

- Kruseman, G.P. and De Ridder, N.A., (1983). Analysis and Evaluation of Pumping Test Data. *Bull. 11. International Institute for Land Reclamation and Improvement, / ILRI. Wageningen.*
- Kunetz, G., (1966). Principles of Direct Current Resistivity Prospecting. *Berlin, Gebruder Borntraeger. 103 pp.*
- Levinson, A.A., (1974). Introduction to Exploration Geochemistry. *Applied Publishing Ltd.*
- Linsley, R.K. and Franzini, J.B., (1987). Water - Resources Engineering. *Mc Graw - Hill Book Company, Inc. 3rd Edition.*
- Lissa van, R.V., Mannen van H.J.R., and Odera, F.W., (1987). The Use of Remote Sensing and Geophysics for Groundwater Exploration in Nyanza Province, Kenya. *DHV Consulting Engineers, Kisumu.*
- Majanga, F.I., (1987). Forward Modelling for Time-Domain Airborne Electromagnetic data interpretation for groundwater exploration in South-Coastal areas of Kenya. *M.Sc. Thesis, International Institute for Aerospace Survey and Earth Sciences / ITC. Deft, The Netherlands. (Unpublished)*
- Mailu, G.M., (1983). The Hydrogeology of the Athi Basin. *M.Sc Thesis, University of Nairobi, (Unpublished)*

- Maina, L.W., (1983).** Groundwater Chemistry of the Area to the immediate North of Nairobi conservation Area. *M.Sc. Thesis, University of Nairobi. (Unpublished).*
- Mathiez, H.P. and Huot G., (1966).** Geophysical Prospecting and Groundwater Exploration: Examples of Application in West Africa. *Inter African committee for Hydrologic Studies. Paris.*
- Mathu, E.M., Ogola, J.S., Ochieng, J. and Wachira, J., (1989).** An Introduction to the Geology and Tectonic History of Kenya: *Field Excursion Guide. UNESCO/IGCP Project 236: Conference and Field Excursions, Nairobi, Kenya.*
- McCann, D.H., (1974).** Hydrogeologic investigation of Rift Valley Catchments. *United Nations - Kenya Government Geothermal Exploration Project. (Unpublished).*
- McLaughlin, T.G., (1966).** Groundwater in Huerfano County, Colorado, U.S. *Geol. Survey, Water Supply paper No.1865 pp 38-43.*
- Miller, J.M., (1952).** Geology of the Mariakani -Mackinnon Road Area. *Geol Surv. Kenya, Report No.20 32 pp.*

Mlengu, J.M.K., (1981). Operation and Maintenance Practice for Rural Water Supply in Kilimanjaro Region Tanzania. *M.Sc. Thesis, Tampere University of Technology, Finland (Unpublished)*.

Morris, D.B., (1964). The Application of Resistivity method to Groundwater Exploration of Alluvial Basins in semi-arid Areas. *Journal of the Institution of Water Engineers, Vol 18, No 1*.

Mwangi, M.N., (1981). Resistivity Survey for groundwater in Msambeni. *M.Sc. Thesis, University of Nairobi. (Unpublished)*

Nilsson, L., (1983). Pumping Test single Hole Technique. *VIAK AB, Gothenburg, Sweden. Proceedings International Symposium in METHODS AND INSTRUMENTATION FOR THE INVESTIGATION OF GROUNDWATER SYSTEMS. Netherlands Organization for Applied scientific Research (TNO) and Unesco.*

Njau, B.E., (1981). Hydrogeological Investigations in Water Master Plans of Tanzania. *M.Sc. Thesis. Tampere University of Technology, Finland. (Unpublished)*.

Norconsult International, (1986). Water Resources Inventory for the Kwale District. *(Unpublished)*.

- Ojany, F.F. and Ogendo, R.B., (1973). Kenya: A Study in Physical and Human Geography. *Longman Kenya Ltd, Nairobi.*
- O'Neill, D.J., (1975). Improved linear filter coefficients for application in apparent resistivity computations. *Bull. Aust. Soc. Explor. Geophys. Vol.6, pg 104 - 109.*
- Ongweny, G.S.O., (1973). The significance of the geographic and geologic factors in the variation of groundwater chemistry in Kenya. *M.Sc. Thesis, University of Nairobi. (Unpublished).*
- Orellana, E. and Mooney, H.M., (1966). Master Table and Curves for vertical electrical sounding over layered structures. *Interciencia, Madrid, 34 p*
- Parasnis, D.S., (1979). Principles of Applied Geophysics. (3rd Edition) *London, Chapman and Hall. 275pp.*
- Piper, A.M., (1944). A graphic procedure in the geochemical interpretation of water analysis. *Am. Geophys. Union Trans, Vol. 25 pp 914-923.*
- Rawlings, B.S. and Greaves, M.C., (1960). Determination of silver in Lead concentrates by Atomic Absorption Spectroscopy. *Natures, 188: pp 137-138.*

- Rijkswaterstaat, The Netherlands, (1980). Standard Graphs for Resistivity Prospecting European Association of Exploration Geophysicists. (E.A.E.G.)
- Sanders, L.D., (1959). Geology of Mid-Galena Area. *Geological Survey of Kenya. Report No 46 - 50 pp.*
- Sanders, L.D., (1963). Geology of the Voi-South Yatta Area. *Geol. Surv., Kenya. Report No 54, Nairobi.*
- Sheikh, A. and Biwott, L.K., (1985). The South-Coast Handpump Project: Progress Report (Unpublished).
- Survey of Kenya, (1970). National Atlas of Kenya. *Third Edition Government of Kenya.*
- Terra Surveys Ltd, (1978). Interpretation Report, Airborne electromagnetic Survey. Barringer "INPUT" System of Area Six (Tiwi Aquifer). *Ministry of Nat. Resources, Mines and Geol. Dept. (Unpublished).*
- Thambu, G.K., (1987). Variations in Quantity and Quality of Groundwater in the South-Coast Region, Kenya. *M.Eng. Degree Thesis, University of Manitoba, Winnipeg, Canada (Unpublished).*

- Theis, C.V., (1935). The Relationship between the lowering of Piezometric surface and the rate and duration of discharge of a well using groundwater storage. *Am. Geophys. Union. Trans. Vol.16 pp 510-524.*
- Thomson, A. C., (1954). Geology of Malindi Area. *Report No 36 Nairobi. 63 pp Geol., Surv. Kenya*
- Todd, D.K., (1959). Groundwater Hydrology. John Wiley and sons. London.
- Unz, M., (1953). Apparent Resistivity curves for dipping beds. *Geophysics Vol. 18, pp 116-137.*
- Van Dam, J.C. and Menlenkamp, J.J., (1968). Some Results of the Geo-Electrical Resistivity method in Groundwater Investigations in the Netherlands. *Geophysical Prospecting, Vol. 15 pp 92.*
- Walton, C.W., (1970). Groundwater Resource Evaluation. *McGraw-Hill, Kekakusha Ltd. Tokyo.*
- Ward, R.C., (1967). Principles of Hydrology. *McGraw-Hill Publishing company Ltd. London, New York, Toronto, Sydney.*
- Williams, C.A.J., (1958). Geology of Hadu-Fundi Area, North of Malindi, *Geol. Survey Kenya. Report 52, Nairobi, 1962. pp 66*

Winani, P., (1977). Geology and Soil geochemistry of Jombo-Dziririni Area.
Mines and Geol. Dept. Investigation Note 17/4 Nairobi. pp

Wood, M. M., (1930). Report on the geological collections from the Coastal
Lands of Kenya. *Man. of Geol. Depart. of Hunterian, Museum,
Glasgow, Univ. VOL.IV.*

World Health Organisation, (1973). Groundwater Resources in Kenya. *Report
No. 7. Sectional study and National Programming for community and
Rural Water Supply, sewerage and water pollution control.*

World Health Organisation, (1984). Guidelines for (W.H.O) Drinking Water
quality. *W.H.O, Geneva, Vol.I. 139 pp.*

Zohdy, A.A.R., (1965). The auxiliary point method of electrical sounding
interpretation and its relationship to the Dar Zarrouk parameters.
Geophysics, Vol. 30, pg 644 - 660.

Zohdy, A.A.R., Eaton, G.P. and Mabey, D.R., (1980). Application of Surface
Geophysics to Groundwater Investigations. *U.S. Geological Survey.*

FIELD DATA SHEET FOR RESISTIVITY

DATE

LOCATION

WELL NO.

DATE

ADDITIONAL DATA

REMARKS

NO.	TIME	DEPTH	RESISTIVITY
1	10.00	0.00	
2	10.05	1.00	
3	10.10	2.00	
4	10.15	3.00	
5	10.20	4.00	
6	10.25	5.00	
7	10.30	6.00	
8	10.35	7.00	
9	10.40	8.00	
10	10.45	9.00	
11	10.50	10.00	
12	10.55	11.00	
13	11.00	12.00	
14	11.05	13.00	
15	11.10	14.00	
16	11.15	15.00	
17	11.20	16.00	
18	11.25	17.00	
19	11.30	18.00	
20	11.35	19.00	
21	11.40	20.00	
22	11.45	21.00	
23	11.50	22.00	
24	11.55	23.00	
25	12.00	24.00	
26	12.05	25.00	
27	12.10	26.00	
28	12.15	27.00	
29	12.20	28.00	
30	12.25	29.00	
31	12.30	30.00	
32	12.35	31.00	
33	12.40	32.00	
34	12.45	33.00	
35	12.50	34.00	
36	12.55	35.00	
37	13.00	36.00	
38	13.05	37.00	
39	13.10	38.00	
40	13.15	39.00	
41	13.20	40.00	
42	13.25	41.00	
43	13.30	42.00	
44	13.35	43.00	
45	13.40	44.00	
46	13.45	45.00	
47	13.50	46.00	
48	13.55	47.00	
49	14.00	48.00	
50	14.05	49.00	
51	14.10	50.00	
52	14.15	51.00	
53	14.20	52.00	
54	14.25	53.00	
55	14.30	54.00	
56	14.35	55.00	
57	14.40	56.00	
58	14.45	57.00	
59	14.50	58.00	
60	14.55	59.00	
61	15.00	60.00	
62	15.05	61.00	
63	15.10	62.00	
64	15.15	63.00	
65	15.20	64.00	
66	15.25	65.00	
67	15.30	66.00	
68	15.35	67.00	
69	15.40	68.00	
70	15.45	69.00	
71	15.50	70.00	
72	15.55	71.00	
73	16.00	72.00	
74	16.05	73.00	
75	16.10	74.00	
76	16.15	75.00	
77	16.20	76.00	
78	16.25	77.00	
79	16.30	78.00	
80	16.35	79.00	
81	16.40	80.00	
82	16.45	81.00	
83	16.50	82.00	
84	16.55	83.00	
85	17.00	84.00	
86	17.05	85.00	
87	17.10	86.00	
88	17.15	87.00	
89	17.20	88.00	
90	17.25	89.00	
91	17.30	90.00	
92	17.35	91.00	
93	17.40	92.00	
94	17.45	93.00	
95	17.50	94.00	
96	17.55	95.00	
97	18.00	96.00	
98	18.05	97.00	
99	18.10	98.00	
100	18.15	99.00	
101	18.20	100.00	

APPENDIX A

Field Sheet of the Resistivity Data

(showing AB/2, MN/2 and geometric factor, K)

PROJECT KIDIANI AREA GROUNDWATER SURVEY

LOCALITY VES NO. ELEVATION

OPERATOR AZIMUTH DATE

INSTRUMENT TYPE CONFIGURATION FORMATION

MN/2 (m)	AB/2 (m)	K	$\Delta V/I$	e_a (Ohm-m)
0.5	1.6	7.26		
	2.0	11.8		
	2.5	18.8		
	3.2	31.4		
	4.0	49.5		
	5.0	77.8		
	6.3	124		
	8.0	200		
	10.0	313		
0.5	13	530		
5	10	23.56		
	13	45.24		
	16	72.6		
	20	118		
	25	188		
5	32	314		
10	25	82.4		
	32	145		
	40	236		
	50	377		
	63	608		
	80	990		
	100	1560		
	130	2640		
	160	4010		
	200	6270		
	250	9800		

APPENDIX B

Computer Generated Model Curves
and Field Data.

NGULUKU CEDA - F15

1. Measurement name : NGULUKU CEDA
2. Maximum L/2 : 250
3. X-coordinate : ?
4. Y-coordinate : ?
5. Date : 890514
6. Elevation : 120
7. Direction : 070

NGULUKU CEDA

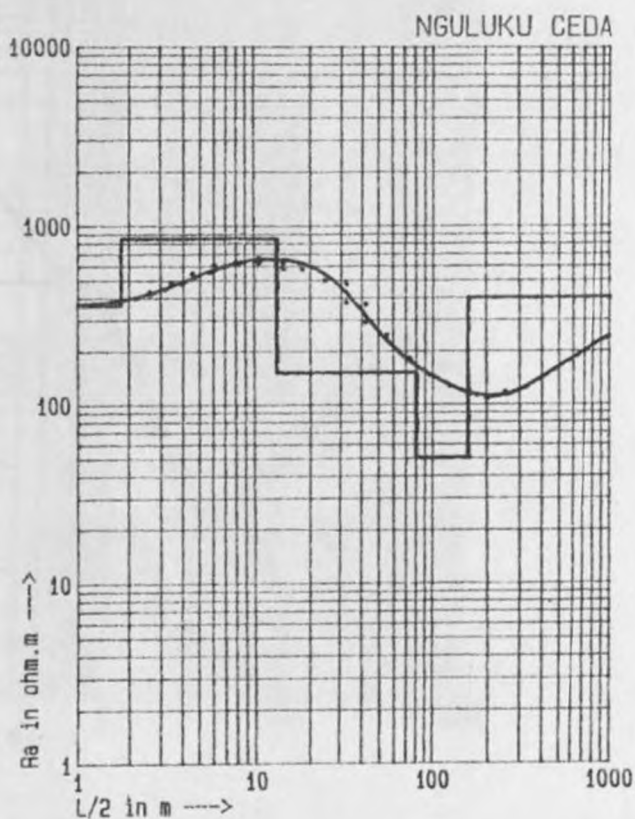
ward apparent resistivities.

L/2	Pa	Nr.	L/2	Pa
2.6	430.7	12.	32.0	373.2
3.4	483.5	13.	32.0	480.6
4.5	548.3	14.	42.0	289.6
6.0	609.7	15.	42.0	366.0
8.0	634.3	16.	55.0	245.0
10.5	627.6	17.	73.0	180.8
10.5	666.9	18.	95.0	145.3
14.0	621.7	19.	125.0	125.4
14.0	579.3	20.	160.0	111.2
18.0	575.9	21.	200.0	107.1
24.0	497.8	22.	250.0	116.8

1. NGULUKU CEDA

Resistivity model(s).

nr.	Depth(m)	Res.(ohm)	Modelnr.
1.	1.8	360.0	begin 1
2.	13.0	850.0	
3.	80.0	150.0	
4.	160.0	50.0	
5.	9999.0	400.0	end of 1



NIMBODZE - F16

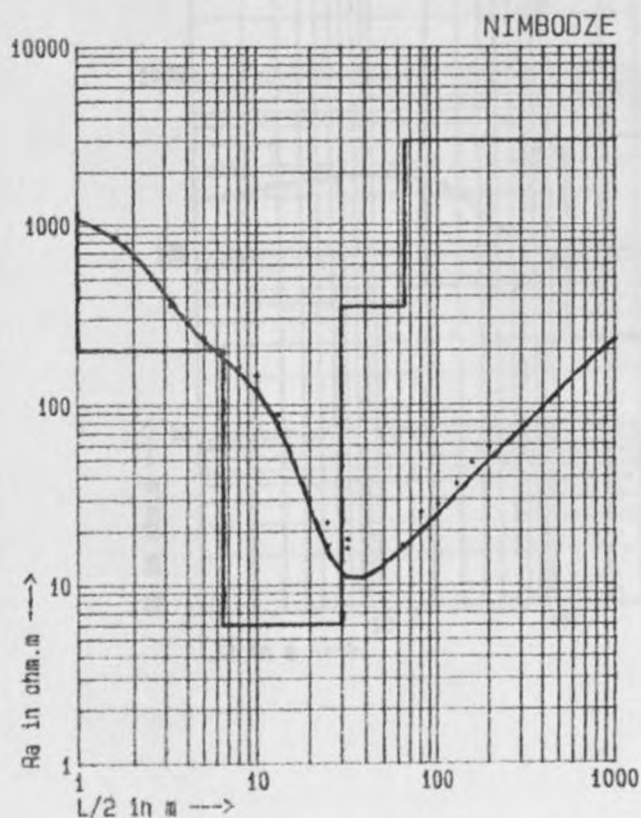
1. Measurement name : NIMBODZE
2. Maximum L/2 : 200
3. X-coordinate : ?
4. Y-coordinate : ?
5. Date : 890513
6. Elevation : 30
7. Direction : 085

NIMBODZE

Measured apparent resistivities.

L/2	Pa	Nr.	L/2	Pa
1.6	850.9	14.	20.0	30.3
2.0	656.1	15.	25.0	16.5
2.5	498.2	16.	25.0	22.3
3.2	355.8	17.	32.0	17.8
4.0	281.2	18.	32.0	15.8
5.0	235.0	19.	40.0	11.2
6.3	195.5	20.	50.0	13.5
8.0	161.0	21.	63.0	16.6
10.0	122.1	22.	80.0	25.4
10.0	145.6	23.	100.0	28.2
13.0	79.3	24.	130.0	36.6
13.0	87.9	25.	160.0	47.7
16.0	48.1	26.	200.0	58.4

NIMBODZE



Resistivity model(s).

Depth(m)	Res.(ohm)	Modelnr.
1.0	1200.0	begin 1
6.5	200.0	
30.0	6.00	
65.0	350.0	
999.0	3000.0	end of 1

LABOUR CAMP - F17

- 1. Measurement name : LABOUR CAMP
- 2. Maximum L/2 : 250
- 3. I-coordinate : ?
- 4. Y-coordinate : ?
- 5. Date : 890513
- 6. Elevation : 60
- 7. Direction : 120

LABOUR CAMP

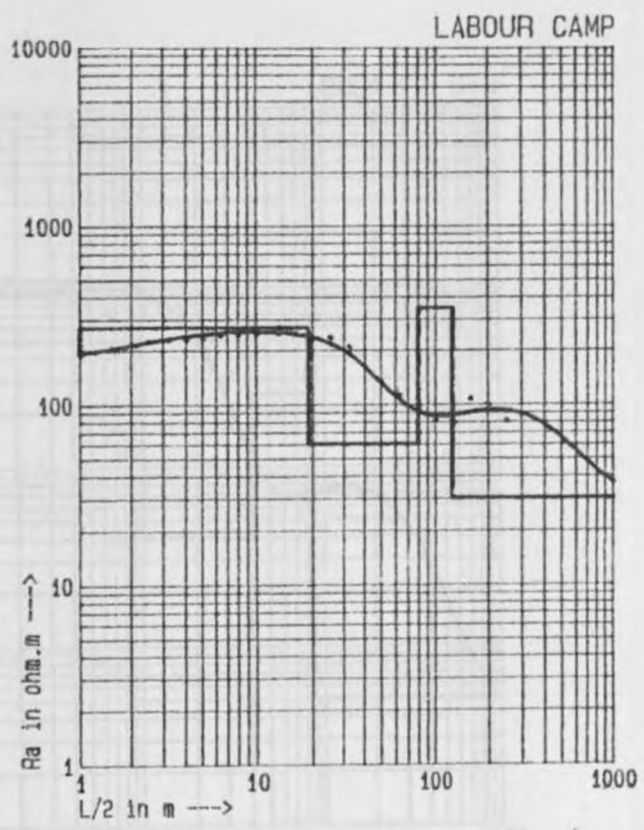
apparent resistivities.

L/2	Pa	Nr.	L/2	Pa
1.6	204.0	15.	25.0	217.5
2.0	216.5	16.	25.0	235.7
2.5	225.4	17.	32.0	190.9
3.2	228.9	18.	32.0	209.2
4.0	230.2	19.	40.0	160.0
5.0	232.6	20.	50.0	132.0
6.3	242.9	21.	63.0	112.0
8.0	245.8	22.	80.0	91.4
10.0	248.2	23.	100.0	81.3
12.0	257.6	24.	130.0	78.9
15.0	248.6	25.	160.0	107.1
18.0	270.5	26.	200.0	99.7
22.0	249.7	27.	250.0	80.4
28.0	232.5			

LABOUR CAMP

activity model(s).

Depth(m)	Res.(ohm)	Modelnr.
1.0	190.0	begin 1
19.0	270.0	
80.0	60.0	
125.0	350.0	
999.0	30.0	end of 1



BUDA F. STN - F18

1. Measurement name : BUDA F. STN
2. Maxime L/2 : 250
3. X-coordinate : ?
4. Y-coordinate : ?
5. Date : 890304
6. Elevation : 60
7. Direction : 050

BUDA F. STN

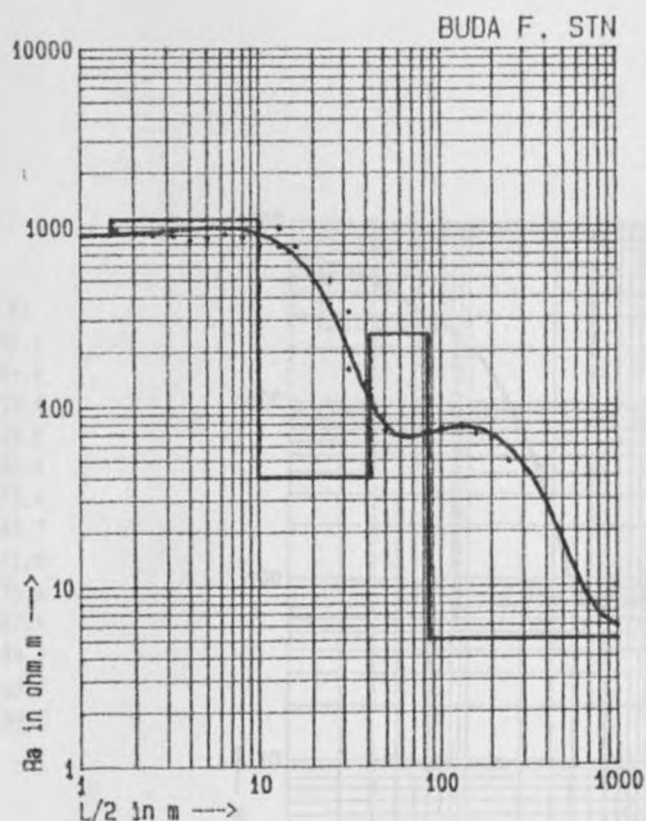
and apparent resistivities.

L/2	Pa	Nr.	L/2	Pa
1.5	958.3	15.	25.0	362.8
1.0	929.8	16.	25.0	498.5
1.5	895.0	17.	32.0	158.7
3.2	882.3	18.	32.0	333.5
4.0	832.6	19.	40.0	135.2
5.0	845.1	20.	50.0	72.8
6.3	908.9	21.	63.0	68.1
8.0	868.3	22.	80.0	70.3
10.0	782.5	23.	100.0	75.6
10.0	1001.3	24.	130.0	79.2
13.8	743.2	25.	160.0	69.1
15.0	981.7	26.	200.0	65.0
16.0	745.9	27.	250.0	49.0
20.0	489.7			

BUDA F. STN

Resistivity model(s).

Depth(m)	Res.(ohm)	Modelnr.
1.5	900.0	begin 1
10.0	1100.0	
42.0	40.0	
85.0	250.0	
999.0	5.00	end of 1



10 100 1000

L/2 in m →

number 5: FOREST EDGE - F19

1. Measurement name : FOREST EDGE
2. Maximum L/2 : 250
3. X-coordinate : 7
4. Y-coordinate : 7
5. Date : 890513
6. Elevation : 40
7. Direction : 045

number 5: FOREST EDGE

Measured apparent resistivities.

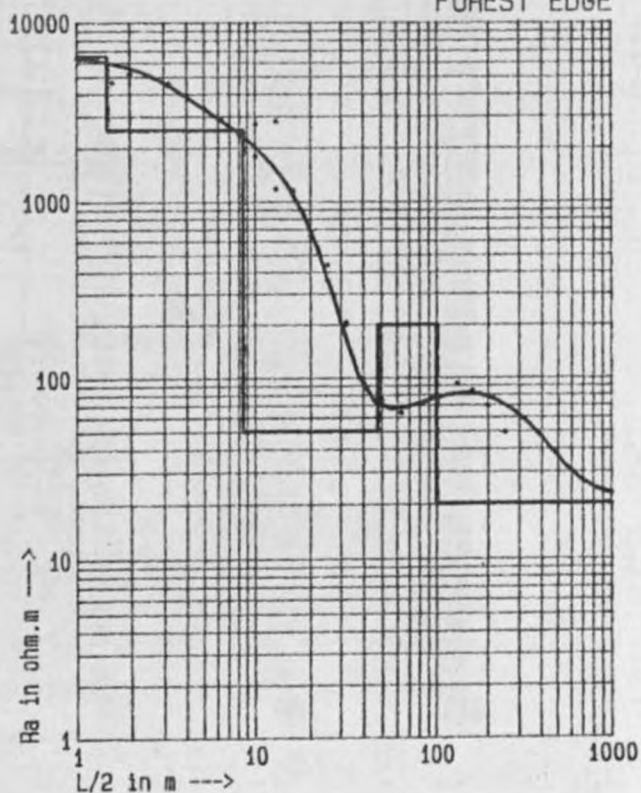
Nr.	L/2	Fa	Nr.	L/2	Pa
1.	1.6	4624.6	15.	25.0	356.1
2.	2.0	5180.2	16.	25.0	440.8
3.	2.5	5094.8	17.	32.0	199.4
4.	3.2	4606.4	18.	32.0	205.0
5.	4.0	3965.0	19.	40.0	93.9
6.	5.0	3361.0	20.	50.0	75.4
7.	6.3	2852.0	21.	63.0	63.3
8.	8.0	2356.0	22.	80.0	71.0
9.	10.0	1790.4	23.	100.0	76.6
10.	10.0	2725.9	24.	130.0	92.4
11.	13.0	1171.3	25.	160.0	84.2
12.	13.0	2824.1	26.	200.0	69.0
13.	16.0	1150.7	27.	250.0	49.0
14.	20.0	838.4			

number 5: FOREST EDGE

Resistivity model(s).

Nr.	Depth(m)	Res.(ohm)	Modelnr.
1.	1.5	6500.0	begin 1
2.	8.5	2500.0	
3.	48.0	50.0	
4.	100.0	200.0	
5.	999.0	20.0	end of 1

FOREST EDGE



NGOJORA - F20

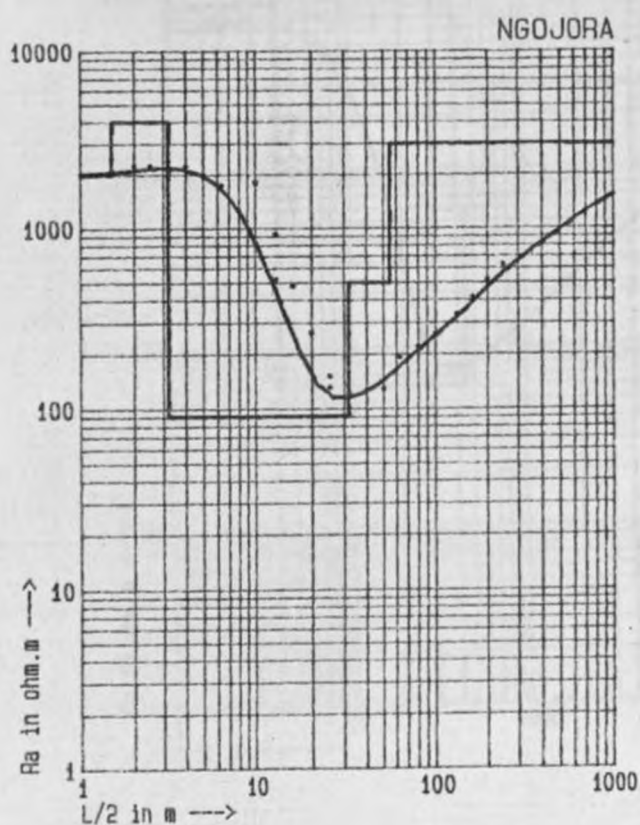
1. Measurement name : NGOJORA
2. Maximum L/2 : 250
3. X-coordinate : ?
4. Y-coordinate : ?
5. Date : 890513
6. Elevation : 30
7. Direction : 020

Number 6: NGOJORA

Measured apparent resistivities.

Nr.	L/2	Pa	Nr.	L/2	Pa
1.	1.6	2054.6	15.	25.0	150.4
2.	2.0	2266.8	16.	25.0	131.0
3.	2.5	2261.6	17.	32.0	120.9
4.	3.2	2470.9	18.	32.0	118.8
5.	4.0	2232.5	19.	40.0	125.8
6.	5.0	2015.0	20.	50.0	128.6
7.	6.3	1736.0	21.	63.0	192.7
8.	8.0	1264.0	22.	80.0	221.4
9.	10.0	820.1	23.	100.0	261.5
10.	10.0	1809.4	24.	130.0	335.6
11.	13.0	518.3	25.	160.0	417.5
12.	13.0	931.9	26.	200.0	521.7
13.	16.0	477.0	27.	250.0	621.2
14.	20.0	263.1			

Number 6: NGOJORA



Resistivity model(s).

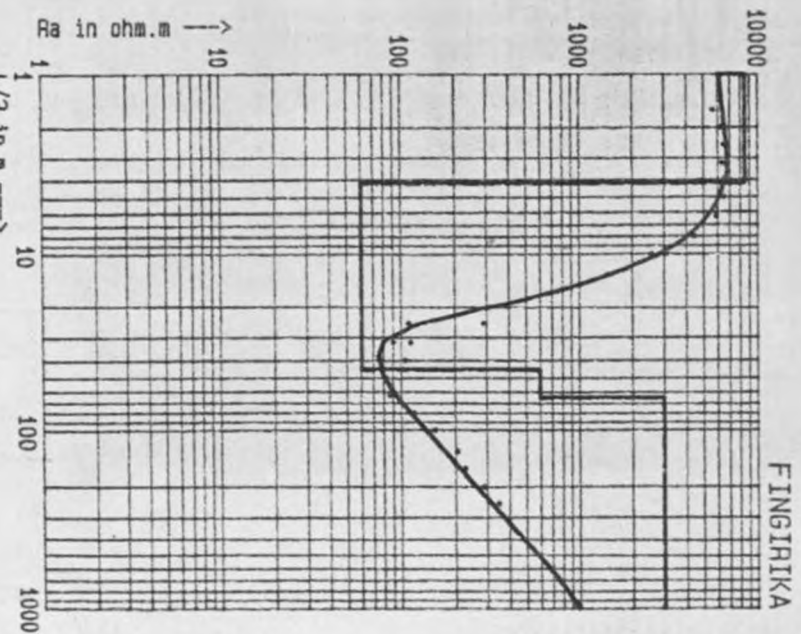
Nr.	Depth(m)	Res.(ohm)	Modelnr.
1.	1.5	2000.0	begin 1
2.	3.2	4000.0	
3.	32.0	90.0	
4.	55.0	500.0	
5.	9999.0	3000.0	end of 1

- 1. Measurement name : FINGERIKA
- 2. Station L/2 : 250
- 3. E-coordinate : 7
- 4. N-coordinate : 7
- 5. Date : 890514
- 6. Elevation : 130
- 7. Direction : 035

Step 7: FINGERIKA

measured apparent resistivities.

L/2	Pa	Nr.	L/2	Pa
1.	1.6 592.3	15.	25.0	109.0
2.	2.0 6254.0	16.	25.0	288.7
3.	2.5 6448.4	17.	32.0	90.1
4.	3.2 6311.4	18.	32.0	113.1
5.	4.0 4490.6	19.	40.0	104.8
6.	5.0 6204.1	20.	50.0	82.6
7.	6.3 5940.4	21.	57.0	86.3
8.	8.0 4400.0	22.	80.0	117.8
9.	10.0 5868.4	23.	100.0	134.4
10.	10.0 1126.4	24.	130.0	205.0
11.	13.0 1479.7	25.	160.0	228.6
12.	15.0 1479.6	26.	200.0	289.8
13.	16.0 755.8	27.	250.0	350.0
14.	20.0 304.4			



Step 7: FINGERIKA

Resistivity model(s).

1. Topsoil Res. (ohm) Model no.

- 1. 1.0 5000.0 begin 1
- 2. 4.2 8500.0
- 3. 45.0 60.0
- 4. 65.0 600.0
- 5. 9999.0 3000.0 end of 1

MUKALA SALIM - F 22

1. Measurement name : MUKALA SALIM
2. Maximum L/2 : 250.
3. X-coordinate : ?
4. Y-coordinate : ?
5. Date : 870226
6. Elevation : 100
7. Direction : 100

Plot 8: MUKALA SALIM

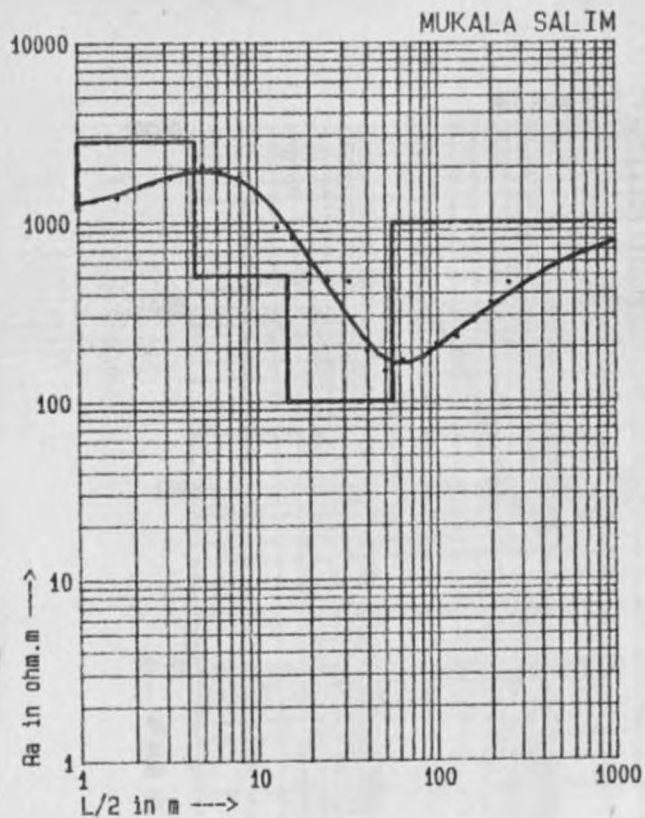
Measured apparent resistivities.

L/2	Pa	Nr.	L/2	Pa
1.6	1772.9	14.	20.0	593.5
2.0	1558.8	15.	25.0	473.8
2.5	1658.2	16.	32.0	465.0
3.2	1767.8	17.	40.0	192.5
4.0	1770.1	18.	50.0	147.4
5.0	2069.0	19.	63.0	170.5
6.3	1918.2	20.	80.0	175.9
8.0	1772.0	21.	100.0	209.5
10.0	1458.6	22.	130.0	229.4
15.0	942.7	23.	160.0	281.2
16.0	827.2	24.	200.0	358.9
16.0	858.1	25.	250.0	461.7
20.0	511.9			

Plot 8: MUKALA SALIM

Resistivity model(s).

Depth (m)	Res. (ohm)	Model nr.
1.	1200.0	begin 1
2.	2800.0	
3.	500.0	
4.	100.0	
5.	9999.0	end of 1



1. Measurement name : MIWUMONI P SCH

2. Station L/2 : 250

3. X-coordinate : 7

4. Y-coordinate : 7

5. Date : 890226

6. Elevation : 100

7. Direction : 030

25: MIWUMONI P SCH

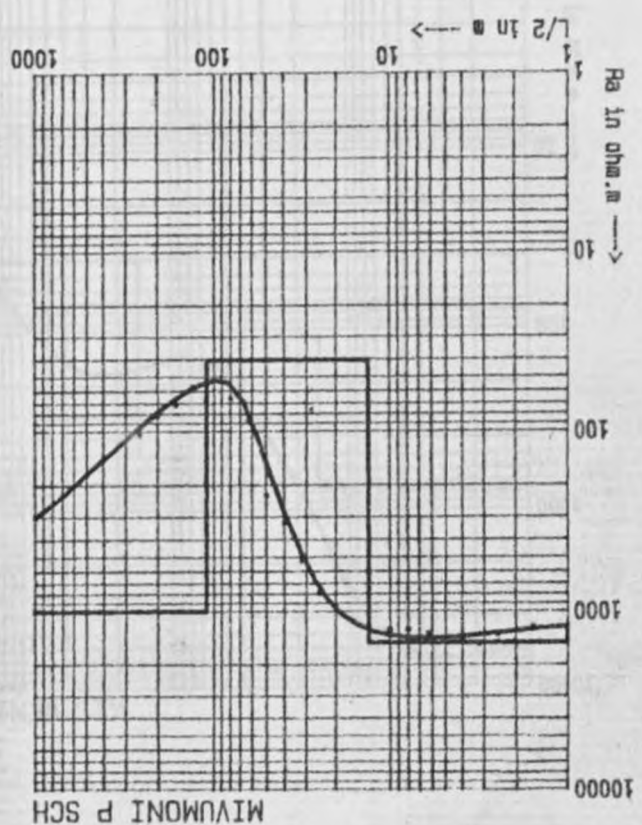
and apparent resistivities.

L/2	Pa	Mr.	L/2	Pa
1.5	1213.1	15.	25.0	759.5
2.0	1470.3	16.	25.0	793.5
2.5	1346.1	17.	32.0	521.6
3.2	1526.0	18.	32.0	500.3
4.0	1425.6	19.	40.0	322.1
5.0	1402.7	20.	50.0	227.0
6.3	1323.1	21.	63.0	85.7
8.0	1290.0	22.	80.0	65.3
10.0	1248.9	23.	100.0	51.0
10.0	1305.2	24.	130.0	56.1
13.0	160.7	25.	160.0	71.4
15.0	117.7	26.	200.0	82.6
15.0	1135.5	27.	250.0	104.4
20.0	922.8			

25: MIWUMONI P SCH

activity model(s).

Depth Res.(ohm) Modelnr.
 1.0 1200.0 begin 1
 13.0 1500.0
 40.0
 1000.0 end of 1



MIWUMONI P SCH

KISIWENI - F24

1. Measurement name : KISIWENI
2. Maximum L/2 : 250
3. X-coordinate : 7
4. Y-coordinate : 7
5. Date : 890226
6. Elevation : 60
7. Direction : 020

Number 9: KISIWENI

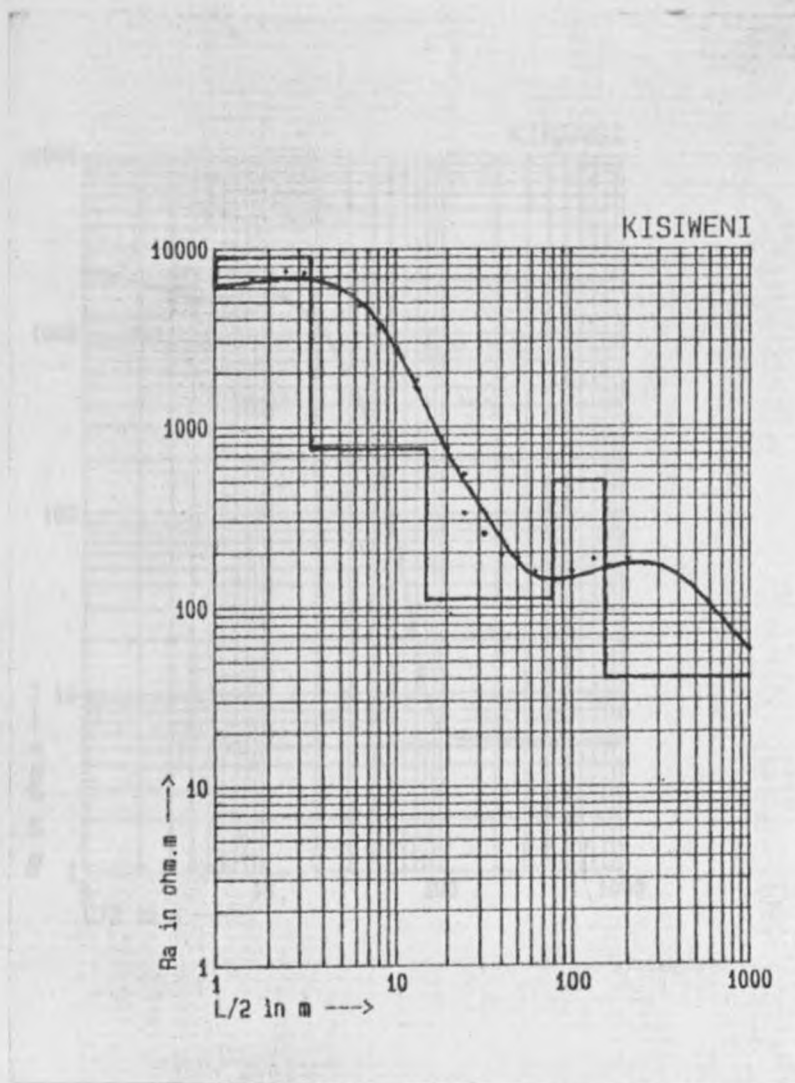
Measured apparent resistivities.

Mr.	L/2	Pa	Mr.	L/2	Pa
1.	1.5	6050.2	15.	25.0	327.7
2.	2.0	6985.6	16.	25.0	548.8
3.	2.5	7463.6	17.	32.0	249.9
4.	3.2	7316.2	18.	32.0	251.6
5.	4.0	6662.7	19.	40.0	191.6
6.	5.0	5681.7	20.	50.0	184.7
7.	6.3	4724.4	21.	63.0	154.4
8.	8.0	3512.0	22.	80.0	203.0
9.	10.0	2585.4	23.	100.0	155.5
10.	10.0	2799.0	24.	130.0	182.9
11.	13.0	1791.4	25.	160.0	165.7
12.	13.0	1619.6	26.	200.0	183.1
13.	16.0	1094.1	27.	250.0	170.0
14.	20.0	756.4			

Number 9: KISIWENI

Resistivity model(s).

Mr.	Depth(m)	Res.(ohm)	Modelnr.
1.	1.0	6000.0	begin 1
2.	3.5	7000.0	
3.	15.0	750.0	
4.	80.0	110.0	
5.	150.0	500.0	
6.	9999.0	40.0	end of 1



KIRANGA - F25

1. Measurement name : KIRANGA
 2. Maximal L/2 : 130
 3. X-coordinate : ?
 4. Y-coordinate : ?
 5. Date : 870514
 6. Elevation : 30
 7. Direction : 320

Order 10: KIRANGA

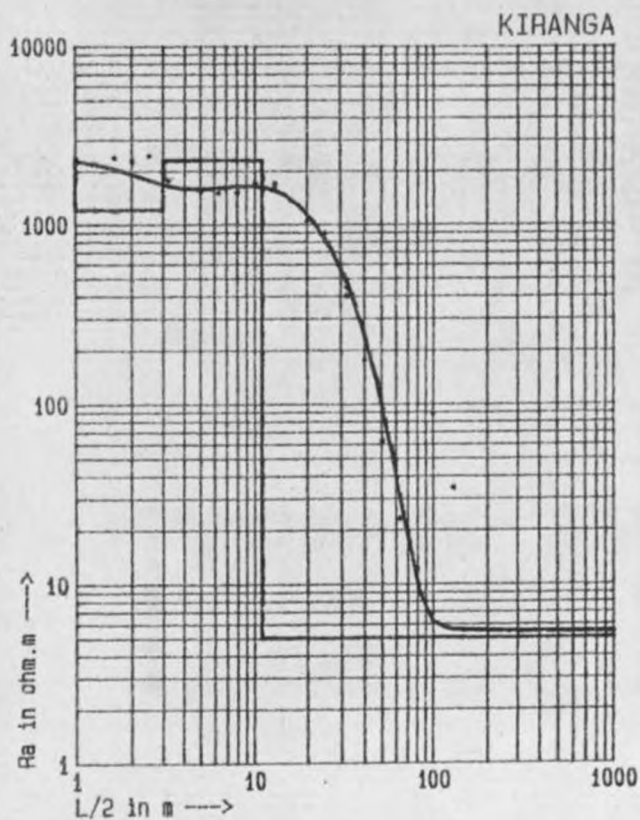
Measured apparent resistivities.

Nr.	L/2	Pa	Nr.	L/2	Pa
1.	1.6	2365.8	13.	16.0	1359.1
2.	2.0	2264.6	14.	20.0	1038.4
3.	2.5	2429.0	15.	25.0	797.1
4.	3.2	1758.4	16.	25.0	894.0
5.	4.0	1608.8	17.	32.0	394.7
6.	5.0	1521.0	18.	32.0	445.2
7.	6.3	1485.0	19.	40.0	176.1
8.	8.0	1500.0	20.	50.0	61.6
9.	10.0	1671.4	21.	63.0	23.0
10.	10.0	1708.1	22.	80.0	12.1
11.	13.0	1611.2	23.	100.0	87.8
12.	13.0	1705.5	24.	130.0	34.3

Order 10: KIRANGA

Resistivity model(s).

Nr.	Depth(s)	Res.(ohm)	Modelnr.
1.	1.0	2400.0	begin 1
2.	3.0	1200.0	
3.	11.0	2300.0	
4.	9999.0	5.00	end of 1



11: GANZORI - F26

1. Measurement name : GANZORI
 2. Maximum L/2 : 250
 3. X-coordinate : ?
 4. Y-coordinate : ?
 5. Date : 990227
 6. Elevation : 60
 7. Direction : 090

number 11: GANZORI

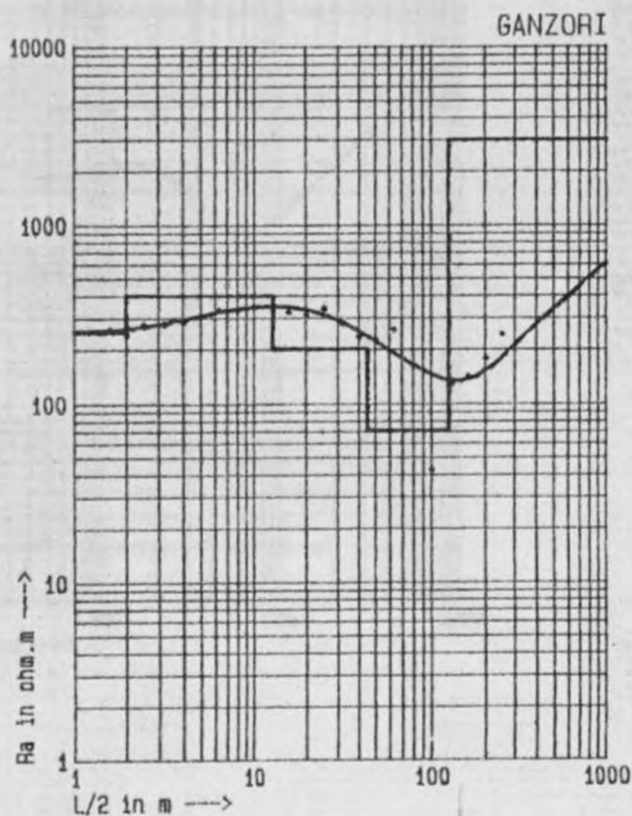
Measured apparent resistivities.

Nr.	L/2	Pa	Nr.	L/2	Pa
1.	1.6	260.1	15.	25.0	336.5
2.	2.0	237.2	16.	25.0	338.7
3.	2.5	277.9	17.	32.0	274.1
4.	3.2	272.1	18.	32.0	283.2
5.	4.0	291.7	19.	40.0	232.2
6.	5.0	303.8	20.	50.0	225.8
7.	6.1	334.0	21.	63.0	257.8
8.	8.0	330.0	22.	80.0	163.4
9.	10.0	348.2	23.	100.0	42.1
10.	10.0	347.8	24.	130.0	129.4
11.	13.0	358.5	25.	160.0	142.8
12.	13.0	347.4	26.	200.0	179.0
13.	14.0	322.3	27.	250.0	243.0
14.	20.0	310.3			

number 11: GANZORI

Resistivity model(s).

Nr.	Depth (m)	Res. (ohm)	Model nr.
1.	2.0	250.0	begin 1
2.	13.0	400.0	
3.	45.0	200.0	
4.	105.0	70.0	
5.	999.0	3000.0	end of 1



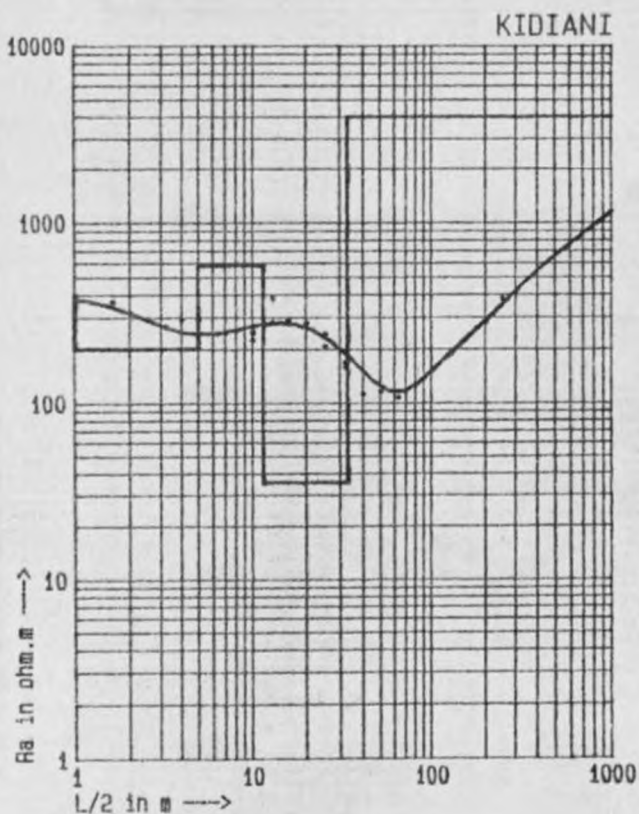
KIDIANI - F27

- 1. Measurement name : KIDIANI
- 2. Maximum L/2 : 250
- 3. Y-coordinate : ?
- 4. Y-coordinate : ?
- 5. Date : 890227
- 6. Elevation : 90
- 7. Direction : 010

12: KIDIANI

Measured apparent resistivities.

L/2	Pa	Nr.	L/2	Pa
1.5	363.0	15.	25.0	241.2
2.0	317.4	16.	25.0	206.0
2.5	291.2	17.	32.0	168.0
3.2	266.9	18.	32.0	155.9
4.0	292.5	19.	40.0	111.4
5.0	291.8	20.	50.0	116.1
6.3	242.7	21.	63.0	106.8
8.0	254.6	22.	80.0	124.4
10.0	222.9	23.	100.0	150.1
10.0	247.9	24.	130.0	187.7
13.0	382.1	25.	160.0	235.2
13.0	281.4	26.	200.0	281.4
16.0	289.7	27.	250.0	380.1
20.0	277.3			



13: KIDIANI

Resistivity model(s).

Depth(m)	Res.(ohm)	Modelnr.
1.0	400.0	begin 1
5.0	200.0	
11.5	580.0	
33.0	35.0	
9999.0	4000.0	end of 1

ID: MKURUMUJI - F28

1. Measurement name : MKURUMUJI
 2. Maximum L/2 : 250
 3. I-coordinate : ?
 4. Y-coordinate : ?
 5. Date : 890520
 6. Elevation : 80
 7. Direction : 080

Order 17: MKURUMUJI

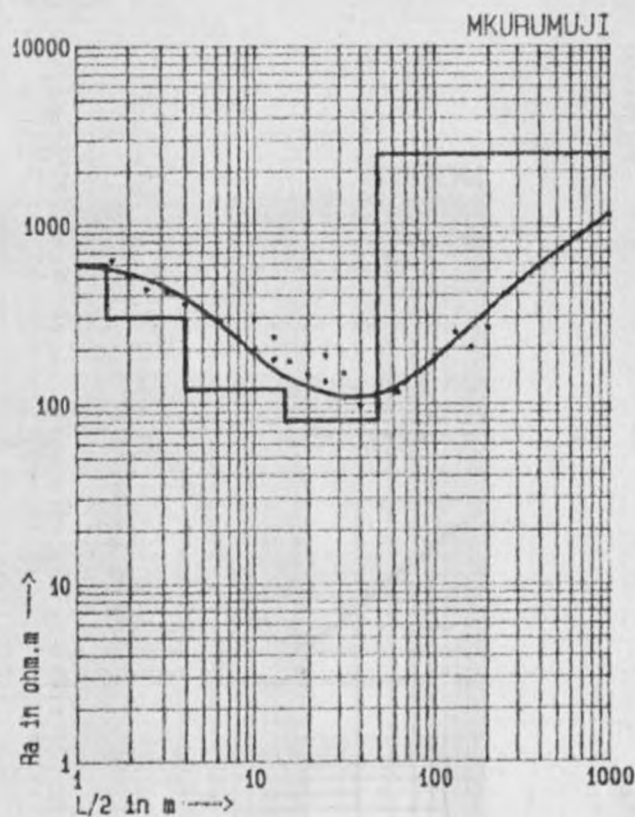
Measured apparent resistivities.

Nr.	L/2	Pa	Nr.	L/2	Pa
1.	1.6	628.7	15.	25.0	132.2
2.	2.0	507.4	16.	25.0	186.2
3.	2.5	432.4	17.	32.0	107.1
4.	3.2	419.2	18.	32.0	147.3
5.	4.0	357.4	19.	40.0	96.5
6.	5.0	326.8	20.	50.0	96.5
7.	6.3	288.8	21.	63.0	116.1
8.	8.0	236.0	22.	80.0	150.0
9.	10.0	198.8	23.	100.0	185.6
10.	12.5	290.0	24.	130.0	249.0
11.	15.0	175.4	25.	160.0	205.7
12.	17.5	233.4	26.	200.0	261.6
13.	16.0	170.6	27.	250.0	404.6
14.	10.0	143.5			

Order 17: MKURUMUJI

Resistivity model(s).

No.	Depth (m)	Res. (ohm)	Model no.
1.	1.5	600.0	begin 1
2.	4.0	300.0	
3.	15.0	120.0	
4.	80.0	80.0	
5.	2500.0	2500.0	end of 1



14: NZEVNI -F29

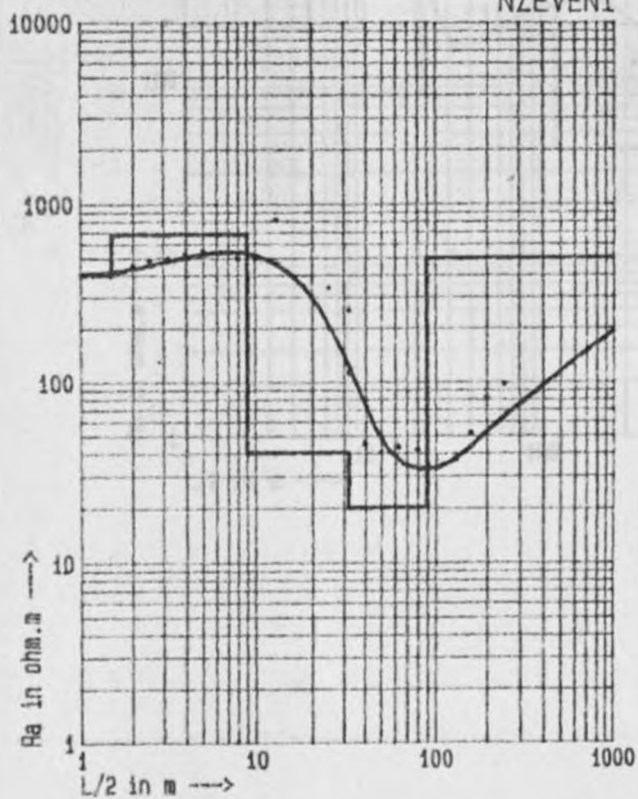
- 1. Measurement name : NZEVNI
- 2. Maximum L/2 : 250
- 3. X-coordinate : ?
- 4. Y-coordinate : ?
- 5. Date : 870228
- 6. Elevation : 70
- 7. Direction : 075

Water 14: NZEVNI

Measured apparent resistivities.

Nr.	L/2	Pa	Nr.	L/2	Pa
1.	1.5	417.5	15.	25.0	198.5
2.	2.0	453.1	16.	25.0	337.8
3.	2.5	486.9	17.	32.0	111.2
4.	3.2	499.9	18.	32.0	253.2
5.	4.0	526.7	19.	40.0	45.1
6.	5.0	547.7	20.	50.0	40.0
7.	6.3	539.4	21.	63.0	43.2
8.	8.0	502.0	22.	80.0	41.6
9.	10.0	504.6	23.	100.0	32.8
10.	12.5	501.8	24.	130.0	37.0
11.	15.0	822.0	25.	160.0	52.1
12.	17.5	463.7	26.	200.0	91.5
13.	20.0	394.2	27.	250.0	98.0
14.	25.0	297.4			

NZEVNI



Water 14: NZEVNI

Resistivity model(s).

Mo. (ohm.m)	Res. (ohm)	Modelnr.
500.0	400.0	begin 1
400.0	600.0	
20.0	40.0	
20.0	20.0	
500.0	500.0	end of 1

4. BUDA FOREST II - F30

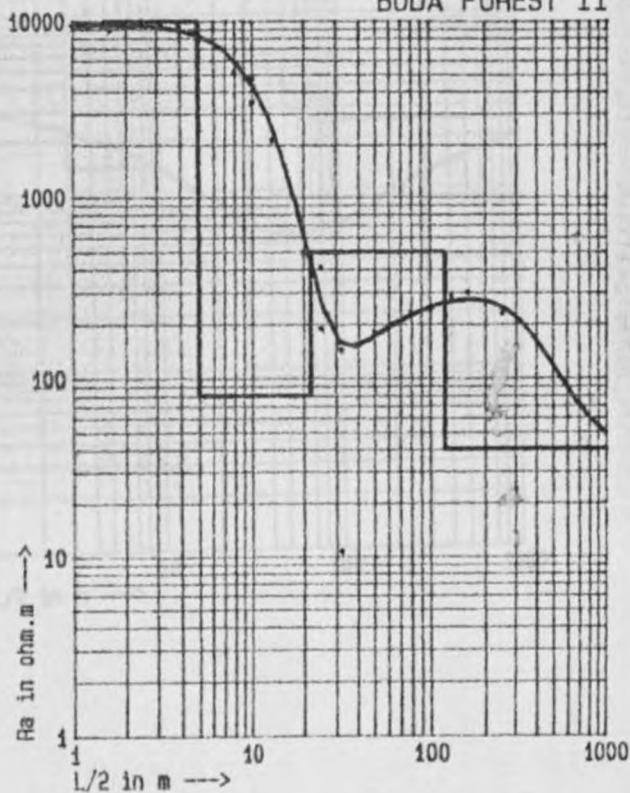
- 1. Measurement name : BUDA FOREST II
- 2. Maximum L/2 : 250
- 3. I-coordinate : ?
- 4. V-coordinate : ?
- 5. Date : 890513
- 6. Elevation : 60
- 7. Direction : 015

15: BUDA FOREST II

measured apparent resistivities.

L/2	Pa	Nr.	L/2	Pa
1.5	8806.4	15.	25.0	188.6
2.0	9251.2	16.	25.0	415.3
2.5	9700.8	17.	32.0	10.7
3.2	9608.4	18.	32.0	144.3
4.0	9291.2	19.	40.0	155.6
5.0	8666.9	20.	50.0	180.9
6.3	7089.4	21.	63.0	201.2
8.0	5120.0	22.	80.0	234.6
10.0	3458.7	23.	100.0	241.8
10.0	4712.0	24.	130.0	287.8
13.0	2135.7	25.	160.0	301.2
15.0	2501.8	26.	200.0	269.6
15.0	1428.6	27.	250.0	230.0
20.0	494.4			

BUDA FOREST II



15: BUDA FOREST II

resistivity model(s).

Depth(m)	Res.(ohm)	Modelnr.
1. 1.5	9500.0	begin 1
2. 5.0	10000.0	
3. 23.0	80.0	
4. 120.0	500.0	
5. 9999.0	40.0	end of 1

Number 16: MWACHANDE BRI. - F31

1. Measurement name : MWACHANDE BRI.

2. Maximum L/2 : 250

3. X-coordinate : 7

4. Y-coordinate : 7

5. Date : 89/5/20

6. Elevation : 30

7. Direction : 035

Number 16: MWACHANDE BRI.

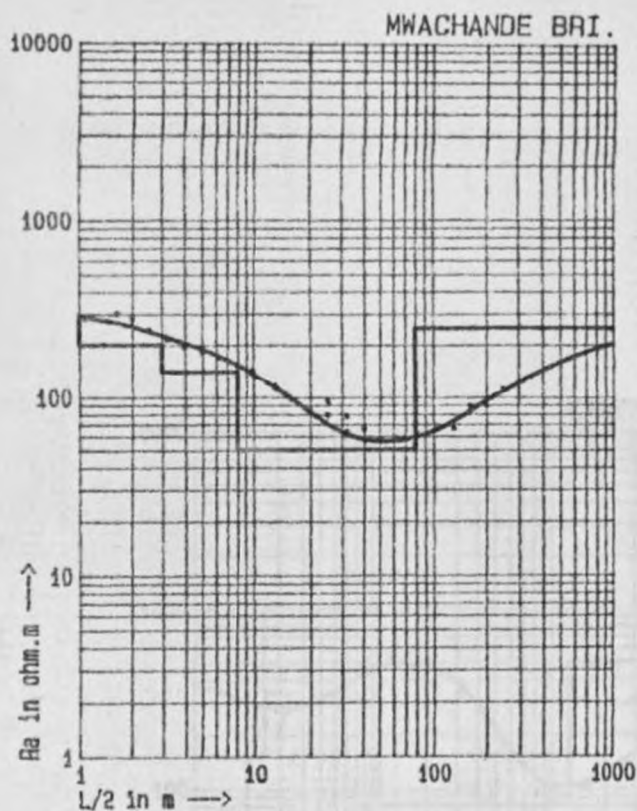
Measured apparent resistivities.

Nr.	L/2	Pa	Nr.	L/2	Pa
1.	1.6	302.7	15.	25.0	79.0
2.	2.0	280.8	16.	25.0	95.7
3.	3.5	243.1	17.	32.0	63.7
4.	3.2	213.9	18.	32.0	78.2
5.	4.0	192.6	19.	40.0	65.1
6.	5.0	181.3	20.	50.0	56.8
7.	6.3	168.9	21.	63.0	57.3
8.	8.0	151.4	22.	80.0	63.3
9.	10.0	134.0	23.	100.0	64.1
10.	10.0	142.8	24.	130.0	66.3
11.	15.0	111.8	25.	160.0	89.4
12.	15.0	115.4	26.	200.0	89.0
13.	16.0	96.7	27.	250.0	113.7
14.	20.0	82.0			

Number 16: MWACHANDE BRI.

Resistivity model(s).

Nr.	Depth(m)	Res.(ohm)	Modelnr.
1.	1.0	300.0	begin 1
2.	1.0	200.0	
3.	3.0	140.0	
4.	5.0	50.0	
5.	250.0	250.0	end of 1



17: KAMENE B/H - F32

- 1. Measurement name : KAMENE B/H
- 2. Maximum L/2 : 250
- 3. X-coordinate : ?
- 4. Y-coordinate : ?
- 5. Date : 890521
- 6. Elevation : 60
- 7. Direction : 090

Order 17: KAMENE B/H

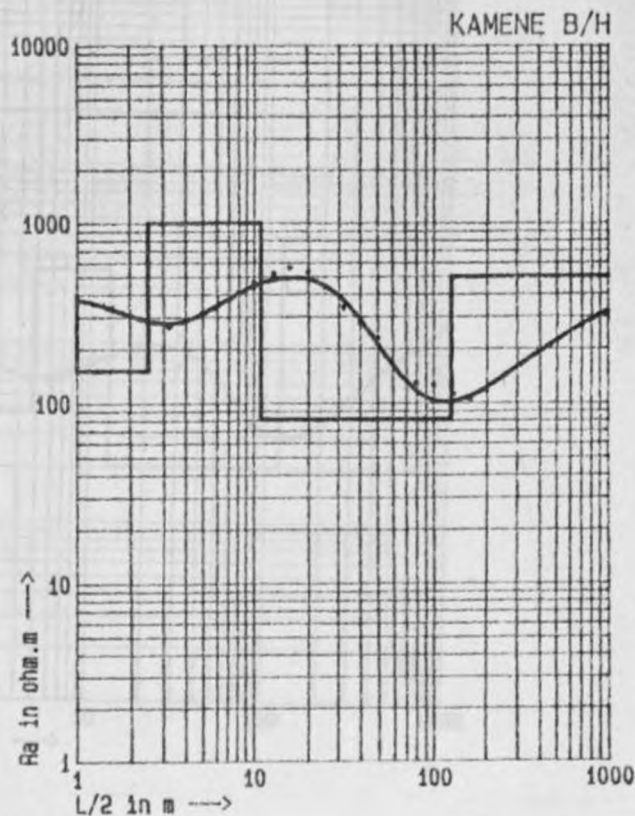
Measured apparent resistivities.

Nr.	L/2	Pa	Nr.	L/2	Pa
1.	1.6	336.1	15.	25.0	439.9
2.	2.0	306.8	16.	25.0	435.9
3.	2.5	273.9	17.	32.0	337.6
4.	3.2	263.1	18.	32.0	333.5
5.	4.0	286.1	19.	40.0	274.7
6.	5.0	317.4	20.	50.0	227.7
7.	6.0	355.9	21.	63.0	151.4
8.	8.0	412.0	22.	80.0	128.8
9.	10.0	467.0	23.	100.0	124.5
10.	10.0	430.7	24.	130.0	119.1
11.	13.0	523.6	25.	160.0	103.1
12.	13.0	513.0	26.	200.0	116.0
13.	16.0	561.2	27.	250.0	139.2
14.	20.0	526.3			

Order 17: KAMENE B/H

Resistivity model(s).

Nr.	Depth(m)	Res.(ohm)	Modelnr.
1.	1.0	400.0	begin 1
2.	2.5	150.0	
3.	15.0	1000.0	
4.	100.0	80.0	
5.	1000.0	500.0	end of 1



- 1. Measurement name : MWALUVANGA
- 2. Maximum L/2 : 250
- 3. X-coordinate : 7
- 4. Y-coordinate : 9
- 5. Date : 090502
- 6. Elevation : 30
- 7. Direction : 040

14: MWALUVANGA

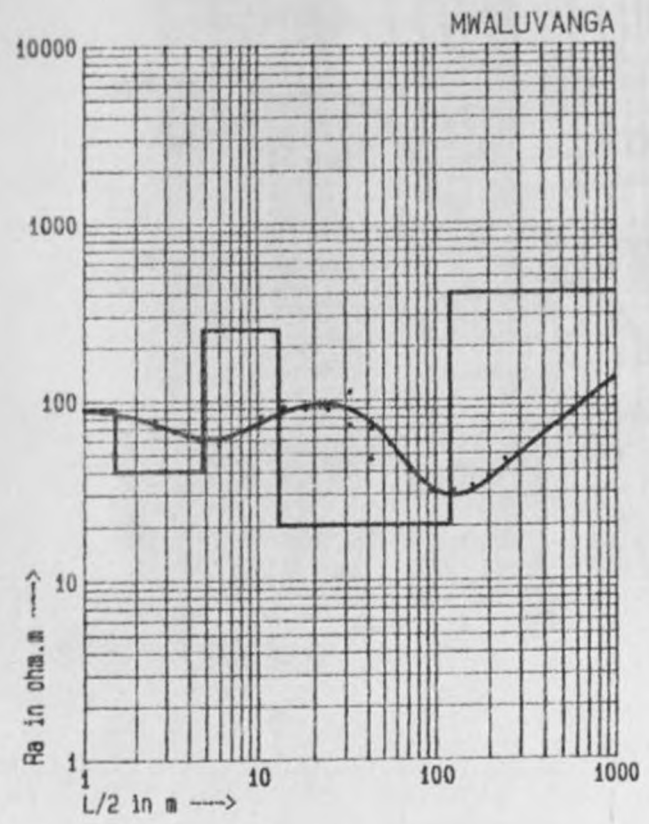
ed apparent resistivities.

L/2	Pa	Nr.	L/2	Pa
3.2	77.2	12.	32.0	71.9
3.4	66.6	13.	32.0	110.9
4.0	59.4	14.	42.0	46.0
6.0	58.2	15.	42.0	68.8
8.0	68.7	16.	55.0	55.7
10.0	78.6	17.	73.0	29.6
12.0	90.4	18.	95.0	31.1
15.0	71.2	19.	125.0	30.7
18.0	47.3	20.	160.0	33.0
20.0	44.4	21.	200.0	37.0
25.0	98.7	22.	250.0	46.0

15: MWALUVANGA

ity model(s).

Depth (m)	Res. (ohms)	Model nr.
0.0	90.0	begin 1
4.0	40.0	
10.0	250.0	
20.0	20.0	
250.0	400.0	end of 1



0: MWACHANDE SCH -F34

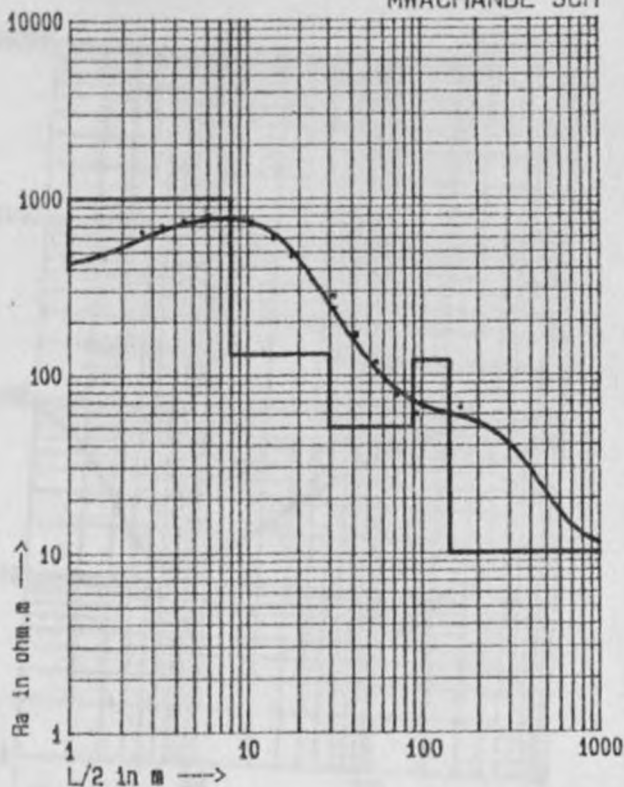
- 1. Measurement name : MWACHANDE SCH
- 2. Radius L/2 : 250
- 3. Y-coordinate : 7
- 4. X-coordinate : 7
- 5. Date : 890209
- 6. Allocation : 125
- 7. Direction : 175

0: MWACHANDE SCH

of apparent resistivities.

L/2	Ra	Nr.	L/2	Ra
2.8	645.4	12.	32.0	336.0
3.4	890.4	13.	32.0	280.2
4.5	743.5	14.	42.0	165.5
6.1	817.6	15.	42.0	170.7
8.0	787.2	16.	55.0	117.2
10.5	717.6	17.	73.0	75.6
16.5	742.1	18.	95.0	59.2
19.0	597.5	19.	130.0	61.1
14.0	597.0	20.	160.0	64.8
18.0	468.0	21.	200.0	53.7
24.0	347.5	22.	250.0	46.2

MWACHANDE SCH



19: MWACHANDE SCH

ativity model(s).

Depth	Ra (ohm)	Model no.
1.0	400.0	begin 1
8.0	1000.0	
20.0	130.0	
30.0	50.0	
140.0	120.0	
200.0	10.0	end of 1

Station 20: KIBWAGA - F35

1. Measurement name : KIBWAGA
2. Marine station : 230730
3. X-coordinate : 7
4. Y-coordinate : 1
5. Date : 27/04/01
6. Elevation : 15
7. Direction : 055

Station 20: KIBWAGA

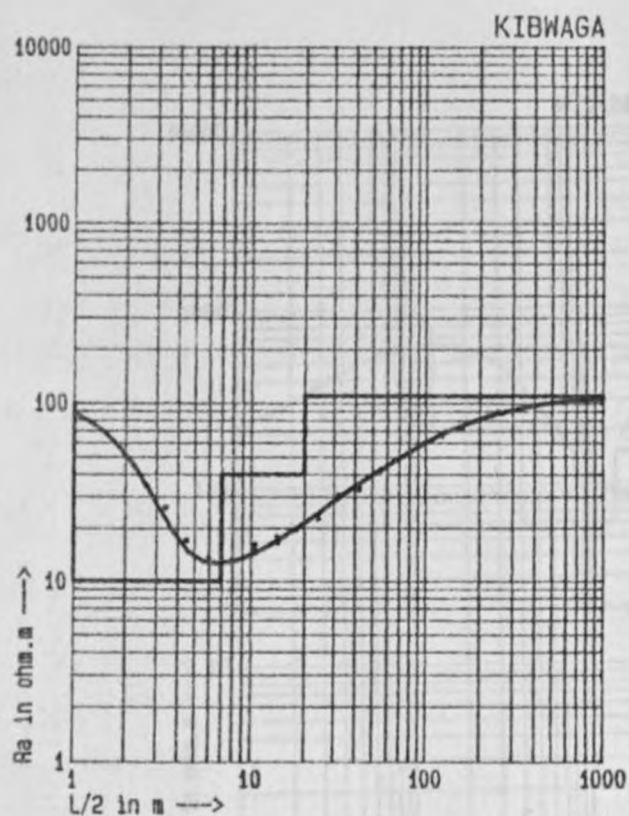
Measured apparent resistivities.

Nr.	L/2	Pa	Nr.	L/2	Pa
1.	2.6	34.4	12.	32.0	39.7
2.	3.4	25.9	13.	32.0	30.1
3.	4.5	16.9	14.	42.0	32.9
4.	6.0	13.5	15.	42.0	33.8
5.	9.0	13.1	16.	55.0	42.2
6.	11.5	16.1	17.	73.0	50.6
7.	16.5	14.9	18.	95.0	58.9
8.	14.0	17.9	19.	125.0	66.1
9.	14.0	16.3	20.	160.0	73.2
10.	18.0	19.7	21.	200.0	80.5
11.	24.0	22.6	22.	250.0	89.8

Station 20: KIBWAGA

Resistivity model(s).

Nr.	Depth	Res.(ohm)	Model nr.
1.	1.0	100.0	begin I
2.	7.0	10.0	
3.	20.0	40.0	
4.	250.0	110.0	end of I



Station 21: MIVUMONI CHUR - F36

1. Measurement name : MIVUMONI CHUR
 2. Maximum L/2 : 250
 3. X-coordinate : ?
 4. Y-coordinate : ?
 5. Date : 890521
 6. Elevation : 90
 7. Direction : 120

Station 21: MIVUMONI CHUR

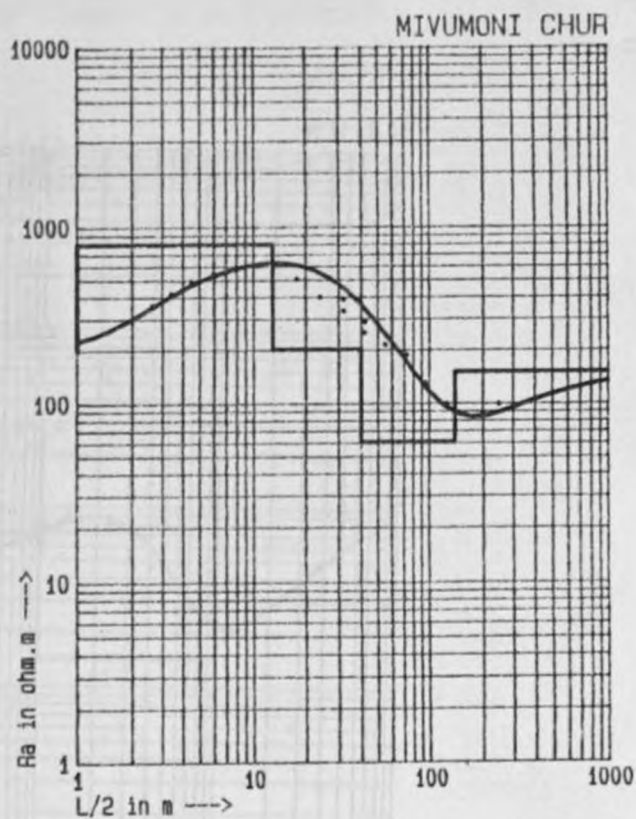
Measured apparent resistivities.

Nr.	L/2	Pa	Nr.	L/2	Pa
1.	2.6	356.8	12.	32.0	330.7
2.	3.4	421.3	13.	32.0	386.2
3.	4.5	492.3	14.	42.0	248.2
4.	6.0	549.1	15.	42.0	286.1
5.	8.0	596.7	16.	35.0	212.8
6.	10.5	610.3	17.	73.0	186.5
7.	10.5	603.3	18.	95.0	129.0
8.	14.0	614.9	19.	125.0	98.7
9.	14.0	621.6	20.	160.0	64.6
10.	18.0	504.9	21.	200.0	86.3
11.	24.0	396.5	22.	250.0	98.8

Station 21: MIVUMONI CHUR

Resistivity model(s).

Nr.	Depth(m)	Res.(ohm)	Modelnr.
1.	1.0	200.0	begin 1
2.	13.0	800.0	
3.	40.0	200.0	
4.	140.0	60.0	
5.	9999.0	150.0	end of 1



- 1. Measurement name : KILULU
- 2. Maximum L/2 : 215
- 3. X-coordinate : ?
- 4. Y-coordinate : ?
- 5. Date : 890521
- 6. Elevation : 90
- 7. Direction : 095

72: KILULU

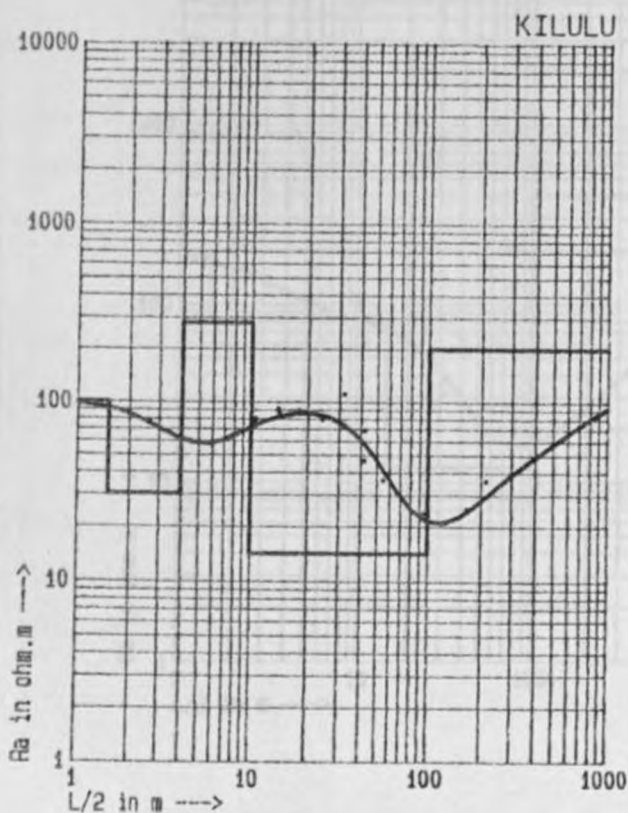
Measured apparent resistivities.

L/2	Pa	Nr.	L/2	Pa
2.6	77.3	12.	32.0	71.9
3.4	66.6	13.	32.0	110.9
4.5	59.4	14.	42.0	46.0
6.0	56.2	15.	42.0	68.7
8.0	64.2	16.	55.0	35.9
10.5	76.6	17.	75.0	28.0
10.5	80.4	18.	95.0	23.5
14.0	91.2	19.	125.0	21.0
14.0	87.3	20.	165.0	25.0
18.0	89.4	21.	215.0	36.0
24.0	78.7			

72: KILULU

Resistivity model(s).

Depth(m)	Res. (ohm)	Modelnr.
1.5	100.0	begin 1
4.8	30.0	
10.0	280.0	
190.0	14.0	
999.0	200.0	end of 1



LIKONI - F38

1. Measurement name : LIKONI
2. Maximum L/2 : 250
3. X-coordinate : ?
4. Y-coordinate : ?
5. Date : 890520
6. Elevation : 40
7. Direction : 070

LIKONI

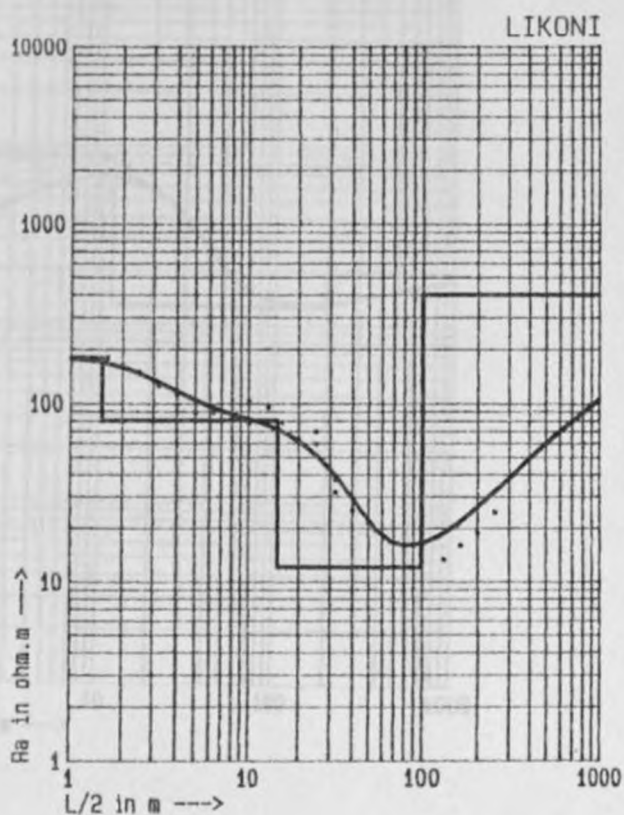
red apparent resistivities.

L/2	Pa	Nr.	L/2	Pa
1.6	177.9	15.	25.0	69.2
2.0	160.8	16.	25.0	59.0
2.5	148.3	17.	32.0	31.6
3.2	124.3	18.	32.0	37.3
4.0	111.4	19.	40.0	25.0
5.0	88.0	20.	50.0	21.1
6.3	88.2	21.	63.0	17.6
8.0	61.6	22.	80.0	15.8
10.0	76.7	23.	100.0	18.7
10.0	103.2	24.	130.0	13.2
13.0	79.0	25.	160.0	16.0
13.0	95.5	26.	200.0	18.8
16.0	77.6	27.	250.0	24.5
20.0	62.7			

LIKONI

stivity model(s).

Depth(m)	Res.(ohm)	Modelnr.
1.5	180.0	begin 1
15.0	80.0	
100.0	12.0	
9999.0	400.0	end of 1



MZEE KOMO - F40

1. Measurement name : MZEE KOMO
 2. Maximum L/2 : 250
 3. X-coordinate : ?
 4. Y-coordinate : ?
 5. Date : 090518
 6. Elevation : 80
 7. Direction : 975

MZEE KOMO

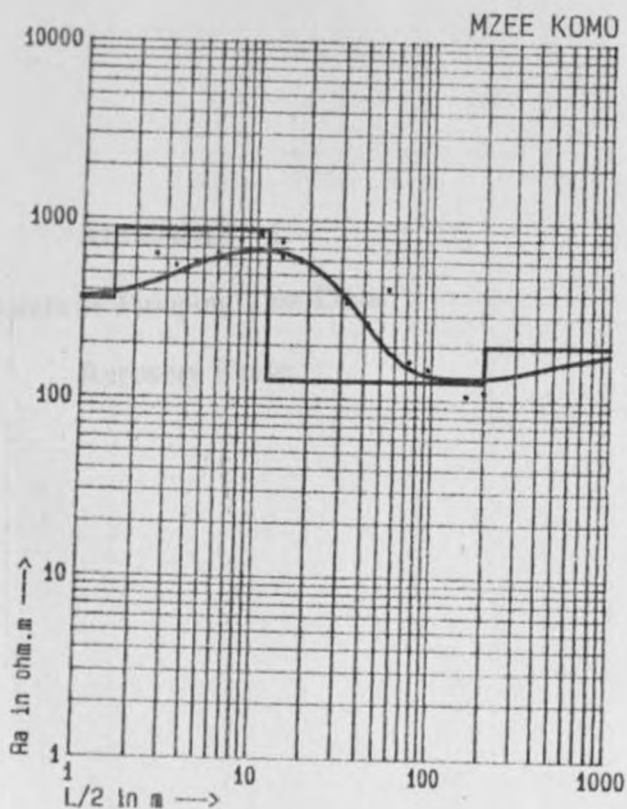
red apparent resistivities.

L/2	Pa	Nr.	L/2	Pa
2.6	637.9	12.	32.0	350.3
3.4	552.5	13.	32.0	373.2
4.5	583.0	14.	42.0	258.3
6.0	656.1	15.	42.0	269.8
8.0	774.7	16.	55.0	423.7
10.5	826.5	17.	73.0	163.4
10.5	689.1	18.	95.0	147.5
14.0	625.6	19.	130.0	125.4
14.0	760.1	20.	160.0	105.0
18.0	590.7	21.	200.0	110.5
24.0	494.2	22.	250.0	200.0

MZEE KOMO

ivity model(s).

Depth	Res. (ohm)	Model	Inr.
1.5	360.0	begin	1
11.7	880.0		
20.0	125.0		
99.0	200.0	end of	1



APPENDIX C			
Borehole Pumping Test Data			
Recovery Phase.			
Time (min)	Flow Rate (gpm)	Water Level (ft)	Water Level (ft)
0	0	25.00	25.00
10	10	24.50	24.50
20	20	24.00	24.00
30	30	23.50	23.50
40	40	23.00	23.00
50	50	22.50	22.50
60	60	22.00	22.00
70	70	21.50	21.50
80	80	21.00	21.00
90	90	20.50	20.50
100	100	20.00	20.00
110	110	19.50	19.50
120	120	19.00	19.00
130	130	18.50	18.50
140	140	18.00	18.00
150	150	17.50	17.50
160	160	17.00	17.00
170	170	16.50	16.50
180	180	16.00	16.00
190	190	15.50	15.50
200	200	15.00	15.00
210	210	14.50	14.50
220	220	14.00	14.00
230	230	13.50	13.50
240	240	13.00	13.00
250	250	12.50	12.50
260	260	12.00	12.00
270	270	11.50	11.50
280	280	11.00	11.00
290	290	10.50	10.50
300	300	10.00	10.00

KIDIANI AREA GROUNDWATER SURVEY					
RECOVERY PHASE					
BOREHOLE NO: 7087.		BOREHOLE NAME: Makutano			
BOREHOLE DEPTH 58 m		MEASURING PT: G/L			
METHOD OF MEASURING		DATE OF TEST: 23-01-89			
WATER LEVEL: Electric Dipper		INITIAL WRL: 27.40 m			
Clock Time & Pumping Time, t, min	Recovery Time t' min	Water Level in m	Residual Drawdown S _r , m	t/t'	
9.45 am	540	0	51.74	24.34	-
	541	1	49.50	22.10	541
	542	2	48.20	20.80	271
	543	3	47.50	20.10	181
	544	4	46.20	18.80	136
	545	5	45.15	17.75	109
	546	6	44.05	16.65	91
	547	7	43.10	15.70	78.1
	548	8	42.30	14.90	68.5
	549	9	41.15	13.75	61
10.00	550	10	40.45	13.05	55
	555	15	38.75	11.35	37
	560	20	37.40	10.00	28
	565	25	36.65	9.25	22.6
	570	30	35.82	8.42	19
	575	35	35.10	7.70	16.4
	580	40	34.35	6.95	14.5
	585	45	33.75	6.35	13
	590	50	33.20	5.80	11.8
	595	55	32.68	5.28	10.8
10.45	600	60	32.43	5.03	10
	615	75	31.85	4.45	8.2
11.15	630	90	30.35	2.95	7
	645	105	29.65	2.25	6.1
11.45	660	120	28.98	1.58	5.5
12.15	690	150	27.40	0.00	4.6

KIDIANI AREA GROUNDWATER SURVEY					
RECOVERY PHASE					
BOREHOLE NO: 7090		BOREHOLE NAME: Mivumoni			
BOREHOLE DEPTH: 61 m		MEASURING PT: G/L			
METHOD OF MEASURING		DATE OF TEST: 16-03-89			
WATER LEVEL: Electric Dipper		INITIAL WRL: 23.70 m			
Clock Time & Pumping Time, t, min	Recovery Time t', min	Water Level in m	Residual Drawdown S _r , m	t/t'	
8.45	540	49.00	25.30	-	
	541	48.10	24.40	541	
	542	47.25	23.55	271	
	543	46.45	22.75	181	
	544	45.67	21.97	136	
	545	44.65	20.95	109	
	546	43.99	20.29	91	
	547	43.39	19.69	78.1	
	548	42.81	19.11	68.5	
	549	42.23	18.53	61	
	550	41.83	18.13	55	
9.00	555	40.93	17.23	37	
	560	40.13	16.43	28	
	565	39.38	15.68	22.6	
	570	38.68	14.98	19	
	575	38.00	14.30	16.4	
	580	37.40	13.70	14.5	
	585	36.85	13.15	13	
	590	36.35	12.65	11.8	
	595	35.87	12.17	10.8	
	600	35.40	11.70	10	
	615	34.20	10.50	8.2	
	630	33.15	9.45	7	
	645	32.10	8.40	6.1	
	660	31.20	7.50	5.5	
11.15	690	29.40	5.70	4.6	
	720	27.80	4.10	4	
12.45	780	23.70	0.00	3.3	

KIDIANI AREA GROUNDWATER SURVEY					
RECOVERY PHASE					
BOREHOLE NO: 7267		BOREHOLE NAME: Kamene			
BOREHOLE DEPTH: 54 m		MEASURING PT: G/L			
METHOD OF MEASURING		DATE OF SURVEY: 13-04-89			
WATER LEVEL Electric Dipper		INITIAL WRL : 17.90 m			
Clock Time & Pumping Time, t, min	Recovery Time t' min	Water Level in m	Residual Drawdown S_r , m	t/t'	
8.45	420	49.00	31.10	-	
	421	48.20	31.30	421	
	422	47.50	29.60	211	
	423	47.05	29.15	141	
	424	46.40	28.50	106	
	425	46.00	28.10	85	
	426	45.15	27.25	71	
	427	44.68	26.78	61	
	428	44.15	26.25	53.5	
	430	43.10	25.20	43	
	435	42.15	24.25	29	
	440	41.55	23.65	22	
	445	40.95	23.05	17.8	
	450	40.15	22.25	15	
	455	39.60	20.70	13	
	460	39.05	21.15	11.5	
	465	38.55	20.65	10.3	
	470	38.00	20.10	9.4	
	475	37.20	19.30	8.6	
9.45	480	36.55	18.65	8.0	

KIDIANI AREA GROUNDWATER SURVEY					
RECOVERY PHASE					
BOREHOLE NO: 7934		BOREHOLE NAME: Kiranga Eshu			
BOREHOLE DEPTH: 70 m		MEASURING PT: G/L			
METHOD OF MEASURING		DATE OF TEST: 31-01-89			
WATER LEVEL: Electric Dipper		INITIAL WRL: 15.10 m			
Clock Time & Pumping Time, t, min	Recovery Time t', min	Water Level in m	Residual Drawdown S _r , m	t/t'	
5.00	300	0	35.85	20.75	-
	301	1	35.10	20.00	301
	302	2	34.80	19.70	151
	302	3	33.00	17.90	101
	304	4	32.05	16.95	76
	306	6	31.20	16.10	51
	308	8	30.50	15.40	38.5
	310	10	28.10	13.00	31
	315	15	27.00	11.90	21
	320	20	26.60	11.50	16
5.30	325	25	24.33	9.23	13
	330	30	22.04	6.94	11
	335	35	20.80	5.70	9.6
	340	40	19.00	3.90	8.5
	345	45	18.94	3.84	7.7
	350	50	17.50	2.40	7
6.00	355	55	17.30	2.20	6.5
	360	60	17.10	2.00	6

KIDIANI AREA GROUNDWATER SURVEY					
RECOVERY PHASE					
BOREHOLE NO: 8221		BOREHOLE NAME: Fuombi			
BOREHOLE DEPTH: 40 m		MEASURING PT: G/L			
METHOD OF MEASURING		DATE OF TEST: 10-03-89			
WATER LEVEL: Electric Dipper		INITIAL WRL: 7.37 m			
Clock Time & Pumping Time, t, min	Recovery Time t' min	Water Level in m	Residual Drawdown S _r , m	t/t'	
6.55	400	0	16.66	9.29	-
	401	1	16.40	9.03	401
	402	2	16.00	8.63	201
	403	3	15.72	8.35	134.3
	404	4	15.34	7.97	101
	406	6	14.30	6.93	67.7
	408	8	13.67	6.30	51
	410	10	13.23	5.86	41
	415	15	12.30	4.93	27.7
	420	20	12.11	4.74	21
7.25	425	25	10.80	3.43	17
	430	30	10.12	2.75	14.3
	435	35	9.78	2.41	12.4
	440	40	9.51	2.14	11
	445	45	9.42	2.05	9.9
7.55	450	50	9.24	1.87	9
	455	55	9.11	1.74	8.3
	460	60	9.05	1.68	7.7
	475	75	8.94	1.57	6.3
	490	90	8.70	1.33	5.4
10.00	505	105	8.61	1.24	4.8
	525	125	8.50	1.13	4.2
	555	155	8.23	0.86	3.6
	585	185	8.15	0.78	3.2
	615	215	8.13	0.76	2.9

KIDIANI AREA GROUNDWATER SURVEY					
RECOVERY PHASE					
BOREHOLE NO: 6721		BOREHOLE NAME: Kivuleni			
BOREHOLE DEPTH: 40 m		MEASURING PT: G/L			
METHOD OF MEASURING		DATE OF TEST: 25-05-89			
WATER LEVEL: Electric Dipper		INITIAL WRL 0.80 m			
Clock Time & Pumping Time, t.min	Recovery Time t' min	Water level in m	Residual Drawdown S _r , m	t/t'	
6.00	483	0	10.70	9.90	-
	484	1	9.86	9.06	484
	485	2	7.80	7.00	242.5
	486	3	7.15	6.35	162
	487	4	6.65	5.85	121.8
	489	6	6.07	5.27	81.5
	491	8	5.94	5.14	61.4
	493	10	5.64	4.84	49.3
	498	15	5.18	4.38	33.2
	503	20	4.90	4.10	25.2
6.30	508	25	4.85	4.05	20.3
	513	30	4.50	3.70	17.1
	518	35	4.08	3.28	14.8
	523	40	3.91	3.11	13.1
	528	45	3.87	3.07	11.7
7.00	533	50	3.73	2.93	10.7
	538	55	3.69	2.89	9.8
	543	60	3.61	2.81	9.1

KIDIANI AREA GROUNDWATER SURVEY					
RECOVERY PHASE					
BOREHOLE NO: 7097		BOREHOLE NAME: Mwachande			
BOREHOLE DEPTH: 70 m		MEASURING PT: G/L			
METHOD OF MEASURING		DATE OF TEST: 20-04-89			
WATER LEVEL: Electric Dipper		INITIAL WRL: 20.06 m			
Clock Time & Pumping Time, t, min	Recovery Time t' min	Water Level in m	Residual Drawdown S _r , m	t/t'	
10.35	720	0	38.00	17.94	-
	721	1	28.60	8.54	721
	722	2	27.00	6.94	361
	723	3	26.00	5.94	241
	724	4	25.60	5.54	181
	726	6	25.07	5.01	121
	728	8	24.75	4.69	91
	730	10	24.47	4.41	73
	735	15	24.24	4.18	49
	740	20	24.03	3.97	37
	745	25	23.84	3.78	29.8
	750	30	23.64	3.58	25
	755	35	23.45	3.39	21.6
	760	40	23.27	3.21	19
	765	45	23.10	3.04	17
	770	50	22.95	2.89	15.4
	775	55	22.82	2.76	14.1
11.35	780	60	22.69	2.63	13
	795	75	22.56	2.50	10.6
	810	90	22.43	2.37	9
	825	105	22.30	2.24	7.9
12.35	840	120	22.07	2.01	7
	865	145	21.72	1.66	6
	925	205	21.71	1.65	4.5
3.00	985	265	21.70	1.64	3.7

KIDIANI AREA GROUNDWATER SURVEY					
RECOVERY PHASE					
BOREHOLE NO:		6673		BOREHOLE NAME: Mnazimoja	
BOREHOLE DEPTH:		50 m		MEASURING PT: G/L	
METHOD OF MEASURING			DATE OF TEST: 25-02-89		
WATER LEVEL: Electric Dipper			INITIAL WRL: 12.60 m		
Clock Time & Pumping Time, t, min		Recovery Time t', min	Water Level in m	Residual Drawdown S _r , m	t/t'
1.35 pm	840	0	23.03	10.43	-
	841	1	22.94	10.34	841
	842	2	22.70	10.10	421
	843	3	22.58	9.98	261
	844	4	22.41	9.81	211
	846	6	22.29	9.69	141
	848	8	21.92	9.32	106
	850	10	21.54	8.94	85
	855	15	19.72	7.12	57
	860	20	19.29	6.69	43
2.05	865	25	18.88	6.28	34.6
	870	30	18.58	5.98	29
	875	35	18.33	5.73	25
	880	40	18.12	5.52	22
	885	45	17.93	5.33	19.7
2.35	890	50	17.71	5.11	17.8
	895	55	17.57	4.97	16.3
	900	60	17.43	4.83	15
	915	75	17.22	4.62	12.2
	930	90	17.13	4.53	10.3
5.35	945	105	16.90	4.30	9
	960	120	16.46	3.86	8
	990	150	15.01	2.41	6.6
	1020	180	14.80	2.20	5.7
	1080	240	14.10	1.50	4.5
7.35	1140	300	13.71	1.11	3.8
	1200	360	13.60	1.00	3.3
	1260	420	13.52	0.92	3
11.35	1320	480	13.46	0.86	2.8
	1380	540	13.40	0.80	2.6
	1440	600	13.36	0.76	2.4

DEPTH (m)	LOG 1	LOG 2	LOG 3	LOG 4	LOG 5	LOG 6	LOG 7
0							
1							
2							
3							
4							
5							
6							
7							
8							
9							
10							
11							
12							
13							
14							
15							
16							
17							
18							
19							
20							
21							
22							
23							
24							
25							
26							
27							
28							
29							
30							
31							
32							
33							
34							
35							
36							
37							
38							
39							
40							
41							
42							
43							
44							
45							
46							
47							
48							
49							
50							

APPENDIX D
Well Logs Data

